AD-A162 777 RADIATION-HARD BREADBOARD STAR TRACKER(U) BALL AEROSPACE SYSTEMS DIV BOULDER CO M W HUBBARD ET AL. SEP 85 BASD/F85-03 N00014-82-C-2488 1/2

UNCLASSIFIED F/G 17/3 NL

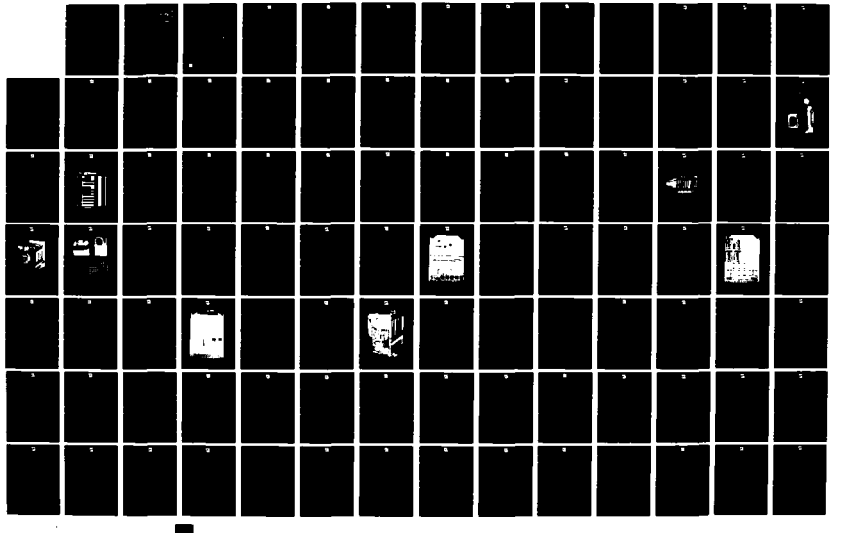

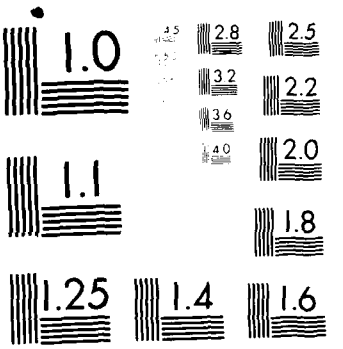

Ball

Final Report for

ADIATION-HARD BREADBOARD STAR TRACKER

F85-03 September 1985

AD-A162 777

DTIC FILE COPY

DTIC
ELECTE
DEC 30 1985
S D

This document has been approved for public release and sale; its distribution is unlimited.

Final Report for

RADIATION-HARD BREADBOARD STAR TRACKER

F85-03 September 1985

Prepared for
Naval Research Laboratory
Washington, D.C.

Contract N00014-82-C-2488

Prepared by

M.W. Hubbard
Principal Engineer

D.L. Murata
Design Engineer

Approved by

J.C. Kollodge
Program Manager

C.A. Cullian
Director
Electro-Optical Products

Ball Aerospace Systems Division

BOULDER COLORADO 80306

TABLE OF CONTENTS

TABLE OF CONTENTS (Continued)

TABLE OF CONTENTS (Concluded)

FOREWORD

This final report summarizes the activities performed by Ball Aerospace Systems Division (BASD) under Naval Research Laboratory (NRL) Contract N000-14-82-C-2488. It presents the results of the design, analyses, and tests conducted. Attachment I to this report contains various program listings, flowcharts, and error messages for the software that was developed for this project.

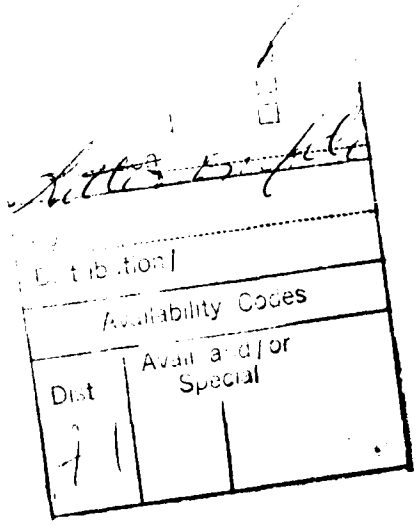

GLOSSARY

A/D	Analog-to-Digital
AGC	Automatic Gain Control
AMD	Advanced Micro Devices
BASD	Ball Aerospace Systems Division
CCD	Charge Coupled Device
CDS	Correlated Double Sample
CID	Charge Injection Device
CMOS	Complementary Metal Oxide Semiconductor
CMRR	Common-Mode Rejection Ratio
CPS	Cycles per Second
CPU	Central Processing Unit
CRT	Cathode Ray Tube
C/S	Command/Status
CTD	Charge Transfer Device
DMA	Defense Mapping Agency
EFL	Effective Focal Length
EMI	Electromagnetic Interference
EPIC	Emulation and Programmable Integrated Circuit
FET	Field Effect Transistor
FOV	Field of View
GE	General Electric
HP	Hewlett Packard
IDT	Image Dissector Tube
IC	Integrated Circuit
I/O	Input/Output
LC	Inductor-Capacitor
LINAC	Linear Electron Accelerator
LSTTL	Low-Power Schottky Transistor-Transistor Logic
MSI	Medium-Scale Integration
NDRO	Nondestructive Readout
NEA	Noise-Equivalent Angle
NMOS	N-Channel Metal Oxide Semiconductor
NRL	Naval Research Laboratory
PASS	Precision Astronomical Survey System
PMI	Precision Monolithics, Inc.

GLOSSARY (Concluded)

PROM	Programmable Read-Only Memory
RAM	Random Access Memory
ROM	Read-Only Memory
S/H	Sample and Hold
SSI	Small-Scale Integration
TEC	Thermoelectric Cooler
TF	Transfer Function
TLD	Thermal Luminescent Dosimeter
TTL	Transistor-Transistor Logic

Section 1
INTRODUCTION

Section 1
INTRODUCTION

1.1 BACKGROUND

Operation in a radiation environment affects the performance of many types of electro-optical sensors. Specifically, noise generated from radiation in the detector and front-end electronics in star trackers can degrade the performance of the sensors. Upsets in the related processing electronics can cause loss of track, data interruptions, and in some cases, failure to recover.

Degradation of performance can occur in a natural charged-particle environment and becomes worse in a weapon-enhanced radiation environment. High total dose results in component and, in turn, system failure to operate.

The objectives of this program, which was conducted by Ball Aerospace Systems Division (BASD) for the Naval Research Laboratory (NRL), were to develop a tracker that could survive a high total dose and to gain a better understanding of the transient effects of radiation on the star tracker performance. Survivability of the star tracker in a radiation environment, both at the component level and at the system level, is of primary importance.

1.2 PROGRAM SUMMARY

The primary goal of this program was the design, fabrication, and test of a breadboard star tracker to verify survivability with a total radiation dose of 10^5 rad. To meet this goal, the following tasks were performed:

- Selection and procurement of radiation parts;
- Design and fabrication of a radiation-hard breadboard star tracker;
- Lens housing design and fabrication;
- Star simulator design and fabrication;
- Design and fabrication of the interface between the star tracker and the command computer;
- Functional testing of the star tracker electronics;

- Preliminary radiation testing of the star tracker electronic circuitry;
- Design and implementation of the test software;
- System testing with the test software;
- Procurement of radiation-hard detectors, including characterization and radiation tests;
- Final radiation testing; and
- Data review and analysis.

1.3 OBSERVATIONS AND CONCLUSIONS

The breadboard design has high performance capabilities and can be packaged in a volume of 4,000 cm^3, with a weight of approximately 10 kg, including shielding. Power consumption is approximately 15W without the thermoelectric cooler (TEC) operating.

Radiation tests were performed at NRL using cobalt 60 for low-rate transient tests and 40 MeV electrons for high-rate and total dose tests. The tests and results are summarized below.

- Low-Rate Transient: 0.6 rad/sec (limited by source capability); no observable effect on performance.

- High Rate: 10^8 rad/sec, loss of track and interruption of performance, recovery time was approximately 1 second; 10^9 rad/sec (limited by source capability), latch-up, recovered when power was cycled off and on.

- High Rate (detector only): 10^{11} rad/sec, loss of track and subsequent recovery, no other observable effect on performance.

- Total Dose: 10^5 rad; no observable degradation.

- Test to Failure: 1.5×10^5 rad, D139 level shifter integrated circuits (IC) in the star tracker level shifter circuit failed.

From these results we can conclude that the program objectives were met. However, further tests and analyses are needed to better understand the transient effects that were observed and the degradation of electronic parts. Additional development is required to improve the hardware to levels significantly above 10^5 rad.

Section 2
GENERAL DESCRIPTION

Section 2
GENERAL DESCRIPTION

2.1 DESIGN APPROACH

The advent of charge transfer devices (CTD) has generated a high interest in their application to advanced sensors for use in pointing and control of space vehicles.

BASD's involvement with the development of a star tracker using CTD technology began in 1975. The charge coupled device (CCD) was used in early work because of its availability. Subsequently, the charge injection device (CID) was used because its nondestructive readout (NDRO) and random access readout offer advantages for star tracking applications.

Evaluation of breadboards with both devices demonstrated the expected performance improvements over other detectors, such as photo tubes and photodiodes.

Another significant advantage of the CTD is that it offers flexibility in operational modes when placed under microprocessor control.

Because of the improved performance and the fact that CTD and microprocessor radiation hardening efforts were being undertaken by the suppliers, the decision was made to use those devices in the design approach.

2.2 CTD SELECTION

2.2.1 Operational Considerations

A CTD is an array of photosensitive picture elements, or pixels, that are formed on a semiconductor chip using IC processing techniques. The pixels are small (~25 μm), so that a very large number can be deposited on a small chip. The device is unique in that the photon-generated electrons are integrated and stored at the respective pixels until removed by commanded readout or recombination.

Many variations of CTDs have been developed. They can typically be placed into one of two general categories: CCDs and CIDs.

The basic difference between CCDs and CIDs is the method of readout and charge removal. The CCD is read out by sequential transfer of charge from pixel to pixel along the columns, similar to a "bucket brigade." The charge signals are detected at the end of the columns and can be related by the clocking sequence to the pixel locations from which they originated. The charge is removed in the readout process.

The CID cannot transfer charge between pixels. Instead, each pixel has a row-connected and a column-connected electrode, which form capacitors between which charge can be transferred. The impulse, which is proportional to the charge during the intrapixel transfer, is detected for signal readout. The charge is not destroyed in this mode, so that multiple readings can be taken while the charge is integrating at the pixel.

The random access, multiple-NDRO capability, combined with high uniformity of response and dark current, make the CID an attractive device for tracking small sources such as stars.

Table 2-1 is a qualitative comparison of CIDs and CCDs; it was made specifically for the star tracking application. Although the chart shows a bias toward the CID, both devices will meet performance requirements for most applications. Parameters that made the CID more attractive for star tracking applications include:

- Lower dark current, which requires less cooling power;
- Defect tolerance and yield, which indicate advantages in producibility;
- Direct accessing of only needed data, which uses less processing;
- Operational flexibility, which reduces system processing requirements and enhances performance; and
- Lower power, which reduces electrical and thermal design efforts.

Table 2-1

COMPARISON OF CID AND CCD

No.	Trade-off Item	CID	CCD
1	Defect Tolerance	+ Defects confined to pixel	- Defects propagate down columns
2	Optical Overload Tolerance	+ Blooming confined to local area	- Blooming propagates down column
3	Charge Storage Capacity	+ 10^6 carriers typical	- 10^5 carriers typical
4	Dark Current Generation	+ 1 ns per cm^2 typical	- 5 ns per cm^2 typical
5	Quantum Efficiency	+ High; 0.4 to 1 μm	+ High; 0.4 to 1 μm
6	Response Uniformity	+ 0.6% rms typical	- 5% rms typical
7	Temporal Noise	+ 30 to 300 carriers typical	+ 50 to 200 carriers typical
8	Cross Talk Sensitivity	+ Confined to adjacent pixel	- Occurs over several pixels
9	Data Address	+ Direct X-Y access to data pixel	- "Bucket brigade" to data pixel
10	Charge Transfer Efficiency	+ One transfer	- Full array transferred
11	Operational Flexibility	+ Destructive or non-destructive readout: on-chip processing	- Destructive full frame readout
12	Power	+ Only required pixels are read at required update rate	- Full array is read at required update rate
13	Yield	+ Three masking operations involved in fabrication	- 5 to 12 masking operations involved in fabrication
14	Technical Maturity	+ Implemented in tracker and tested	+ Implemented in tracker and tested

+ = Advantage
- = Disadvantage

2.2.2 Radiation Considerations

Both devices had been hardened to greater than 10^5 rad (Si) at the time the selection trade-offs were being made (late 1982). However, improvements were in process and postradiation performance data varied with different processes and lots.

Response and noise degradation in the two are similar. However, problems with degradation in charge transfer efficiency and column streaking with high radiation are unique to the CCD; they are not as much of a problem with the CID. In general, because there are fewer operational parameters in the CID that can be affected by radiation, it should have a lower failure rate with increasing radiation.

Based on these comparisons and a detailed review of available data, the CID was selected for the star tracker. The specific device chosen for the NRL radiation-hard breadboard star tracker is the GE ST-256E CID. A TEC was packaged as an integral part of the detector assembly for maximum cooling efficiency.

2.3 PERFORMANCE CAPABILITY

Typical performance parameters of a CID (ST-256) that are critical to system performance are shown in Table 2-2.

Table 2-2
CID PERFORMANCE SUMMARY

PARAMETER	PERFORMANCE
Array Size	256 x 256 pixels
Pixel Size	20 x 20 μm
Dark Current	$<10^4$ E^-/sec-pixel at 0°C
Quantum Yield	>0.4
Pixel Saturation	$>10^6 e^-$
Dark Current Variation	<1.5%
Response Variation	<1%
Readout Noise	<3.9 $E^-/Hz^{1/2}$ read rate
Response Point Spread	Symmetrical about pixel center
Radiation Tolerance	$>10^6$ rad

2.3.1 Tracking Capability

Star trackers require a transfer function (output versus position) to determine location of the star image relative to the center of the nearest pixel.

A major emphasis has been placed on achieving a high interpolation accuracy because it simplifies the system design. An extensive study program at BASD resulted in the development of a unique concept with maximum gain and an accuracy capability better than 1 percent of a pixel. The concept also includes features to enhance acquisition and tracking with radiation background. The transfer function (TF) is continuous and linear, as shown in Figure 2-1.

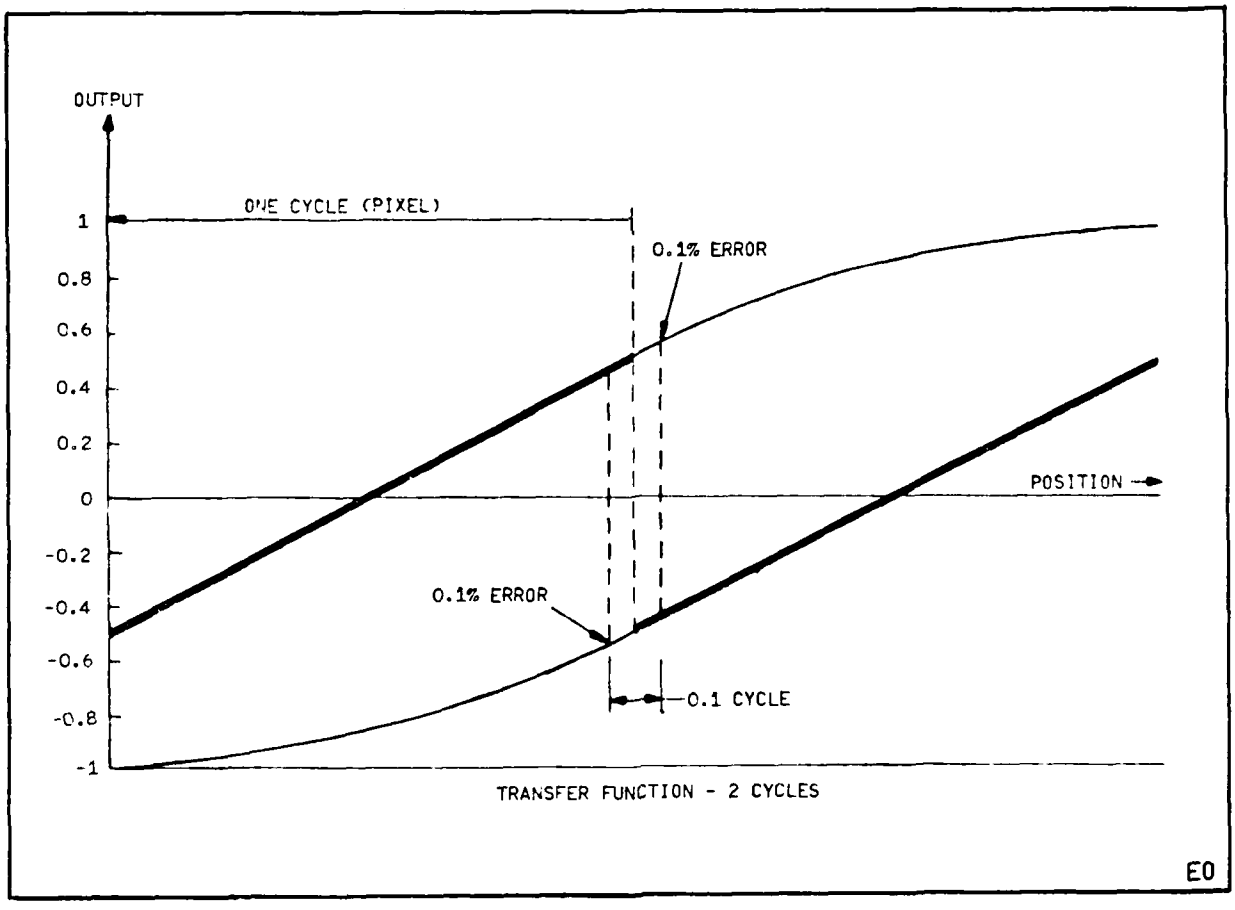

Figure 2-1 Interpixel Transfer Function

The CTD has an inherent resolution equivalent to the number of pixels divided by the interpolation accuracy. Therefore, the TF applies only to position relative to the pixel nearest the star image center. This results in effectively improving the accuracy by a factor equivalent to the number of pixels (N) in the CTD for a given TF accuracy.

This advantage is illustrated in Figure 2-2 for an uncalibrated CID sensor and is projected to be 30 times better than a calibrated image dissector tube (IDT) sensor.

As Figure 2-2 shows, system accuracy can be improved either by increasing the number of pixels (N) or by decreasing the interpolation error (e_i). Therefore, if the interpolation accuracy is not met for a given system performance, the deficiency can be overcome by increasing the number of pixels in the CTD.

The alternative of increasing the number of pixels to make up for excessive interpolation errors has a significant impact on system configuration, producibility, and cost, especially for very high accuracy systems.

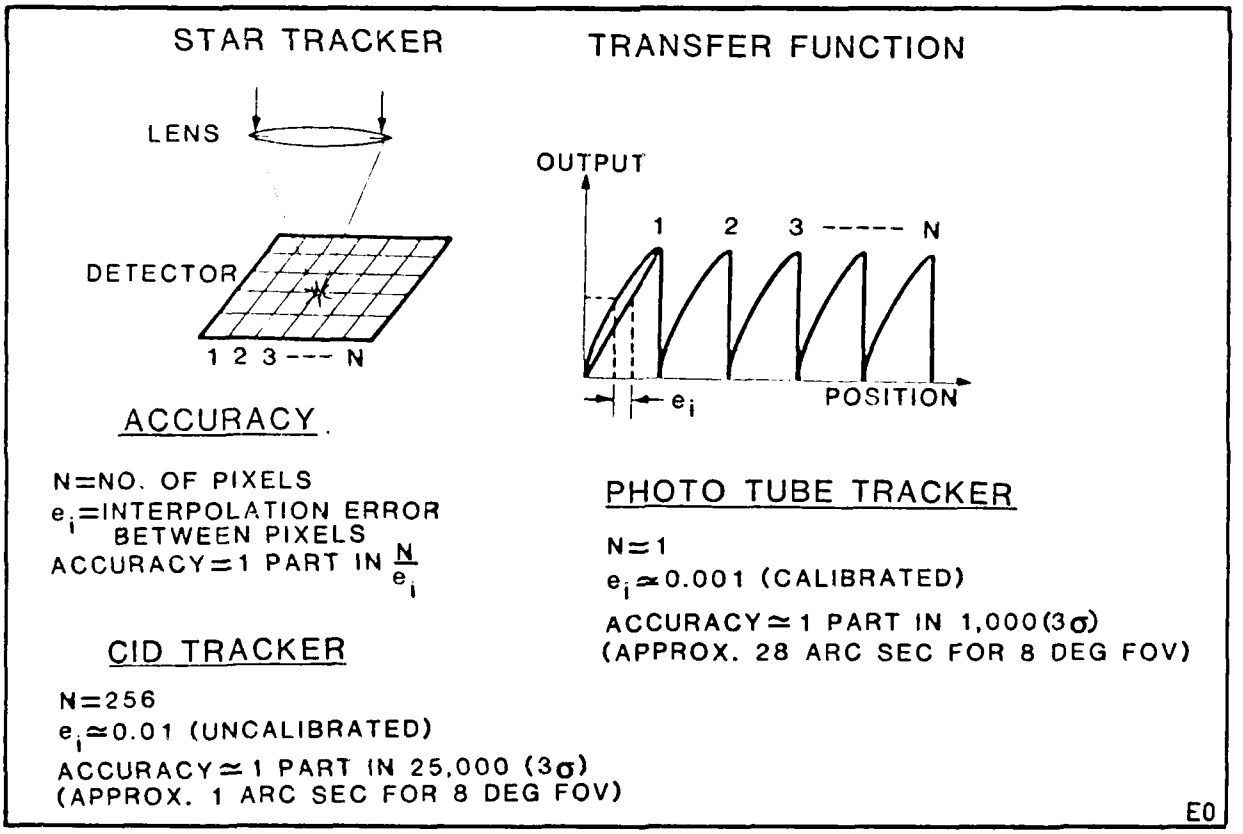

Figure 2-2 Mosaic Focal Plane Tracking Concept

The breadboard circuitry was designed to accommodate the tracking concepts previously developed by BASD.

By using those concepts and by sizing the tracker optics for sensitivity to 5.6 M_V stars, the basic performance capability can be tabulated, as shown in Table 2-3.

Table 2-3
STAR TRACKER PERFORMANCE CAPABILITY

PARAMETER	PERFORMANCE
Sensitivity	0 to 5.6 M_V
Star Availability	One at 0.99 probability, Two at 0.95 probability
Field of View (FOV)	7.6 x 7.6 deg
Position Accuracy	<20 arc sec (1σ)
Noise-Equivalent Angle (NEA)	10 arc sec (typical)
Number of Stars	≤3
Acquisition Time	<30 sec
Acquisition and Tracking Rate	>300 arc sec/sec
Position Update Rate	10 Hz (typical)

Changes in sensitivity, accuracy, and FOV can be made by changing the optics. Various operational modes and parameters can be changed by modifying software.

2.3.2 Typical Configuration and Radiation Considerations

The breadboard design effort has concentrated on minimizing the circuitry and power so that extensive radiation shielding, if needed in final packaging, would not result in intolerable weight.

Although the details of the radiation environment remain to be defined, the general approach for a radiation-hard design included the following key elements:

- Selection of the hardest parts available and affordable,
- Use of the fewest parts possible, and
- Accommodation of the maximum shielding possible.

The tracker functions and performance requirements were minimized, which required minimum processing and control electronics. The resultant small size for the tracker allows for extensive shielding without significant weight and volume penalties.

Radiation-hard parts were available with current technology that would perform after a total dose of 10^5 rad or greater. A preliminary review of worst-case natural and enhanced environments indicated that the total dose for most missions could be reduced to 10^5 rad, with approximately 1.5 cm or less equivalent aluminum shielding.

A packaging concept for the tracker is shown in Figure 2-3. The rugged front-end structure of the tracker typically required for mechanical stability and thermal control inherently provides the required shielding for the front hemisphere. The spacecraft offers shielding for the aft hemisphere; thus, a relatively thin structure is shown for the electronics. However, an additional 2.5 kg have been budgeted into the star tracker's mass (Figure 2-3) in the event that additional shielding is required.

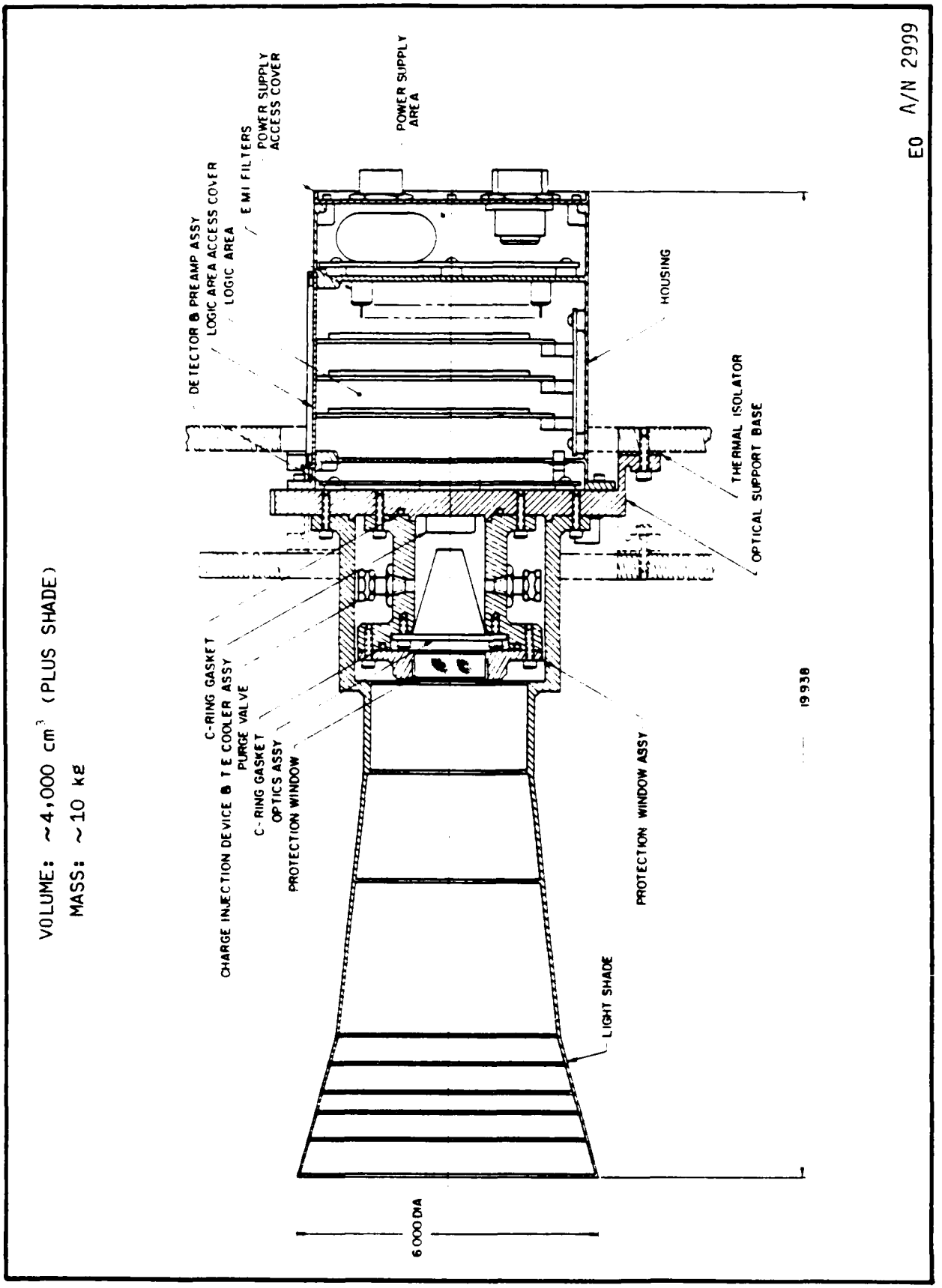

Figure 2-3 Star Tracker Packaging Design Concept

Section 3
HARDWARE DESIGN

Section 3
HARDWARE DESIGN

This section presents an overview of the hardware design. Appendix A provides additional information on the control, interface, and operating procedures. Attachment I contains program listings and flowcharts of the software developed for the project.

3.1 SYSTEM CONFIGURATION

3.1.1 System Overview

A +28 Vdc power supply is used to obtain the power needed to operate the star tracker.

The star tracker electronics and optics are mounted to a card cage construction. Interfaced with the star tracker is the test computer, a Hewlett Packard (HP) Series 200 Model 16 (HP 9816). The computer controls star tracker operation using commands generated to the star tracker.

The star simulator is a cylindrical tube connected to the front of the star tracker. Inside the far end of the tube is a five-pinhole matrix. A light source illuminates through the pinholes to provide simulated stars for the star tracker to detect. The matrix of pinholes may be rotated using a +12 Vdc motor attached to the star simulator.

An XY display is interfaced to the star tracker for easy observation of star tracker operation. The display shows the partition search pattern, and the location and tracking of stars. Each dot on the XY display represents a 4 x 4 pixel array.

Figure 3-1 is a block diagram of the overall system. Figure 3-2 shows the test computer, star tracker, and interface box.

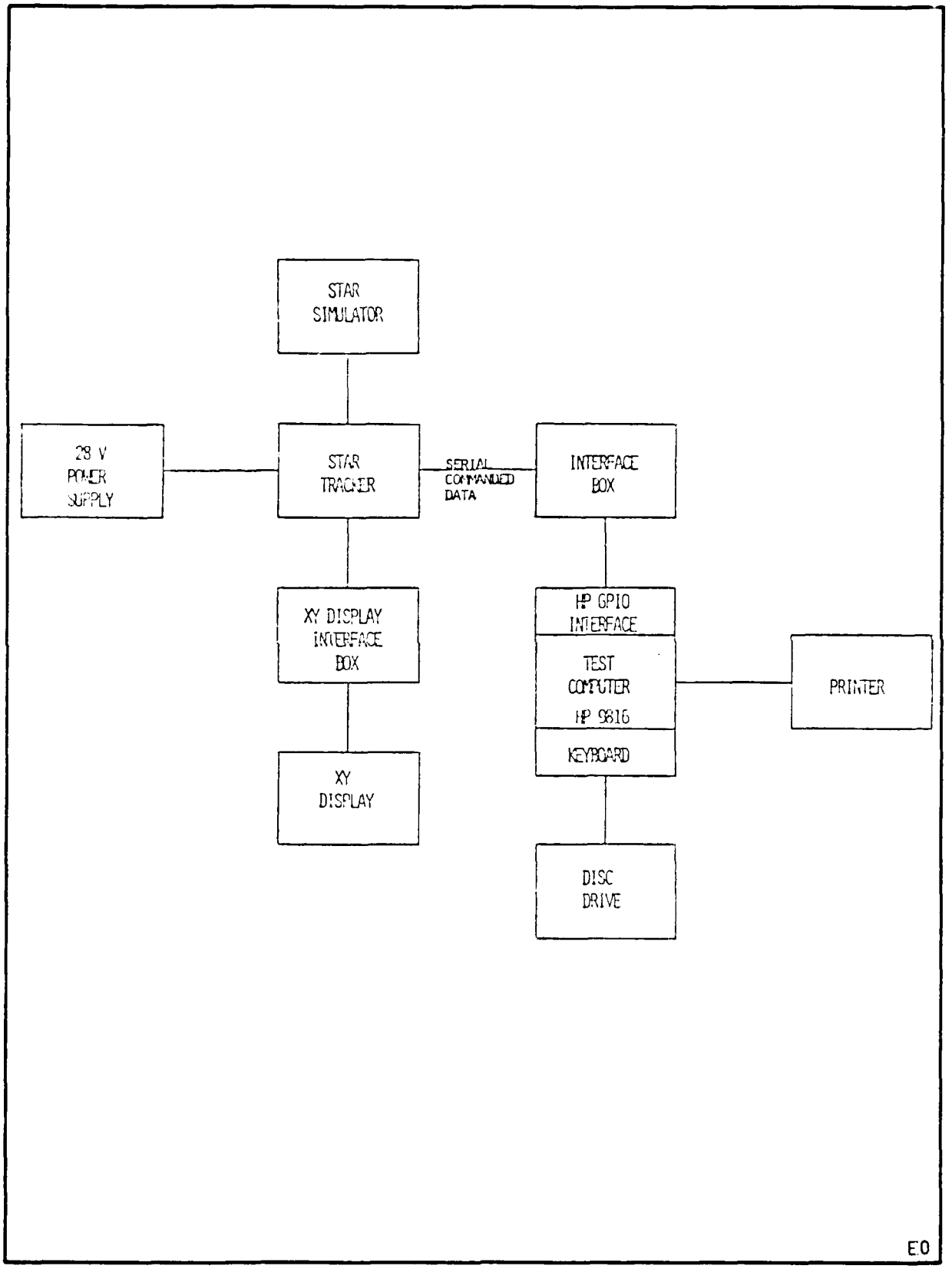

Figure 3-1 Overall Hardware System Block Diagram

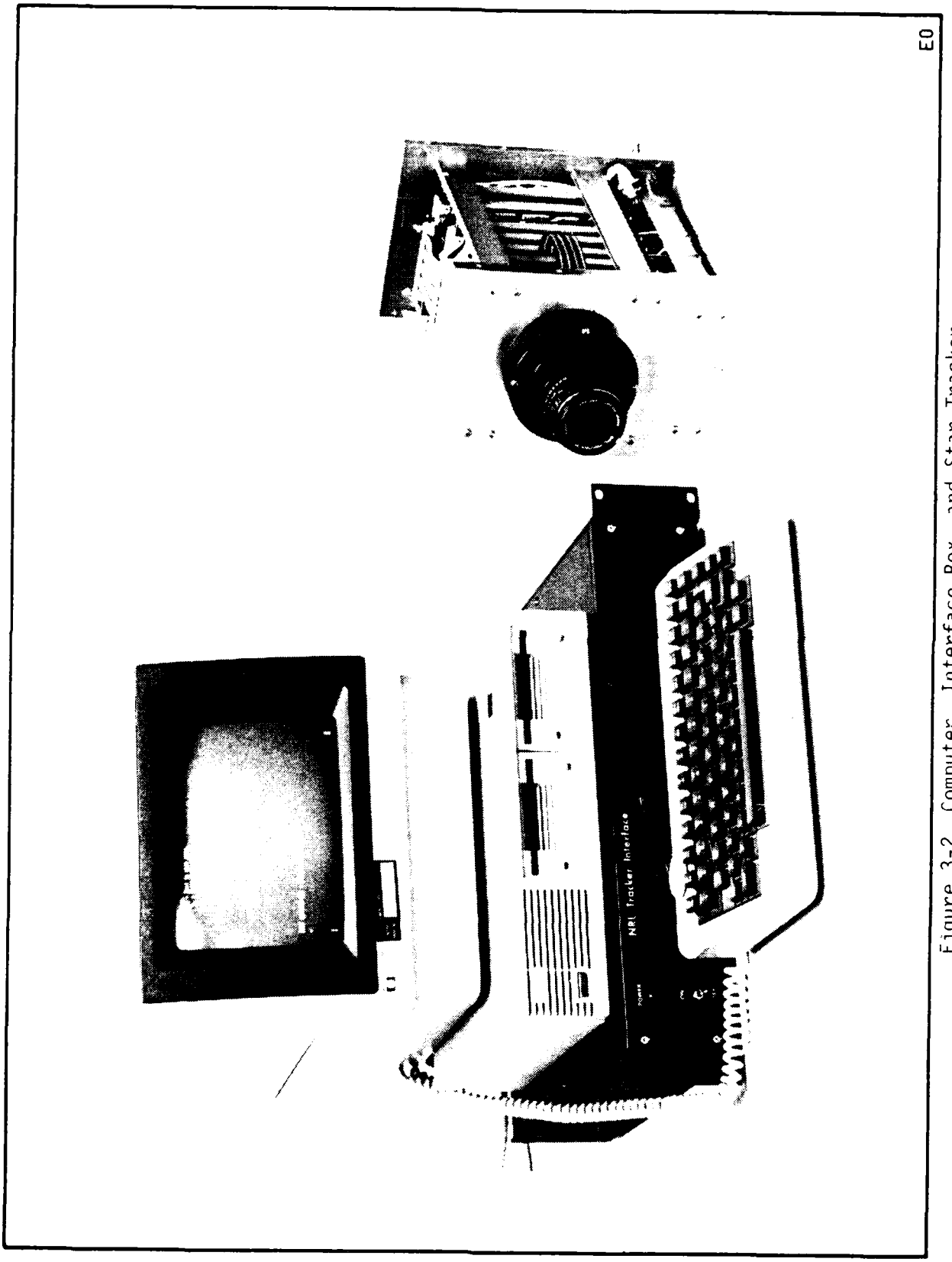

Figure 3-2 Computer, Interface Box, and Star Tracker

3.1.2 Star Tracker Card Cage and Bus

The following three wire-wrapped boards are included in the 6-1/2 x 9 in. star tracker card cage (shown in Figure 3-3):

- Focal plane electronics;
- Level shifters and low-noise regulators; and
- Microprocessor, input/output (I/O) ports, and memory.

The star tracker power supply is mounted on the back of the card cage. The bus board running along the bottom of the star tracker has 56 bus lines. Because of cut bus lines between the microprocessor board and the level shifter board, an additional connector board was installed. This connector board allows the microprocessor to talk to the remaining star tracker electronics and to receive signals from the charge injection device (CID). All star tracker power lines run through the entire length of the bus board.

Tables 3-1 and 3-2 list the bus lines running through the star tracker.

3.2 PARTS SELECTION

The parts selection task for the star tracker considered reliability, radiation hardness, power, and speed. MIL-STD 38510 was reviewed for Class "S" parts that could be designed into a star tracker. Because there are not enough suitable Class S parts for this design and the cost of developing new parts was beyond the scope of this program, it was decided not to use Class S parts. However, regardless of the design approach used, the number of part types would be minimized, and manufacturers with Class S equivalent parts would be used. Because N-channel metal oxide semiconductor (NMOS) devices are generally not radiation-hardened, the choice was between bipolar or hardened complementary metal oxide semiconductor (CMOS) parts. The NRL breadboard star tracker uses a combination of the two choices. To keep total power to less than 15W, the CMOS was preferred. The choice of an 8-bit CMOS over a 16-bit bipolar system microprocessor affected some performance parameters. These CMOS parts are still adequate for star acquisition and tracking if rates are modest.

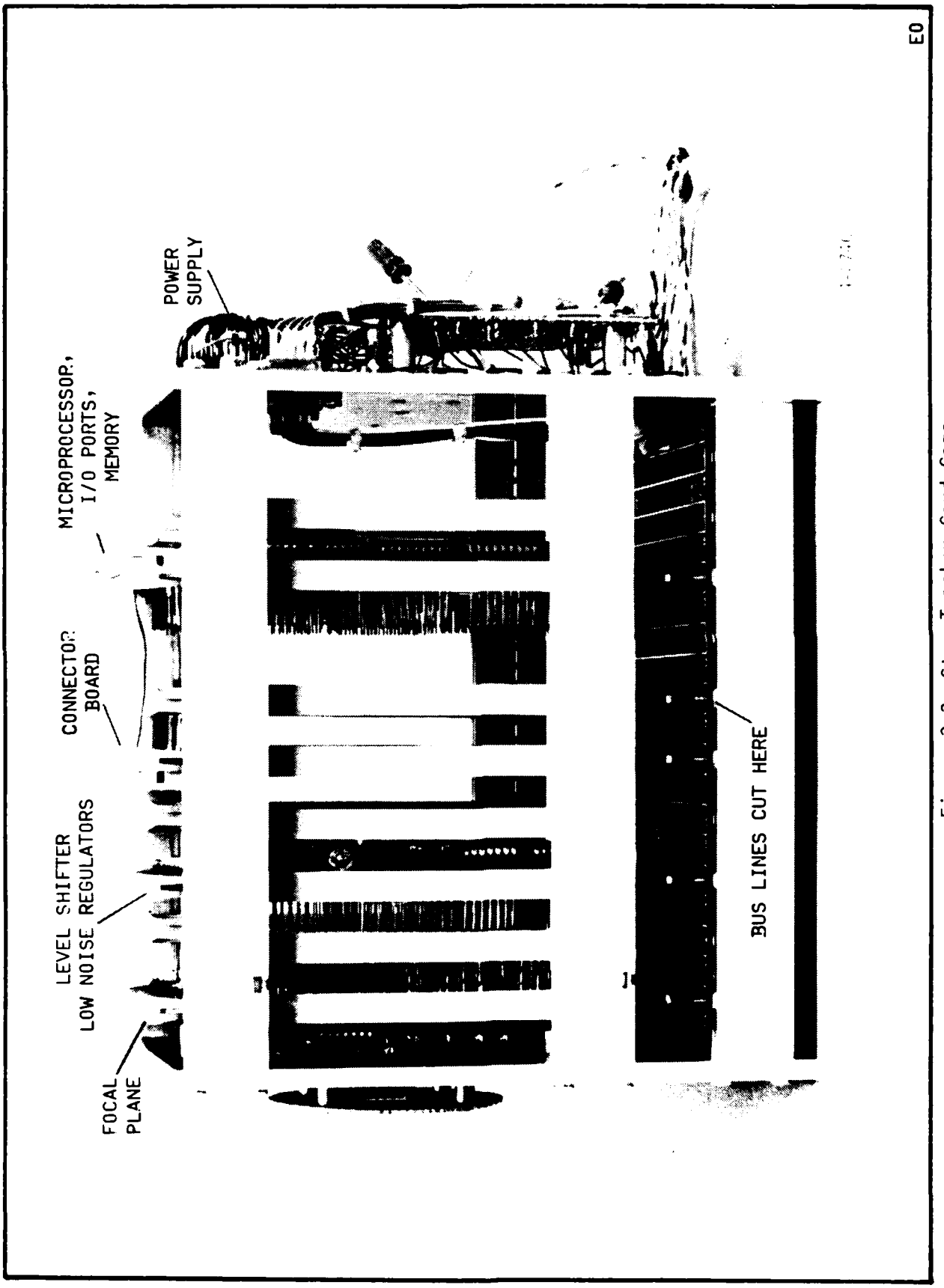

Figure 3-3 Star Tracker Card Cage

Table 3-1

MICROPROCESSOR BOARD BUS

LINE	FUNCTION	LINE	FUNCTION
1	+5V (A)	29	
2	+5V (A)	30	
3	+5V RTN (A)	31	
4	+5V RTN (A)	32	
5	-20V	33	
6	-20V RTN	34	
7	+5V (B) TEC	35	
8	+5V RTN (B) TEC	36	
9	CFLAG+	37	
10	CFLAG-	38	
11	CCLK+	39	
12	CCLK-	40	
13	CDATA+	41	
14	CDATA-	42	
15	+DATA	43	
16	-DATA	44	
17	+CLK	45	
18	-CLK	46	+ACK
19	+FLAG	47	-ACK
20	-FLAG	48	
21		49	Microprocessor CLK
22		50	
23		51	
24		52	
25		53	±15V RTN
26		54	±15V RTN
27		55	+15V
28		56	-15V

Table 3-2

LEVEL SHIFTER BOARD/FOCAL PLANE BOARD BUS

LINE	FUNCTION	LINE	FUNCTION
1	+5V (A)	29	MUX1
2	+5V (A)	30	MUX2
3	+5V RTN (A)	31	SC
4	+5V RTN (A)	32	Spare
5	-20V	33	
6	-20V RTN	34	
7	+5V (B) TEC	35	B0 (LSB)
8	+5V RTN (B) TEC	36	B1
9	RVD (RE)	37	B2
10	Spare	38	B3
11	CVD	39	B4
12	CVG	40	B5
13	IG	41	B6
14	S/H	42	B7
15	RES	43	B8
16	ID	44	B9
17	E1	45	B10
18	E2	46	B11 (MSB)
19	E3	47	
20	E4	48	
21	U/D	49	Microprocessor CLK
22	L/R	50	
23	VIN	51	
24	HIN	52	
25	VØ1	53	±15V RTN
26	VØ2	54	±15V RTN
27	HØ1	55	+15V
28	HØ2	56	-15V

3.2.1 Consultants and Vendor Surveys

A number of representatives from various firms were contacted during the design phase to determine the state of the art in radiation-hardened parts. Important design criteria were that the parts be available and affordable to the program. It was decided not to develop new parts, other than the CID detector (at General Electric).

Consultants. D. Meyers of Fairchild, G. Brucker of RCA, E. Peterson of NRL, and others were contacted to determine the state-of-the-art technology of radiation-hardened microelectronics and to arrive at a reasonable star tracker electronics design. Cost, schedule, and availability were major considerations throughout the program. Advice from consultants allowed us to keep our efforts within scope. Should our final radiation testing reveal problems, some of the areas will require further investigation, analysis, and testing.

RCA. RCA is active in the hardening of CMOS semiconductors. Many of the 4000 Series devices can be hardened to 10^6 rad levels. In fact, BASD designed a focal plane using these part types for the Precision Astronomical Survey System (PASS) program for the Defense Mapping Agency (DMA).

These 4000 series parts could easily be incorporated into the present design to replace transistor-transistor logic (TTL) parts and to further reduce power consumption. The TTL parts were used because of low cost, radiation hardness, and availability.

The hardened CMOS 1802 and family seemed an ideal solution to the tracker microprocessor hardware and power problems. However, the machine speed and architecture were unacceptable. Software development would have been more costly because of the architecture, which provided no powerful instructions.

RCA's emulation and programmable IC (EPIC) family chip set can emulate any microprocessor and can even create a custom design. However, a custom design of this type was beyond the scope of the breadboard star tracker program. Several other companies that make radiation-hardened parts were contacted, as discussed below.

National Semiconductor. National Semiconductor offers hardened CMOS 4000 Series parts. Their NSC800 CMOS Z-80 and support chips would have been ideal if they could have been hardened. About $100,000 per part was estimated for the hardening effort. This choice was dropped because the microprocessor was too new, and hardening appeared unlikely in the near future.

Tracor. Tracor has used the RCA EPIC chip set to emulate the Navy AN/UYK-20 16-bit computer and is developing a machine to execute the MIL-STD-1750A instruction set. Because these machines were new and unproven, they were considered too risky and costly for developing a star tracker. The volume of these boxes is considerable, 8 x 8 x 8 in., and the problem of developing software and installing ROM in the box is formidable.

Martin Marietta Denver Aerospace. Martin Marietta has developed a complete computer, the AMACS-1680, using the RCA EPIC chip set. This machine has a custom instruction set that does not emulate any commonly used machines. They have developed an assembler to run on a VAX computer and are developing a high-level language compiler. The unit has several custom gate arrays that were of questionable hardness. They proposed a breadboard unit and software support for $150,000, which was out of scope for this program.

Advanced Micro Devices. Advanced Micro Devices makes the bipolar bit-slice 2900 Series logic, a forerunner to the EPIC set, for custom computer design. The main problem with this approach is high power consumption, and a much more complex electronics design task.

Applied Technology. The ATAC computer is built around the 2900 Series logic. It is a well-proven, 16-bit-capable minicomputer. The problem with it is large size and power requirements (60W). Because we had decided not to use bit-slice designs of any type, our remaining choice was radiation-hardened microprocessors.

Fairchild. Fairchild builds a state-of-the-art microprocessor that executes the MIL-STD-1750A instruction set. It is very powerful for a central processing unit (CPU) on a chip. At the start of the program, the F9450 chip was not

fully functional, but its predecessor, the F9445, was. The F9445 is a 16-bit machine that emulates the Data General Nova. Both of these were advertised to be radiation-hard to at least 10^5 rad (Si). The F9445 has good speed, a moderately complete instruction set, and somewhat more power than desired (greater than 2W).

Sandia National Laboratories. Sandia is a leader in radiation-hardened microelectronics. Sandia has an impressive facility and a real interest in supplying hardware. Their SA3000 microprocessor was most applicable to the star tracker design, although it is lacking somewhat in performance. Sandia's SA3001 support chip replaces many MSI chips, and features CMOS power, a small random access memory (RAM), and a timer. The tracker was configured to use these parts for I/O functions to the detector and the outside world.

Harris Semiconductors. Harris was considered mainly for read-only memory (ROM) and random access memory (RAM). With the transfer of hardening technology from Sandia to Harris, they are offering a number of digital products. Large CMOS memories are one of their more developed products. It was desirable to have an all-CMOS programmable read only memory (PROM) and RAM. Harris responded to a request to harden a 6641 PROM for $50,000, but this was out of scope for this program. A bipolar PROM was chosen to store the tracker program. Because the Harris 6514 CMOS RAM was already hard and suitable for the design, parts were ordered.

3.2.2 Computer and Microprocessor Trade-offs

Table 3-3 lists the microprocessors and some of the considerations used in our trade-off analysis for selecting the computer.

Two approaches to the microprocessor electronics were selected as primary candidates. The first design approach used the Fairchild F9445 microprocessor and was functionally tested with simple test programs. The design was dropped because of a major effort required to code the flowcharts. A Sandia SA3000 was used in the second design approach, but the hardened parts were not immediately available. The program could continue without significant delay by using compatible NMOS versions for the microprocessor and support parts for early testing. The SA3000 was chosen to be used in the primary microprocessor electronics design.

Table 3-3
COMPUTER TRADE-OFFS

MICROPROCESSOR	MAJOR CONSIDERATION
MOT 6800	Not radiation hard
MOT 68000	Not radiation hard
RCA 1802	Low speed and instruction set
FCH 9445	Code development and support
FCH 9450	Some instructions not working
SA 3000	Availability
TI 9900	Availability
TI 9989	Hardness questionable
AMD 2911	Limited information

Table 3-4 compares the major parameters of the Sandia SA3000 and the Fairchild F9445.

Table 3-4
MICROPROCESSOR TRADE-OFFS

PARAMETER	SA3000	F9445
Technology	CMOS	Bipolar
Power	0.05W	2W
Instruction Cycle	2 μs	1.5 μs
Memory Size	64K	32K
Data Size	8-bit	16-bit
Arithmetic	+ -	+ - x /
I/O	8-bit	16-bit
Software Support	Large	Small
Hardware Support	Large	Minimal
Manufacturing Support	Large	Minimal
Availability	Long lead	Available now

3.2.3 Analog Parts

Analog parts are a major concern in a radiation environment because of gradual circuit performance changes as dose is accumulated. Some design steps have been taken to alleviate problems such as using Darlington transistors and low-value resistors in bias circuits. However, the best solution is to use parts that are inherently radiation hard.

Precision Monolithics, Inc. (PMI) has semiconductor processing that yields analog parts with reasonable performance in radiation. To keep a low parts type count and to stay with a single manufacturer, all the signal processing electronics were designed around PMI parts. Because PMI has a large selection of devices, no compromises were made with the circuit design. These parts are hardened by normal processing; therefore, commercial parts could be used for the breadboard. The consistency of this processing should be further investigated since its specific purpose is not to make the parts radiation hard. Table 3-5 lists the analog parts used.

The linear voltage regulators selected were the uA7800 and uA7900 Series bipolar devices. These regulators use more total power, but are safer and more predictable in a radiation environment than are the more efficient switching regulators.

Table 3-5
ANALOG PARTS SUMMARY

FUNCTION	TYPE	MANUFACTURER
Preamplifier	OP-227 OP-27	PMI PMI
Restore	SMP-11	PMI
Sample/Hold	SMP-11	PMI
Multiplexer	MUX-24	PMI
Buffer	OP-227	PMI
Comparator	CMP-05	PMI
Reference Voltage	REF-01	PMI
A/D Converter	DAC-312	PMI
Successive Approximation Register	AM2504	Advanced Micro Devices (AMD)
Level Shifter	D139	Siliconix
Low-Noise Regulator	OP-01	PMI

3.2.4 Digital Parts

Table 3-6 lists the digital parts used.

Table 3-6
DIGITAL PARTS SUMMARY

FUNCTION	TYPE	MANUFACTURER	REASON
Processor	SA3000	Sandia	CMOS
I/O Port	SA3001	Sandia	CMOS
Logic	LSTTL	Various	Available
Line Driver/ Receiver	26LS31 26LS33	AMD	Bipolar/ Other Program
PROM	82S191	Signetics	Bipolar
RAM	HS-6514	Harris	CMOS

The goal was to use all CMOS parts, if they were available, at a reasonable cost. Where this was not possible, bipolar equivalent types were substituted.

3.3 CIRCUIT DESIGN

3.3.1 NRL Star Tracker

The radiation-hardened star tracker shown in Figure 3-4 is a self-contained unit with a power consumption of less than 20W with the TEC operating. It includes:

- Commercial camera lens,
- CID with TEC,
- Focal plane signal conditioning electronics,
- Level shifters with low-noise regulators,
- Signal processing electronics, and
- Power supply.

The star tracker lens is a commercial camera lens made by Pentax. It has an effective focal length (EFL) of 50 mm and an f-number of 1.7.

Included as part of the focal plane signal conditioning electronics are:

- Preamplifier,
- Restore,
- Sample and hold, and
- Analog-to-digital converter.

The signal processing electronics include:

- Microprocessor,
- RAM and ROM,
- I/O ports, and
- Logic circuits.

The power supply incorporates an electromagnetic interference (EMI) filter circuit for radiation purposes.

Figure 3-5 is a block diagram of the NRL radiation-hard breadboard star tracker.

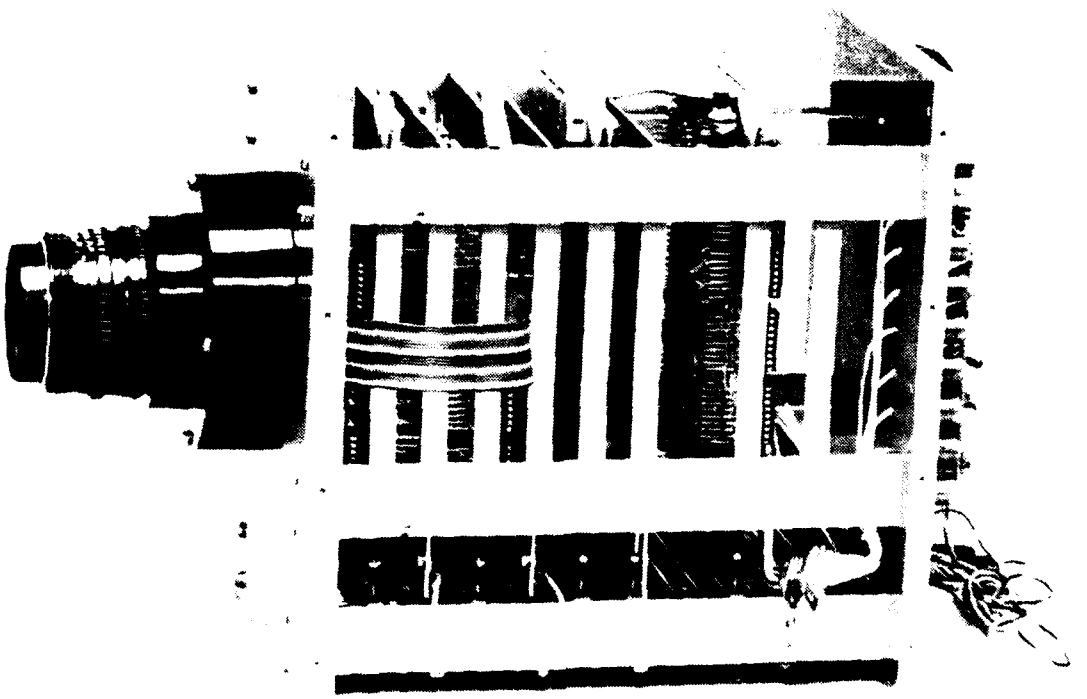

EO

Figure 3-4 NRL Radiation-Hard Breadboard Star Tracker

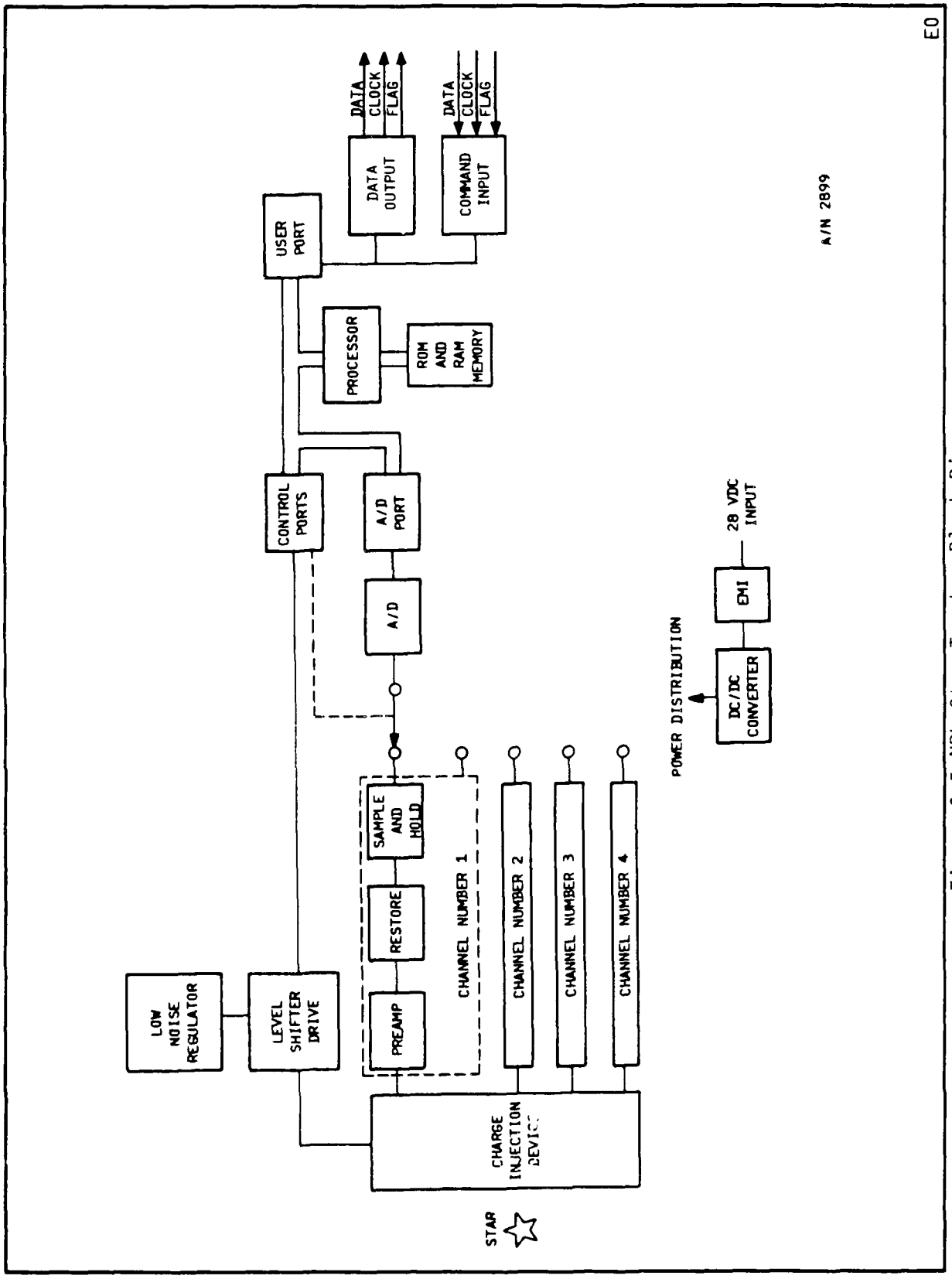

Figure 3-5 NRL Star Tracker Block Diagram

3.3.2 Detector

The detector (manufactured by General Electric) is a CID Model ST-256E mounted to a TEC. The CID is a 256 x 256 pixel array with a pixel size of 20 x 20 μm and is contained in a 44-pin, hermetically sealed chip carrier. Figures 3-6, 3-7, and 3-8 show the CID, TEC assembly, chip carrier, and pixels. Figure 3-9 is a block diagram of the CID.

Each pixel has, in effect, a row-connected and a column-connected capacitor between which charge can be transferred. The displacement current during intrapixel transfer is detected for signal readout. Multiple readings can be taken while charge is integrating at the pixel because the charge is not destroyed during intrapixel transfer.

The array is designed for parallel row readout, and the signals are processed using double-read nondestructive readout (NDRO). By using nondestructive multiple readouts, fixed pattern noise, readout noise, and 1/f noise are reduced. After the read cycle is complete, charge is removed by injection into the substrate.

3.3.2.1 CID Operation

Figure 3-10 shows how a pixel is addressed on the CID array. Horizontal and vertical shift registers are located along two edges of the array. The registers control switches that are connected to the column and row capacitors. With the registers, four columns and four rows can be accessed simultaneously. The desired columns are chosen by the column drive lines, also called E-lines. A single pixel can be addressed by reading the preamplifier for the intersecting row. Row and column bias gates are provided (opposite the register) for single-line control of the full array.

The sum of a 4 x 4 block of pixels can be read by driving all four E-lines and reading the four preamplifier output voltages simultaneously. Data from a single pixel are acquired by driving one E-line and reading one preamplifier output voltage.

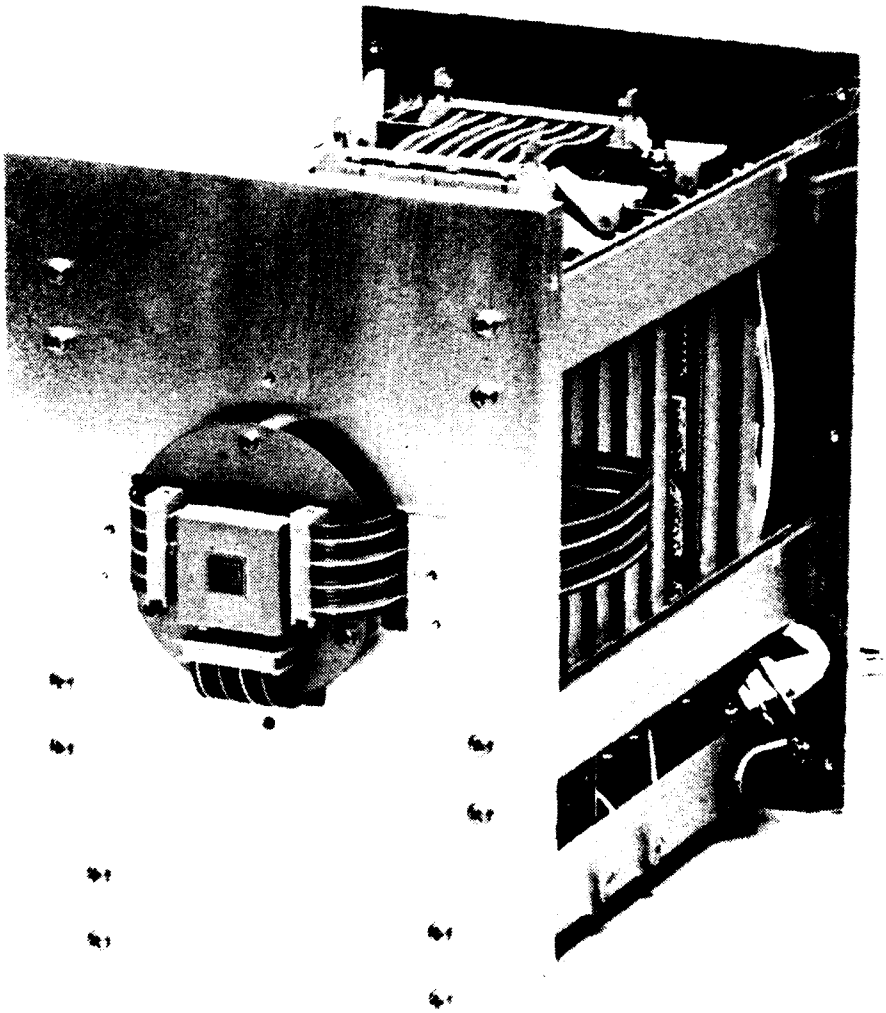

EO

Figure 3-6 CID and Chip Carrier

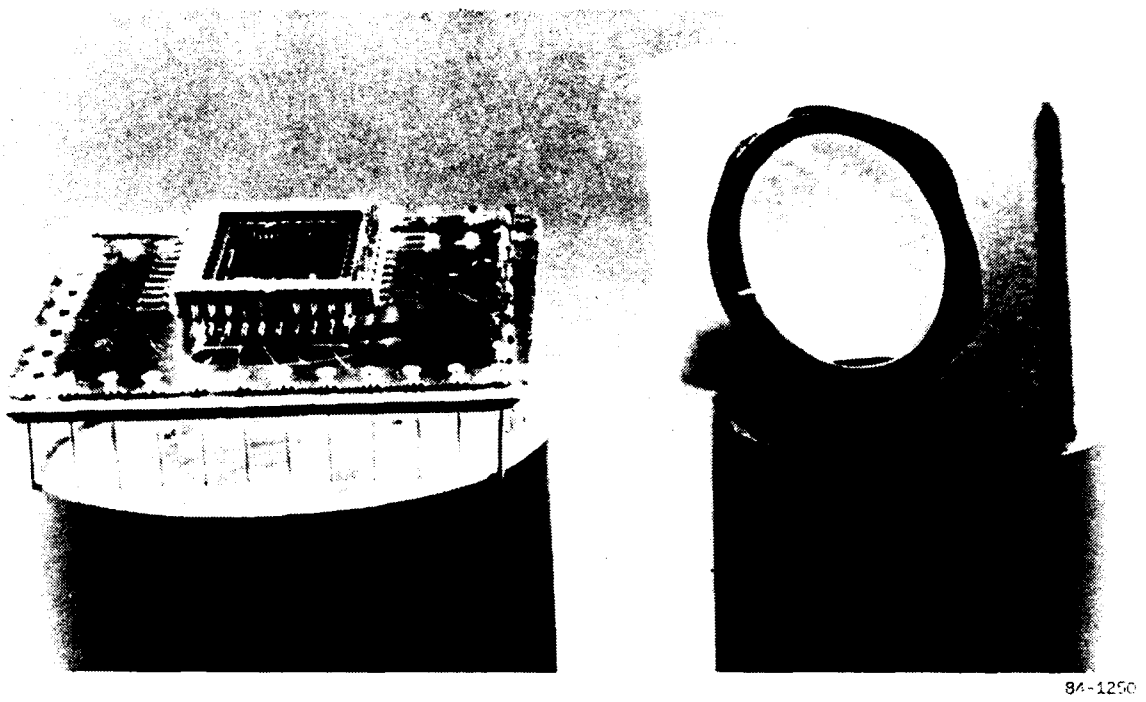

Figure 3-7 Breadboard CID and Thermoelectric Cooler Assembly

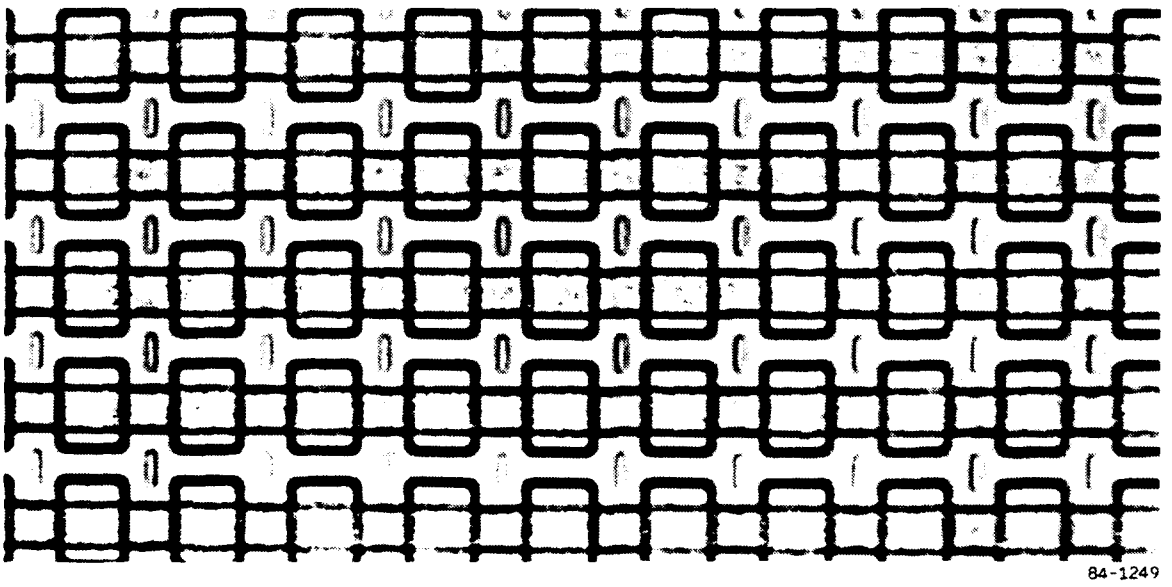

Figure 3-8 CID Pixels

EO

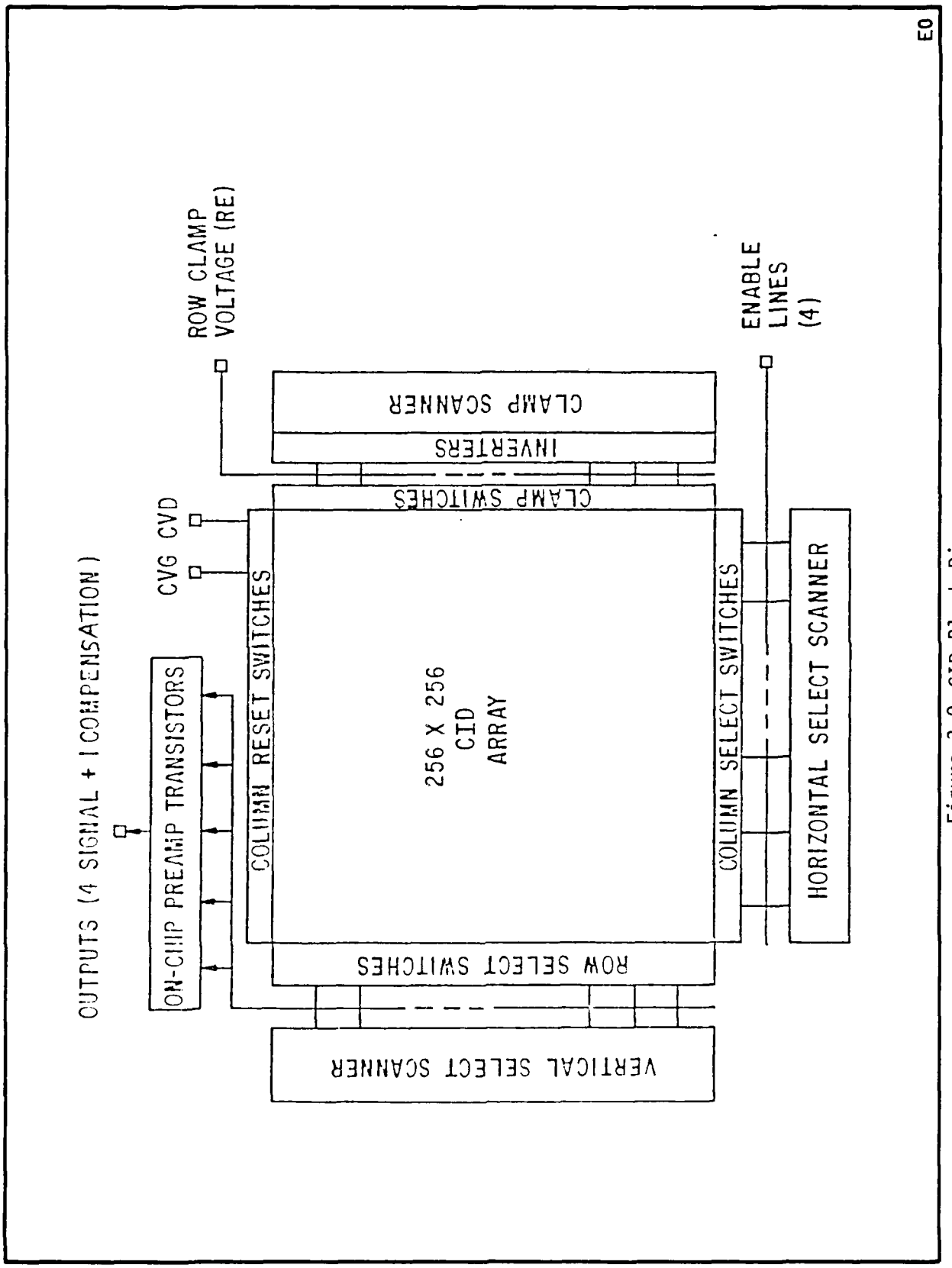

Figure 3-9 CID Block Diagram

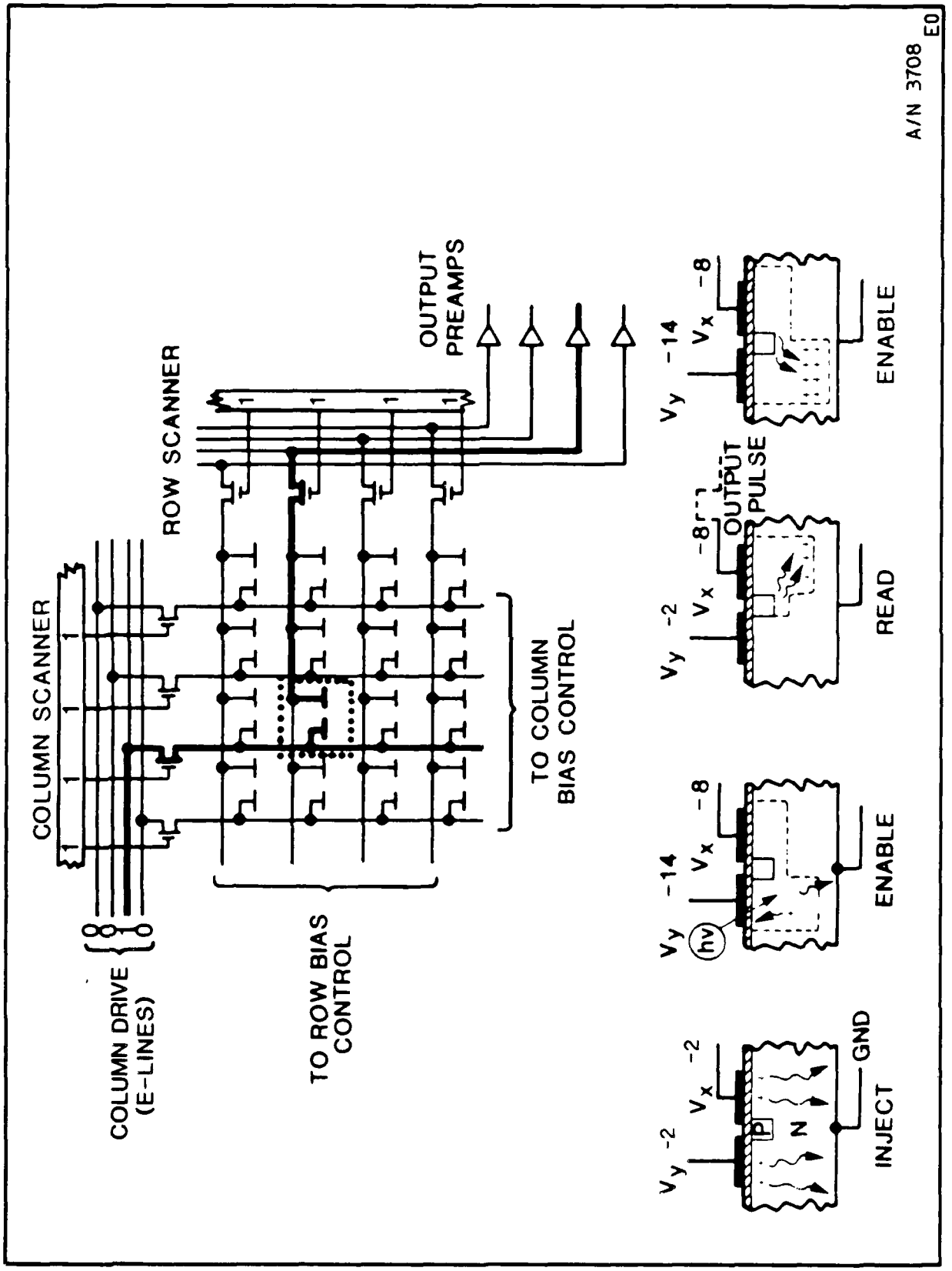

Figure 3-10 Detector Schematic and Addressing Scheme

A typical readout sequence is:

1. The column and row biases are brought to -2V to clear the entire array of stored charges by injection.

2. The row bias is set to -8V, and the column bias is set to -14V for a read enable. The column potential "well," shown in Figure 3-10, stores the photon-generated minority carriers.

3. Column and row biases are floated, and the column is brought to -2V through the E-lines. The collected charge is transferred to the row capacitor, and the displacement current causes a proportional row potential change that is sampled and held for processing.

4. Returning the column bias to -14V and the row bias to -8V transfers the charge back to the column capacitor, and another read cycle can begin.

The accumulated charge is not lost, and repeating the read process would produce the same output, with the signal that had been collected during the first read period added to it. After the desired number of readings has been taken, the charge is injected into the substrate, and the whole process is repeated. A CID schematic diagram is shown in Figure 3-11. Performance parameters for the detectors used on this program are included in Section 6.

3.3.3 Focal Plane Electronics

The focal plane signal conditioning electronics include:

- Preamplifier,
- Restore,
- Sample and hold,
- Multiplexer,
- Buffer,
- Comparator,

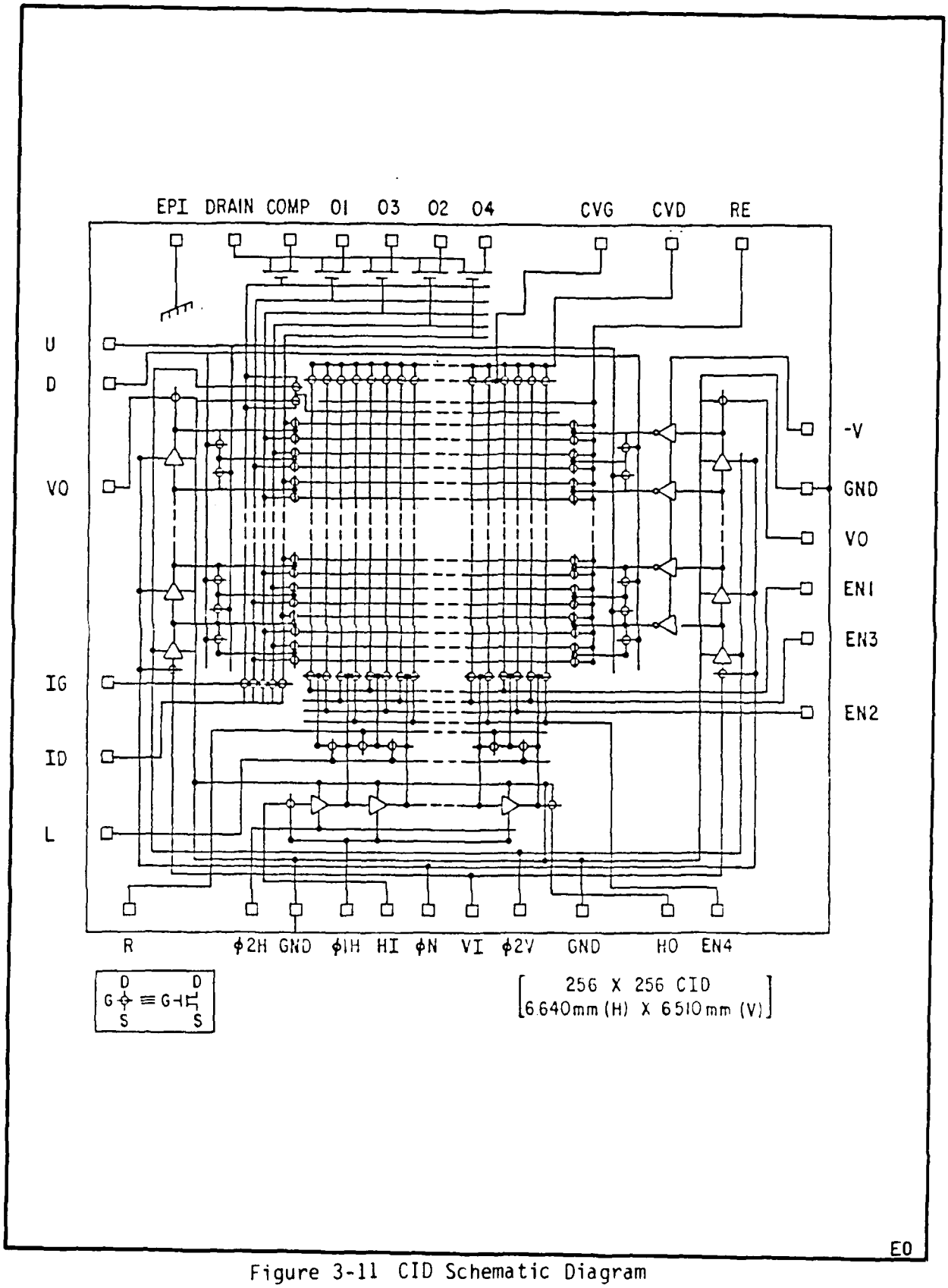

Figure 3-11 CID Schematic Diagram

- Successive approximation register,
- Analog-to-digital (A/D) converter, and
- Reference voltage.

The four CID analog channel signals are passed through a corresponding preamplifier circuit for amplification. Once the signals are amplified, they are restored and then sampled. After the four channel signals are sampled and their values held, each channel signal is selected for further processing. Channel selection is accomplished using a multiplexer. Table 3-7 shows the multiplexer levels required for this task. Once the channel signal is selected, it is buffered and then converted to digital form by an A/D converter. The analog CID signals are digitized to a usable 12-bit form for the microprocessor.

Table 3-7
CHANNEL SELECTION

MUX2	MUX1	CHANNEL
0	0	1
0	1	2
1	0	3
1	1	4

A photograph and schematic diagram of the focal plane electronics are presented in Figures 3-12 and 3-13, respectively. Figure 3-14 is a timing diagram of one sampling cycle.

3.3.4 Preamplifier

The four analog channel signals from the CID are directly connected to their own preamplifier circuit. Since the CID signals have a very low voltage range (millivolts) and are very sensitive, it is desirable to use high accuracy components for the amplification stage. The operational amplifiers used in the preamplifier circuit were chosen for their high accuracy, low input offsets, high direct current gain, high common-mode rejection ratio (CMRR), and low noise characteristics. The operational amplifiers were also chosen for their resistance to radiation effects.

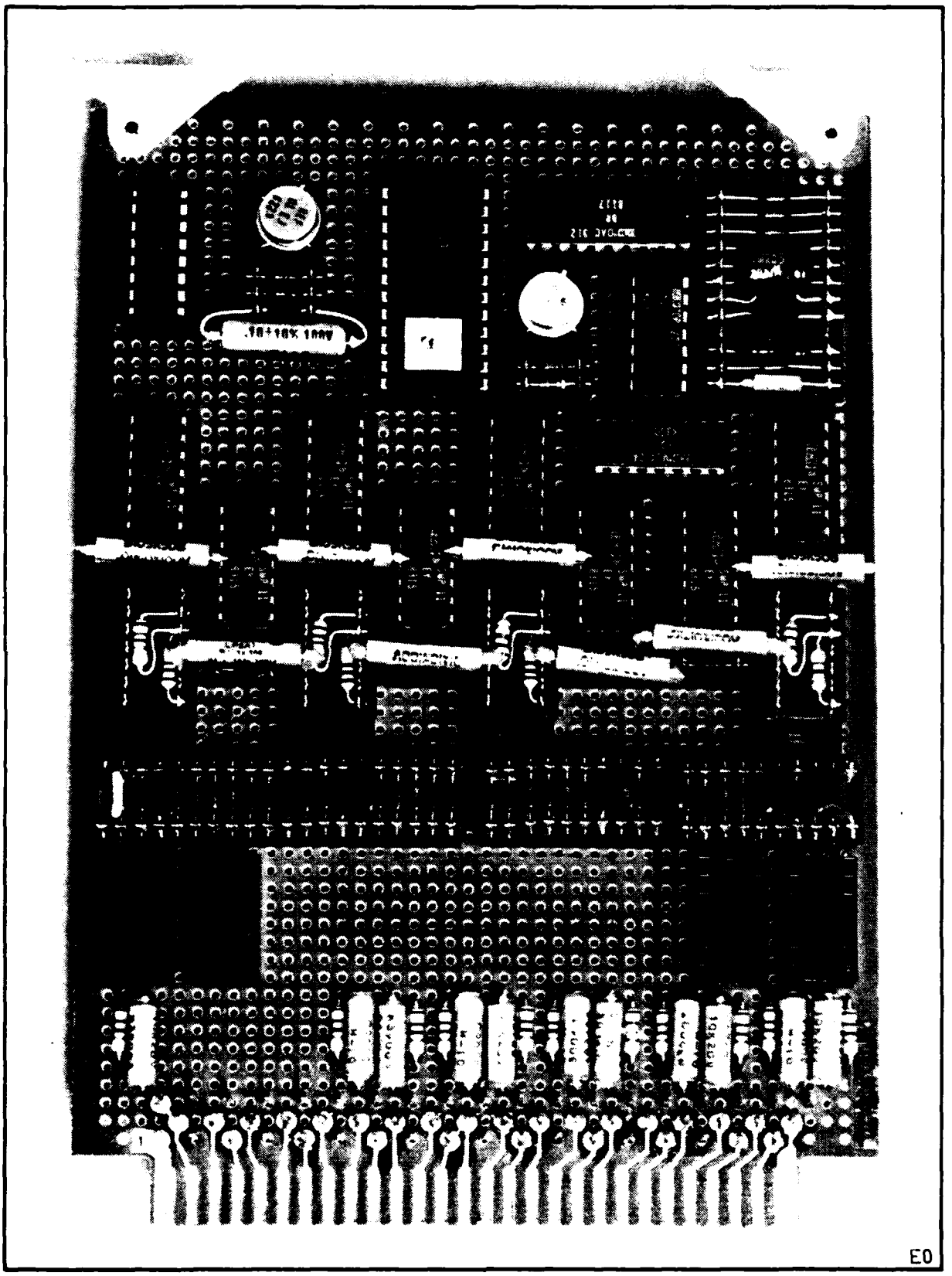

Figure 3-12 Focal Plane Electronics Breadboard

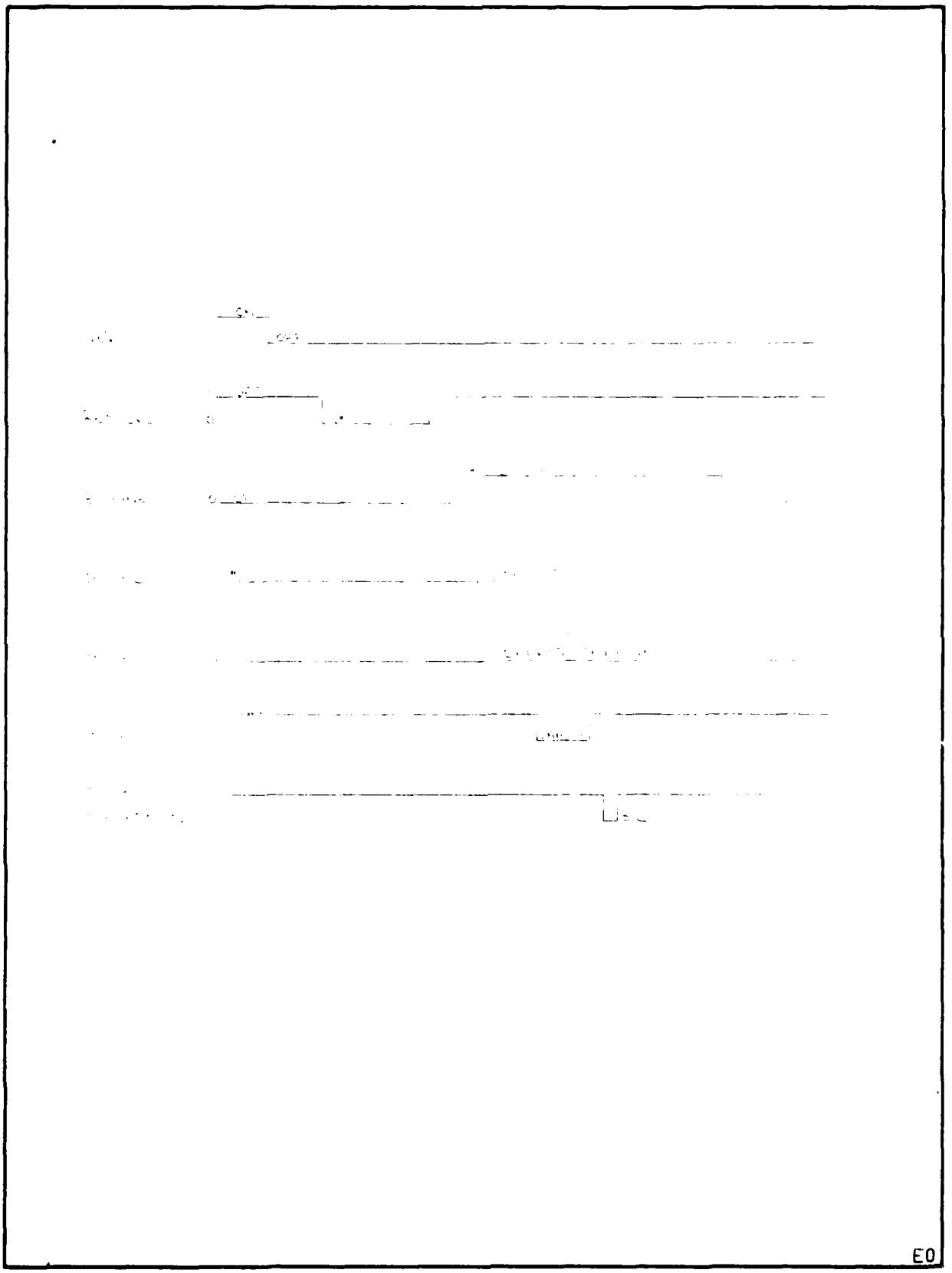

Figure 3-14 Focal Plane Electronics Timing Diagram

The preamplifier circuit has two stages: the first stage has a gain of 10, and the second has a gain of 50. Between the two stages, the total gain of the circuit is 500. Amplification of the CID signals allows for a more reasonable signal value to be sampled for A/D conversion.

3.3.5 Restore

The restore circuit was designed to use the same integrated circuit (IC) as that of the sample-and-hold (S/H) circuit and has a noninverting unity gain.

The amplified CID analog signal from the preamplifier output is held at the hold capacitor input. A reference voltage level is applied to the input of the restore circuit.

When the circuit is not in the restore state, the output is essentially the amplified CID analog signal applied at the hold capacitor input. When the circuit is at the restore state, the output is the amplified CID analog signal shifted by the reference voltage level.

Restore is implemented by applying a logic "0" at the S/H control input of the IC. A logic "1" corresponds to a nonrestore state.

3.3.6 Sample-and-Hold

The four restore output signals are sampled upon entering a logic "0" at the control inputs of the S/H circuits. The restore signals are continuously tracked during the sample mode. After the signals are sampled, they are held by changing the control input to a logic "1".

The IC used in the S/H portion of the focal plane electronics is the SMP-11 manufactured by Precision Monolithics, Inc. The SMP-11 is a precision S/H amplifier with high accuracy, low droop rate, and a fast acquisition time, all needed for data acquisition and signal processing. These amplifiers have noninverting unity gain and two high-input impedance buffer amplifiers connected by a diode bridge switch. Bipolar Darlington circuits and an ion implant

process that creates "super beta" transistors provide the high-input impedance and low droop rates of the SMP-11.

A transconductance, or "super charger," circuit is also part of the SMP-11. It can provide up to 50 mA of charging current to the hold capacitor for smooth, fast charging with minimum noise. The current from the diode bridge controls the settling time of the hold capacitor's final voltage, thus minimizing overshoot and instability.

3.3.7 Level Shifter and Low-Noise Regulators

The CID requires several different voltage levels for proper operation. These voltage levels are -2V, -8V, -14V, -17V, and -20V. All voltages except the -20V are produced by voltage regulators on the breadboard. The -20V is obtained directly from the star tracker power supply.

The voltage regulators are designed for low-noise applications, especially for the sensitivity of the CID. The level shifter breadboard is shown in Figures 3-15 and 3-16.

The D139 drivers are low-level to high-level voltage translators chosen for the following features:

- Inputs directly interface to TTL form,
- Outputs directly interface to field effect transistor (FET) analog switch control,
- Has 30V output swing,
- Has fast translation time (200 nsec maximum),
- Has high input impedance,
- Can drive into pure capacitive loads or moderate resistive loads, and
- Has wide flexibility in actual output voltage levels.

Because of the current source coupling between the input and output and the split power supplies, there is a wide range in the output voltage levels.

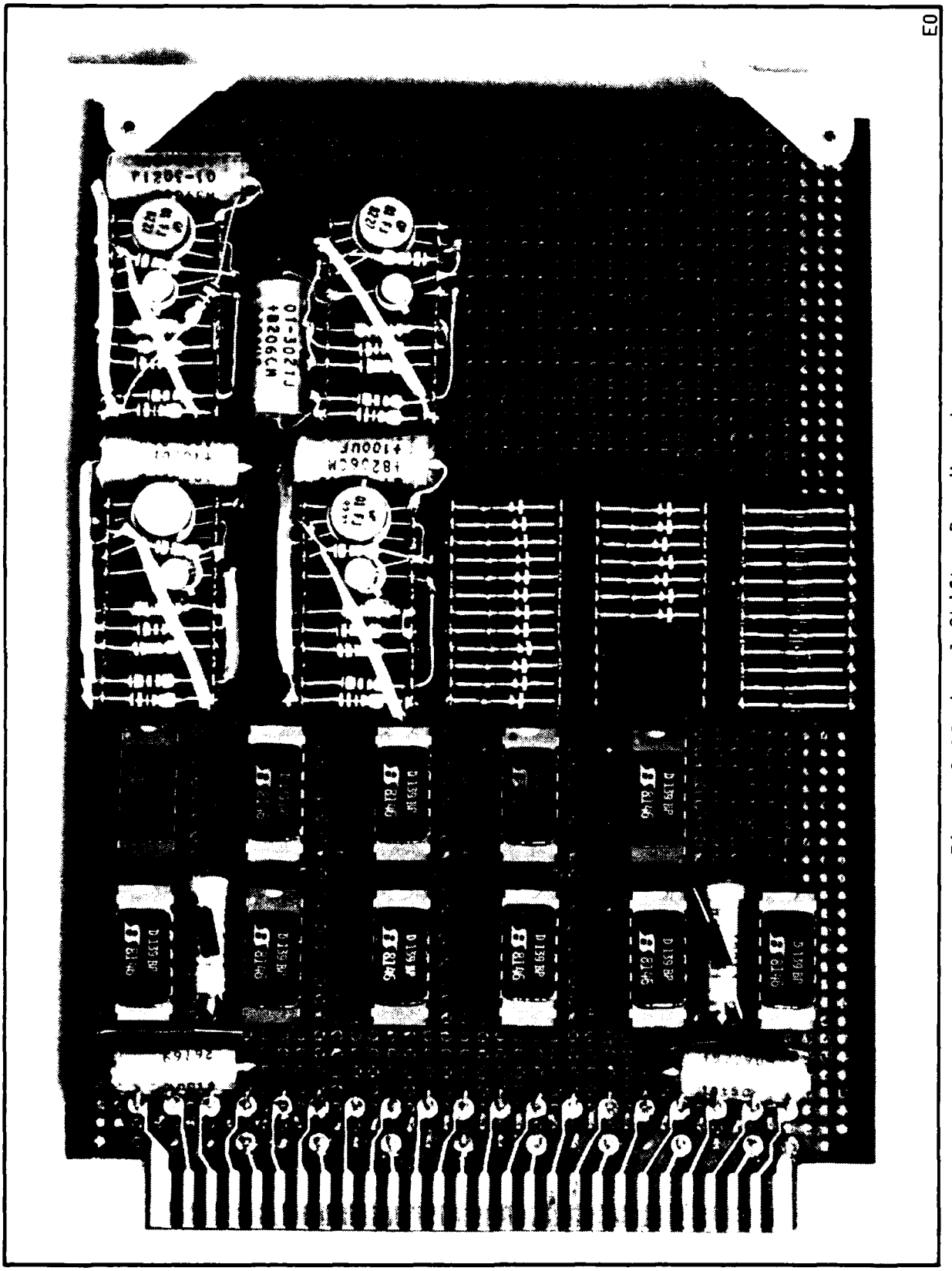

Figure 3-15 Level Shifter Breadboard

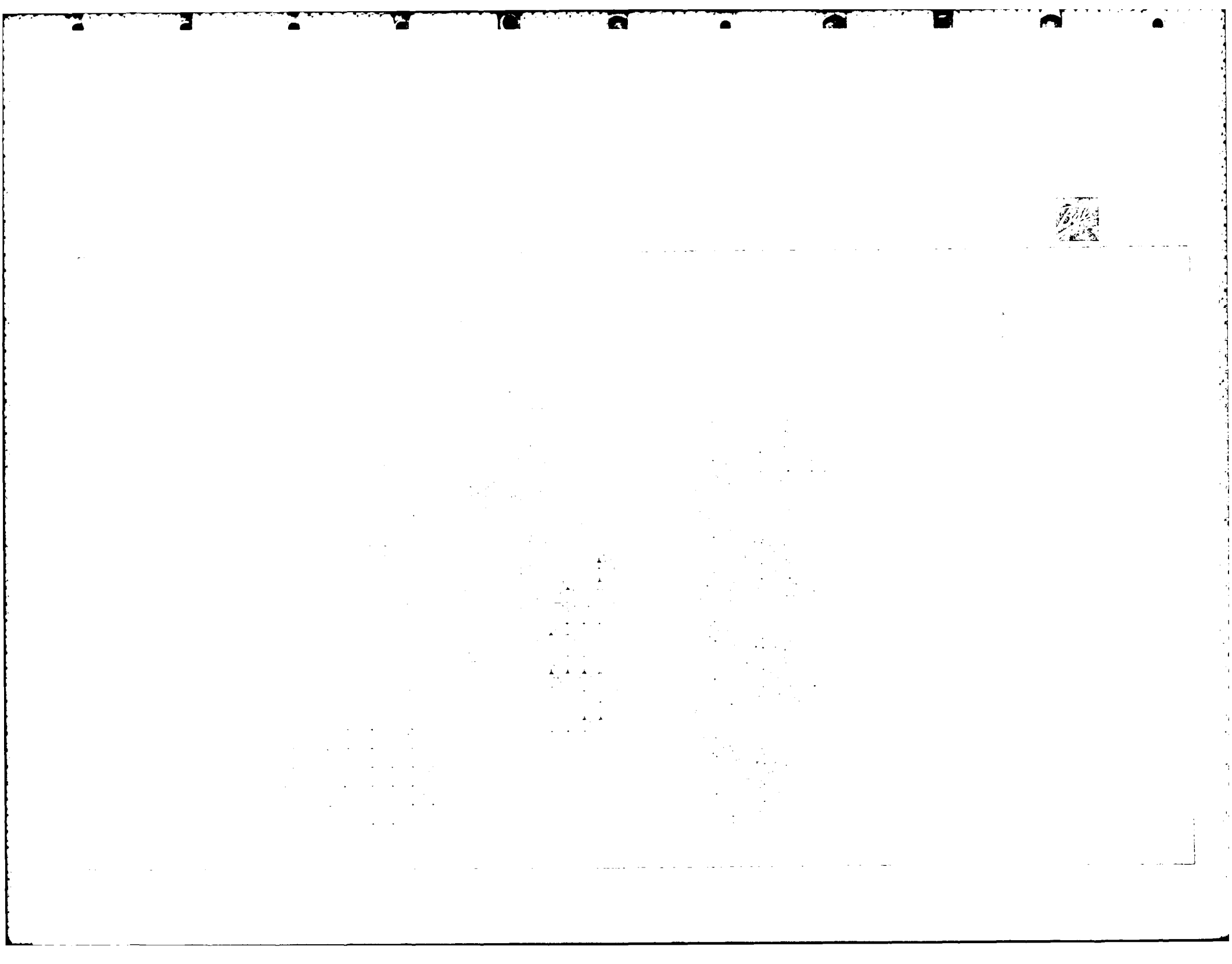

The D139 drivers have complementary outputs; thus, a logic "1" at the input provides a "1" at OUT, and a "0" at $\overline{OUT}$.

Table 3-8 lists the CID signals and their shifted voltage levels.

Table 3-8

CID LEVEL SHIFTER SIGNALS

FUNCTION	HI ("1")	LO ("0")
E1	-2V	-14V
E2	-2V	-14V
E3	-2V	-14V
E4	-2V	-14V
VIN	-17V	0V
HIN	-17V	0V
U	0V	-20V
D	-20V	0V
L	0V	-20V
R	-20V	0V
VØ1	-17V	0V
VØ2	-17V	0V
HØ1	-17V	0V
HØ2	-17V	0V
CVG	-20V	0V
IG	-14V	0V
ID	-2V	-8V
RVD	-2V	-8V
CVD	-2V	-14V

3.3.8 Microprocessor and Support

The microprocessor is a model SA3000, manufactured by Sandia National Laboratories. It is a CMOS radiation-hardened version of the 8085 microprocessor.

The microprocessor electronics are designed for low power usage. The overall design is simplistic and allows for high-density packaging.

The SA3001 I/O ports, also manufactured by Sandia, are radiation hardened. These components include:

- Two 8-bit I/O ports and one 6-bit port,
- 2048-bit static CMOS RAM organized as 256 X 8, and
- 14-bit timer-counter.

The I/O section of the SA3001 contains five registers:

- **Command/Status (C/S) Register.** The same address is assigned to both registers.

- **PA Register.** This 8-bit register can be either an input or an output port.

- **PB Register.** This 8-bit register is functionally the same as the PA register.

- **PC Register.** This register has 6 bits and can be programmed to be an input or output port, or to control signals for the PA and PB registers.

The output of the SA3001 is glitch-free. That is, when a "1" is written to a bit position that was previously a "1," the level at the output pin remains the same.

When the port enters the input mode, the output latch is cleared. Results are unpredictable when reading from an input port with nothing connected to the pins.

Use of the SA3001 provides a smaller parts count. Several more components would have been required to perform the same function as the SA3001. Table 3-9 is an I/O port definition.

Table 3-9

I/O PORT DEFINITION

PORT NO.	TYPE	D7	D6	D5	D4	D3	D2	D1	D0
81H	Output	E4	E3	E2	E1	Spare	Spare	MUX2	MUX1
82H	Output	L/R	U/D	HIN	VIN	Spare	Spare	Spare	Spare
83H	Output			Spare	Spare	HØ2	HØ1	VØ2	VØ1
89H	Input	A/D7	A/D6	A/D5	A/D4	A/D3	A/D2	A/D1	A/D0
8AH	Input	0	0	0	0	A/D11	A/D10	A/D9	A/D8
8BH	Input			Spare	Spare	Spare	Spare	I/O TEST	CMD FLAG
91H	Input	CMD7	CMD6	CMD5	CMD4	CMD3	CMD2	CMD1	CMD0
92H	Output	I/O TEST S/H	RES	CVD	RVD	ID	IG	CVG	Spare
93H	Output			WATCH DOG	CMD S.R. CLEAR	CMD ACK	DATA FLAG	DATA CLK	DATA

The driver and receiver components are bipolar differential parts that provide serial I/O data from and to the ports. The commands are received by a shift register and are put into the appropriate port.

Except for the memory components, all ICs are LSTTL form for simplicity of design and for low power consumption.

To protect against radiation exposure (upsets), current limiting resistors are used. Transorbs are used for the I/O lines to eliminate EMI that could couple into the circuitry. Terminating resistors are also incorporated into the input lines for impedance matching to reduce oscillation.

Figures 3-17 and 3-18 show the microprocessor breadboard. Included on this breadboard are the memory chips and the watchdog circuit described below.

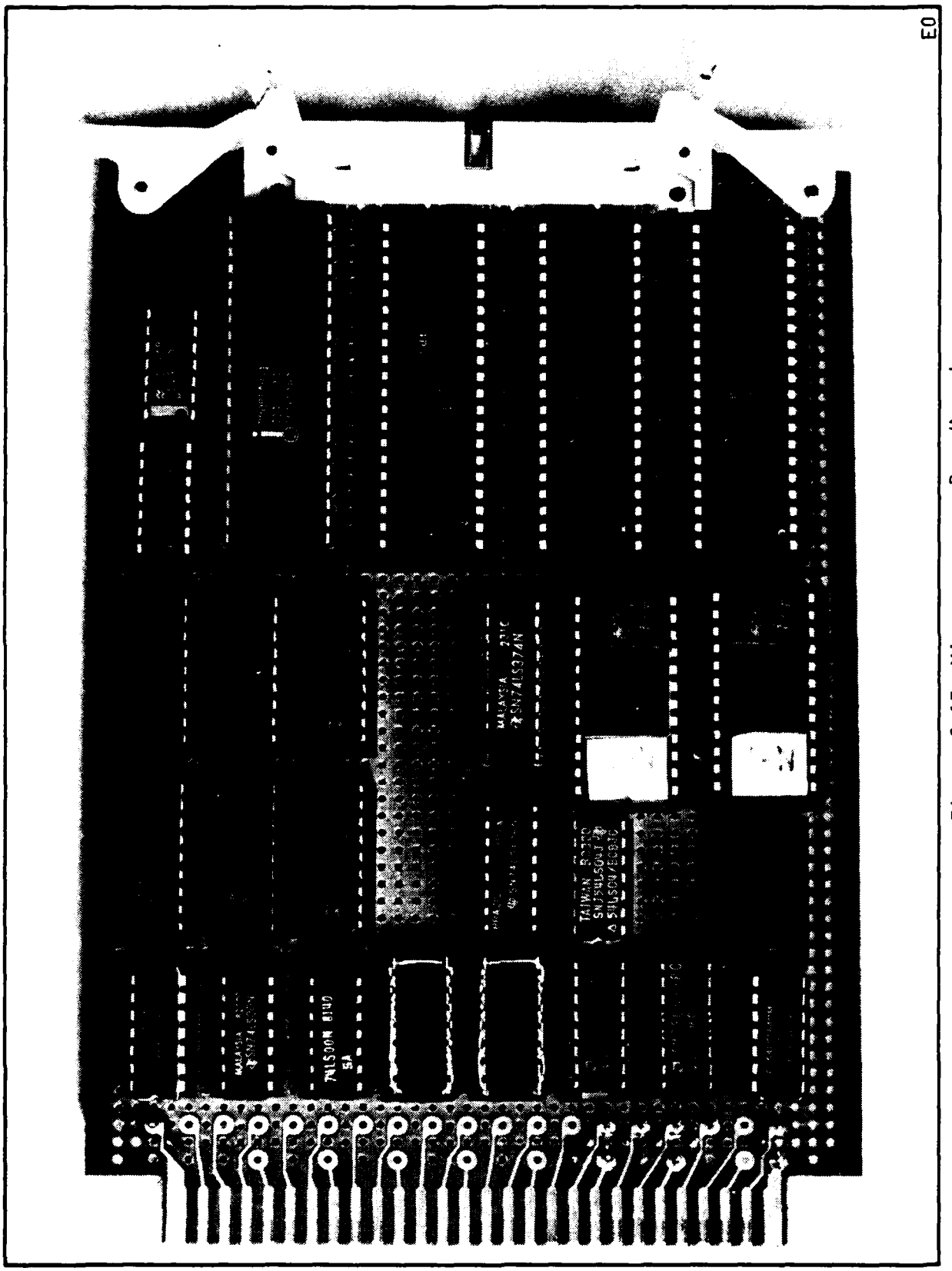

Figure 3-17 Microprocessor Breadboard

3.3.9 Memory

The memory parts are CMOS components. Bipolar fuse-linked PROMs are used to store the tracker program. The board is designed to use 16 kbytes of PROM and 4 kbytes of RAM.

Table 3-10 is a memory map for the star tracker.

Table 3-10
MEMORY MAP

ADDRESS (Hex)	
9000 - 90FF	256 x 8 RAM (I/O port)
8800 - 88FF	256 x 8 RAM (I/O port)
8000 - 80FF	256 x 8 RAM (I/O port)
4C00 - 4FFF	RAM
4800 - 4BFF	RAM
4400 - 47FF	RAM
4000 - 43FF	RAM
2000 - 3FFF	PROM
0000 - 1FFF	PROM

3.3.10 Watchdog Circuit

The watchdog circuit allows recovery from radiation upsets. It is a continuous, self-oscillating, resettable one-shot multivibrator in a closed loop.

The watchdog circuit must be reset approximately every 1.5 sec. If it is not reset, a time-out occurs, and the program counter is set to zero to restart the star tracker program.

3.3.11 Power Supply

The power supply shown in Figure 3-19 incorporates a fairly simple design concept that allows for stability, efficiency, and reliability.

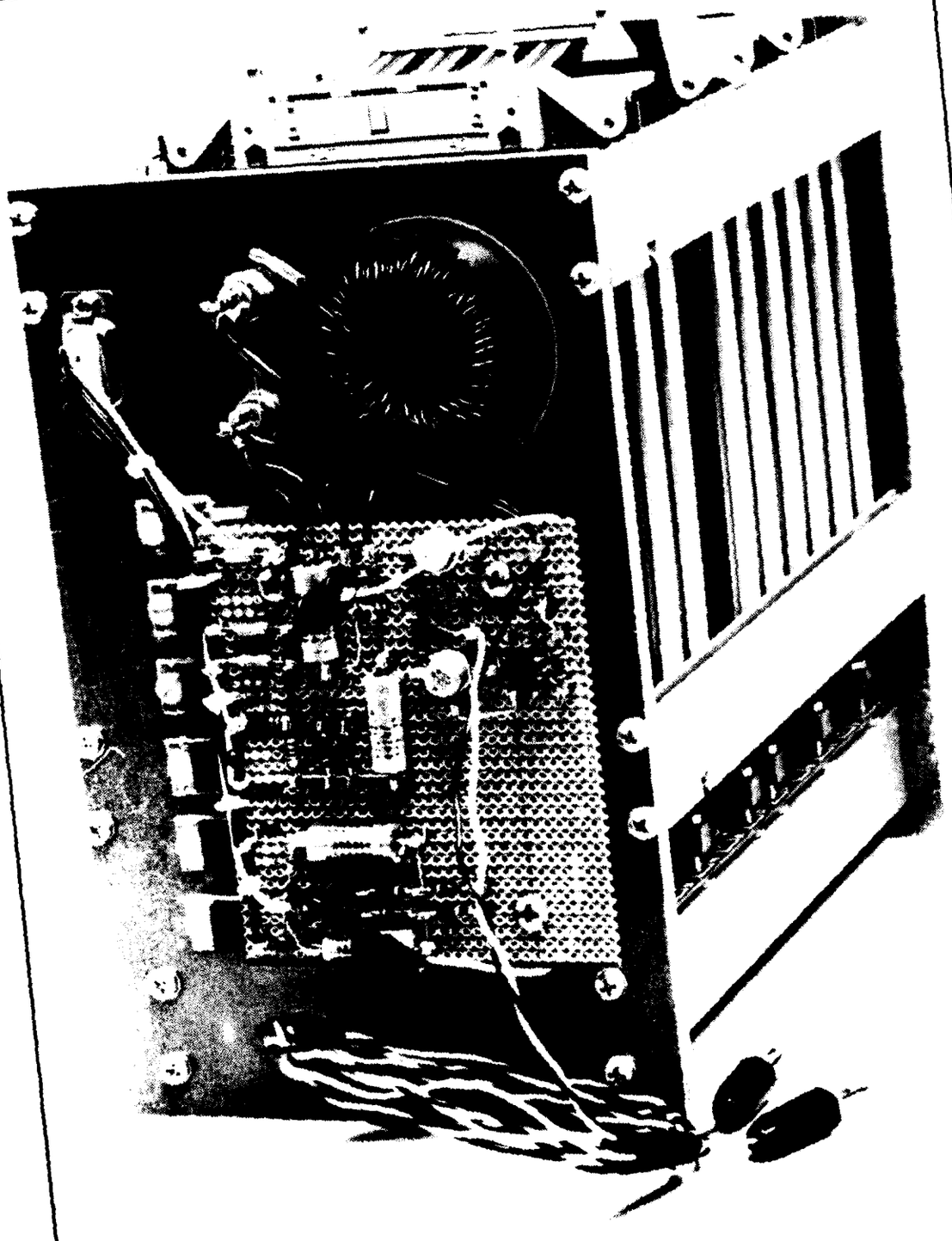

Figure 3-19 Power Supply Breadboard

A +28 Vdc power supply is used to produce +15V, -15V, -20V, and +5V to operate the star tracker. To obtain these voltages, the series uA7800 positive-voltage regulators and the series uA7900 negative-voltage regulators are used. These regulators are of bipolar construction and were chosen for the following reasons:

- Linear regulation,
- Elimination of noise distribution problems associated with single-point regulation,
- Delivery of up to 1.5A of output current, and
- Immunity to overload because of the internal short-circuit current limiting and thermal shutdown features.

Darlington amplifiers are incorporated into the design of this power supply. These transistor configurations are used because of their high-input impedance and to prevent β degradation during radiation exposure. Also, the currents through the transistors can be set independent of each other by adjusting the emitter resistors (1 kΩ) of the 2N2219A transistors.

An EMI filter circuit is included in the design of the power supply (Figure 3-20) for protection against external noise sources. It also prevents power supply noise from leaving the star tracker.

Section 4
SOFTWARE DESIGN

Section 4
SOFTWARE DESIGN

BASD has implemented software programs for radiation test purposes. These programs allow for evaluation of star tracker operation before, during, and after exposure to the radiation environment.

The tracking program uses basic concepts developed on previous BASD programs. Features included in this software are:

- Acquisition and tracking of one moving or stationary target (star);
- Spiral acquisition for the full field of view;
- Breaking track and continuing acquisition on command from the command computer starting from the point of the last acquisition; and
- Outputting data to the command computer.

A program that allows a 1 x 4 block of pixels to be read at the center of the CID array has also been implemented. This program is used to obtain single pixel data and provides a way to check the basic operations of the star tracker electronics. The program performs the following tasks:

- Reads pixels 128,128; 128,129; 128,130; 128,131;
- Drives one E-line (E4);
- Performs one correlated double sample (CDS); and
- Outputs data to the command computer.

To check the A/D readout, a simple test program was developed that performs the following functions using a terminal:

- Sends a restore pulse and a sample pulse to the appropriate circuitry;

- Reads all four channels from the CID to the A/D converter; and

- Prints HEX values from the four channels and displays the values on a terminal using the MCG program, which is a monitor program used for test purposes.

Another simple test program was developed to check RAM and features the following functions using a terminal:

- Reads memory to determine starting and stopping addresses and tests memory between those locations;
- Writes "0" and "1" to each memory location and, after each write, verifies the value;
- Ends the program when all memory is checked or when a memory location fails the test;
- Displays the address of that location on the terminal if a memory location fails the test;
- Displays zeros on the terminal if all memory passes the test; and
- Returns to the MCG program after memory test has been completed.

Section 5
PRELIMINARY RADIATION TESTS

Section 5
PRELIMINARY RADIATION TESTS

5.1 BREADBOARD TESTS

The following breadboard circuits were taken to the NRL linear electron accelerator (LINAC) facility for preliminary radiation testing. All tests were done in the electron beam.

5.1.1 Signal Channel Processor

Normally, the signal processing circuits for CID readout consist of four channels. One channel with an A/D converter was assembled. It was driven by microprocessor test equipment for a correlated double-sample readout. The circuit performance was monitored at a CRT terminal; signal and noise were remotely observed.

5.1.2 Level Shifters and Low-Noise Regulators

All the low-noise regulators and two level shifter circuits were tested as a unit. The circuit was driven with a pulse generator to simulate operation.

5.1.3 Power Supply

The complete star tracker power supply with linear regulators and simulated loads was tested as a unit. The unit was operated with a +28V input. Direct current output voltages were monitored with an oscilloscope and a digital voltmeter.

5.1.4 Microprocessor

At the time of this testing, the SA3000 was not available. However, the F9445 was still being considered, and was tested as a single-board computer. A short program was executed to produce numeric operations that were displayed on a CRT terminal.

5.2 RADIATION TESTS

In general, radiation tests were conducted in a manner consistent with the operation of the LINAC machine. The breadboards were set up at the LINAC waveguide output with metal plates between the board and source to diverge the beam. Thermal luminescent dosimeters (TLD) were placed at five locations on the board to measure dose levels. Calibration showed reasonably even coverage of the entire board.

Radiation was applied at a low duty cycle, high rad/sec rate, i.e., pulses. The pulses were counted to determine dose, after calibration was known. Initially, small doses were accumulated, and the circuits were observed for function. Large numbers of microsecond pulses at approximately 10^7 rad each were generated to achieve greater than 10^5 rad. Table 5-1 summarizes the applied dose test results.

Table 5-1
SUMMARY OF DOSE TESTS

TEST	DOSE
Signal Channel Processor	140 krad
Level Shifter/Low-Noise Regulators	202 krad
Power Supply	999.6 krad
Microprocessor	10.9 krad*

*LINAC down; could not complete test.

5.3 CIRCUIT PERFORMANCE RESULTS

High-level performance data were taken before and after the radiation test, and circuit operation was observed during radiation.

The power supply showed no significant change after radiation. All the voltage regulators were within 10 mV of original settings. There were transients on the regulators when radiation pulses occurred.

The level shifters and low-noise regulators showed no measurable signs of change. Levels and rise times were well within limits.

The F9445 microprocessor was tested, as a part, using a small beam. It was on a board with many nonhardened parts. The only problem observed was upsets when the pulse hit. No conclusion was drawn about this since it was not designed for single-event upsets. The part did survive 10^4 rad, which was the dose when the LINAC failed. The microprocessor always functioned after resets.

Performance of the signal channel was most encouraging. At 80 krad it failed to function. Investigation revealed that the preamplifier bias resistors were too large, and the increase in bias current due to radiation caused saturation. A change of the values by a factor of 10 restored operation. No other parts were changed, and the test was resumed. At the end of the test, all circuits were functioning normally after greater than 10^5 rad. A detailed postradiation test revealed less than 10 mV changes in some amplifier circuits. This is of little consequence because of the differential technique used to read CID pixel values.

Section 6
CID CHARACTERIZATION RADIATION TESTS

Section 6
CID CHARACTERIZATION AND RADIATION TESTS

6.1 CHARACTERIZATION

This section contains ST-256E CID characterization data furnished by General Electric. Of the five detectors purchased from GE, only two (SB10-7-1 and SB10-7-8) were fully characterized. Table 6-1 summarizes the results of the characterization testing.

Table 6-1
ST-256E CHIP CHARACTERIZATION*

PARAMETER	SB10-7-1	SB10-7-8
Dark current (Na/cm^2)	4.557	4.926
Fixed Pattern Noise (Ke^-)	15.14	11.58
Readout Noise (e^-)	570	523
Pixel-to-Pixel Variation in Response (%)	6.95 (5,22 to 64,56)	4.5 (5,193 to 64,236)
Pixel-to-Pixel Dark Current Variation (Na/cm^2)	2.28	2.18
Full Well (Me^-)	1.081	1.079

*Except where noted, pre-radiation data were taken from 1,1 to 248,248 (row, column).

The CID response (A/W) at the pixel or SB10-7-1 is shown in Table 6-2, and Figure 6-1 shows the spectral response curve. Table 6-3 presents the CID response data for SB10-7-8, and Figure 6-2 shows the spectral response curve.

Table 6-2

CID RESPONSE AT THE PIXEL

SB10-7-1

(6/17/85)

CVDL: -1.600V	Full Well: 1.404V
CVDH: -17.00V	Dark Current: 74.0 mV/544.0 mS
RVDL: -2.100V	Backbias: -11.60V
RVDH: -10.60V	Ambient Dark Current: 61.00 mV/217.0 mS
Signal Cap.: 6,800 pf	Readout Efficiency: 1.000

W.L. (MIC)	DV (MV)	DT (MS)	SIGNAL C*V/T (NA)	SIGNAL I-SIG (NA)	REF. DIODE I (NA)	REF. DIODE RES (A/W)	OPT. POWER (NW)	CID RESP. (A/W)	Q.Y.
DARK	61.0	217.0	1.91	--	0.0	--	--	--	--
0.35	141.0	108.3	8.9	6.9	6.0	17.0	102	0.06819	0.242
0.40	194.0	21.6	61.1	59.2	33.0	13.5	447	0.13238	0.411
0.45	183.0	5.4	230.4	228.5	157.0	9.63	1512	0.15117	0.417
0.50	153.0	2.2	477.2	475.3	359.0	7.66	2750	0.17285	0.429
0.55	144.0	1.1	898.3	896.4	820.5	6.49	5329	0.16821	0.380
0.60	190.0	1.1	1185.0	1183.0	1087.5	5.82	6328	0.18701	0.387
0.65	97.0	0.5	1221.0	1220.0	1384.0	5.22	7219	0.16894	0.323
0.70	173.0	0.5	2179.0	2177.0	2465.0	4.81	11849	0.18369	0.326
0.75	112.0	0.5	1410.0	1408.0	2147.0	4.51	9689	0.14536	0.241
0.80	138.0	0.5	1738.0	1736.0	2819.0	4.29	12099	0.14347	0.223
0.85	115.0	0.5	1448.0	1446.0	3650.5	4.11	15011	0.09635	0.141
0.90	189.0	1.1	1179.0	1177.0	4057.5	3.88	15755	0.07472	0.103
0.95	197.00	2.2	614.5	612.6	3524.0	3.82	13448	0.04555	0.060
1.00	162.0	5.4	204.0	202.1	2133.5	4.27	9121	0.02216	0.028
1.05	180.0	10.8	113.3	111.4	1887.5	9.33	17620	0.00632	0.007
1.10	119.0	10.8	74.9	73.0	1419.0	30.2	42854	0.00170	0.002

PEAK RESP. (A/W)/NM	QUANTUM EFF. %	FULL WELL MQe	DARK CURRENT nA/cm^2	STAR CURRENT fA
0.1870 @ 600.	38.7178	1.081	4.557	177.1867

Integrated Resp. (0.4 to 1.1 microns) = 88.40

1,100 nm Resp. = 0.00170

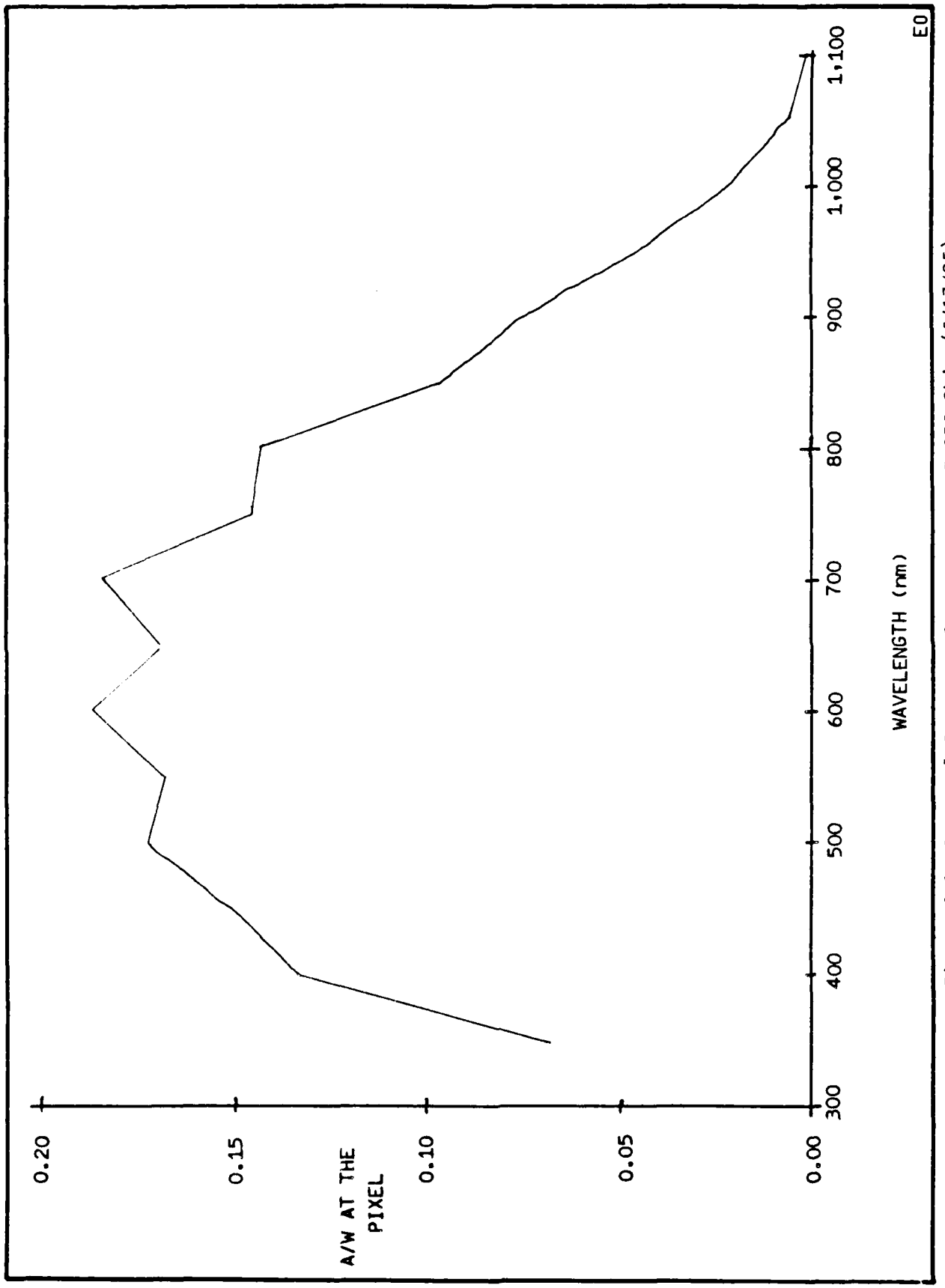

Figure 6-1 Spectral Response for SB10-7-1, ST-256 Chip (6/17/85)

Table 6-3
CID RESPONSE AT THE PIXEL
SB10-7-8
(6/17/85)

CVDL: -1.600V	Full Well: 1.401V
CVDH: -17.00V	Dark Current: 80.0 mV/544.0 mS
RVDL: -2.300V	Backbias: -11.90V
RVDH: -10.30V	Ambient Dark Current: 183.0 mV/544.0 mS
Signal Cap.: 6800 pf	Readout Efficiency: 1.000

W.L. (MIC)	DV (MV)	DT (MS)	SIGNAL C*V/T (NA)	SIGNAL I-SIG (NA)	REF. DIODE I (NA)	REF. DIODE RES (A/W)	OPT. POWER (NW)	CID RESP. (A/W)	Q.Y.
DARK	183.0	544.0	2.29	--	0.0	--	--	--	--
0.35	139.0	108.0	8.8	6.5	6.0	17.0	102	0.06350	0.225
0.40	186.0	21.6	58.6	56.3	31.5	13.5	427	0.13190	0.410
0.45	166.0	5.4	209.0	206.7	144.5	9.63	1391	0.14859	0.410
0.50	141.0	2.2	439.8	437.5	330.0	7.66	2528	0.17309	0.430
0.55	129.0	1.1	804.8	802.5	748.0	6.49	4858	0.16518	0.373
0.60	177.0	1.1	1104.0	1102.0	990.0	5.82	5761	0.19128	0.396
0.65	192.0	1.1	1198.0	1196.0	1259.5	5.22	6570	0.18198	0.348
0.70	127.0	0.5	1599.0	1597.0	2240.0	4.81	10768	0.14831	0.263
0.75	99.0	0.5	1247.0	1244.0	1953.0	4.51	8814	0.14118	0.234
0.80	101.0	0.5	1272.0	1270.0	2560.5	4.29	10990	0.11552	0.179
0.85	212.0	1.1	1323.0	1320.0	3099.0	4.11	12743	0.10361	0.151
0.90	175.0	1.1	1092.0	1089.0	3694.0	3.88	14344	0.07595	0.105
0.95	179.0	2.2	558.3	556.1	3197.5	3.82	12202	0.04557	0.060
1.00	162.0	5.4	204.0	201.7	1974.5	4.27	8441	0.02390	0.030
1.05	171.0	10.8	107.7	105.4	1700.5	9.33	15874	0.00664	0.008
1.10	115.0	10.8	72.4	70.1	1276.5	30.2	38550	0.00182	0.002

PEAK RESP. (A/W)/NM	QUANTUM EFF. %	FULL WELL MQe	DARK CURRENT nA/cm^2	STAR CURRENT fA
0.1913 @ 600.	39.6027	1.079	4.926	172.4736

Integrated Resp. (0.4 to 1.1 microns) = 85.90

1,100 nm Resp. = 0.00182

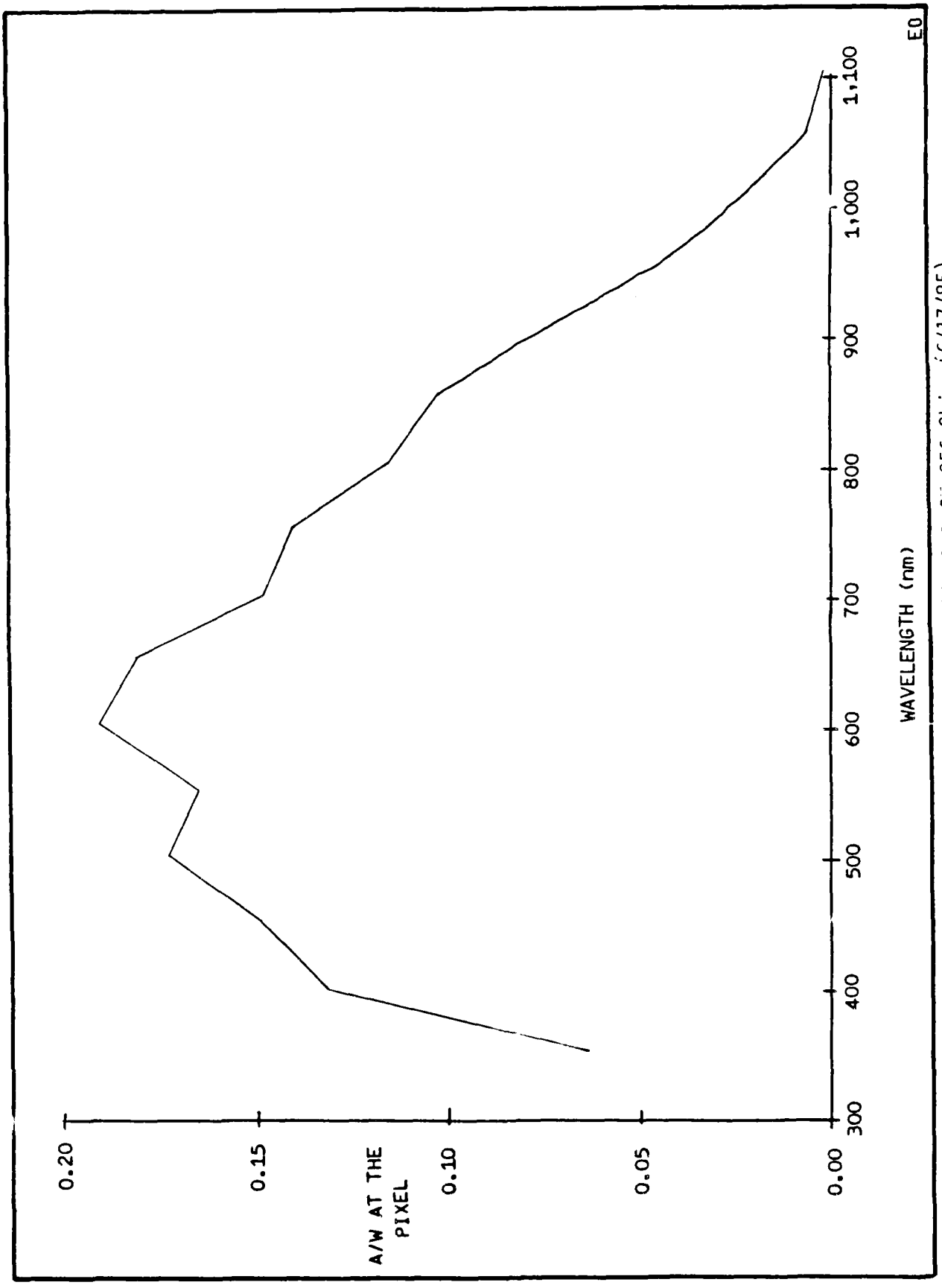

Figure 6-2 Spectral Response for SB10-7-8, Si-256 Chip (6/17/85)

6.2 CID RADIATION TESTING

Radiation testing was performed by GE on a sample of ST-256E CIDs. The results of this testing are shown in Table 6-4 and Table 6-5. Table 6-4 presents before and after radiation data for dark current and full well capacity. Table 6-5 shows the changes in the FET thresholds due to radiation exposure. The total dose of radiation was 10^6 rad.

According to the given data, after exposure to radiation, the dark current seems to increase approximately by a factor of 10, and the full well capacity decreases by half. The FET threshold more than doubles after radiation exposure.

Figures 6-3 through 6-7 show the CID response at the pixel before and after radiation exposure. Figures 6-8 through 6-10 reflect the change in FET thresholds as total dose is accumulated.

Table 6-4

RADIATION (γ) TESTING OF ST-256E CHIPS (10/9/84)

CHIP NO.	PARAMETER	PRERADIATION	POSTRADIATION
5-4-2	Dark Current (Na/cm^2)	22.78	73.70
	Full Well (MQe)	0.978	0.434
5-5-2	Dark Current	12.06	93.13
	Full Well	0.981	0.444
5-6-1	Dark Current	8.04	77.72
	Full Well	0.839	0.466
5-6-2	Dark Current	8.375	9.916*
	Full Well	0.864	0.621
5-7-1	Dark Current	3.35	81.74
	Full Well	1.057	0.520

*Value given by G.E. is not consistent with the other values.

Table 6-5

RADIATION (γ) TESTING OF ST-256E FET THRESHOLDS (10/9/84)

	PRERADIATION THRESHOLD (V)				POSTRADIATION THRESHOLD (V)			
CID NO.	1	2	3	4	1	2	3	4
5-4-2	1.25	1.25	1.25	1.25	3.0	3.0	3.03	3.0
5-4-3	1.26	1.265	1.26	1.26	3.12	3.10	3.12	3.09
5-5-2	1.22	1.22	1.215	1.22	2.845	2.845	2.85	2.845
5-5-4	1.305	1.31	1.31	1.305	2.98	2.98	2.98	2.98
5-6-1	1.26	1.26	1.255	1.26	2.70	2.68	2.68	2.67
5-6-2	1.255	1.25	1.245	1.25	2.68	2.66	2.67	2.66
5-7-1	1.21	1.205	1.205	1.21	2.63	2.63	2.62	2.61

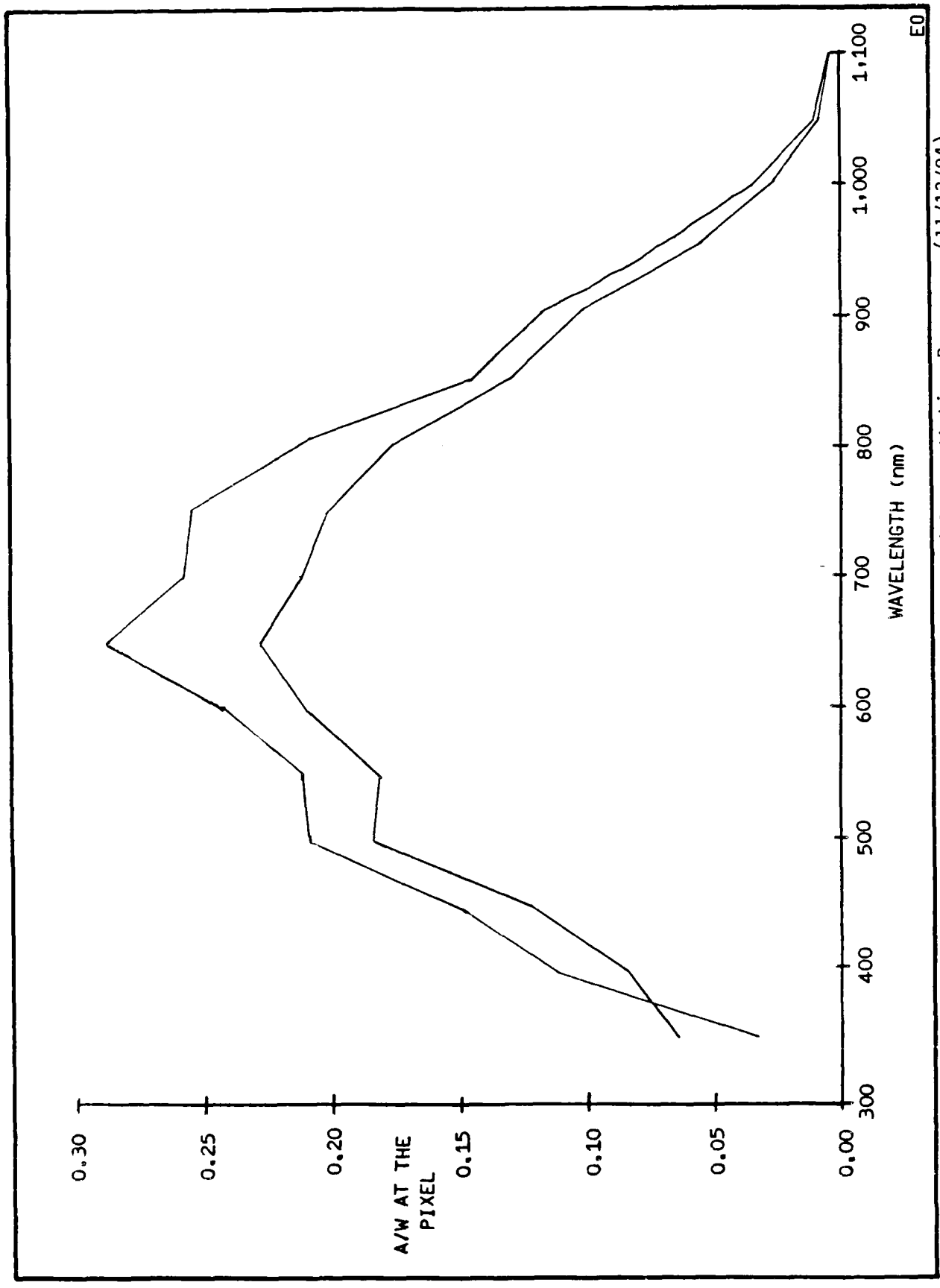

Figure 6-3 Spectral Response for STS-256 5-4-2 Pre- and Postradiation Response (11/13/84)

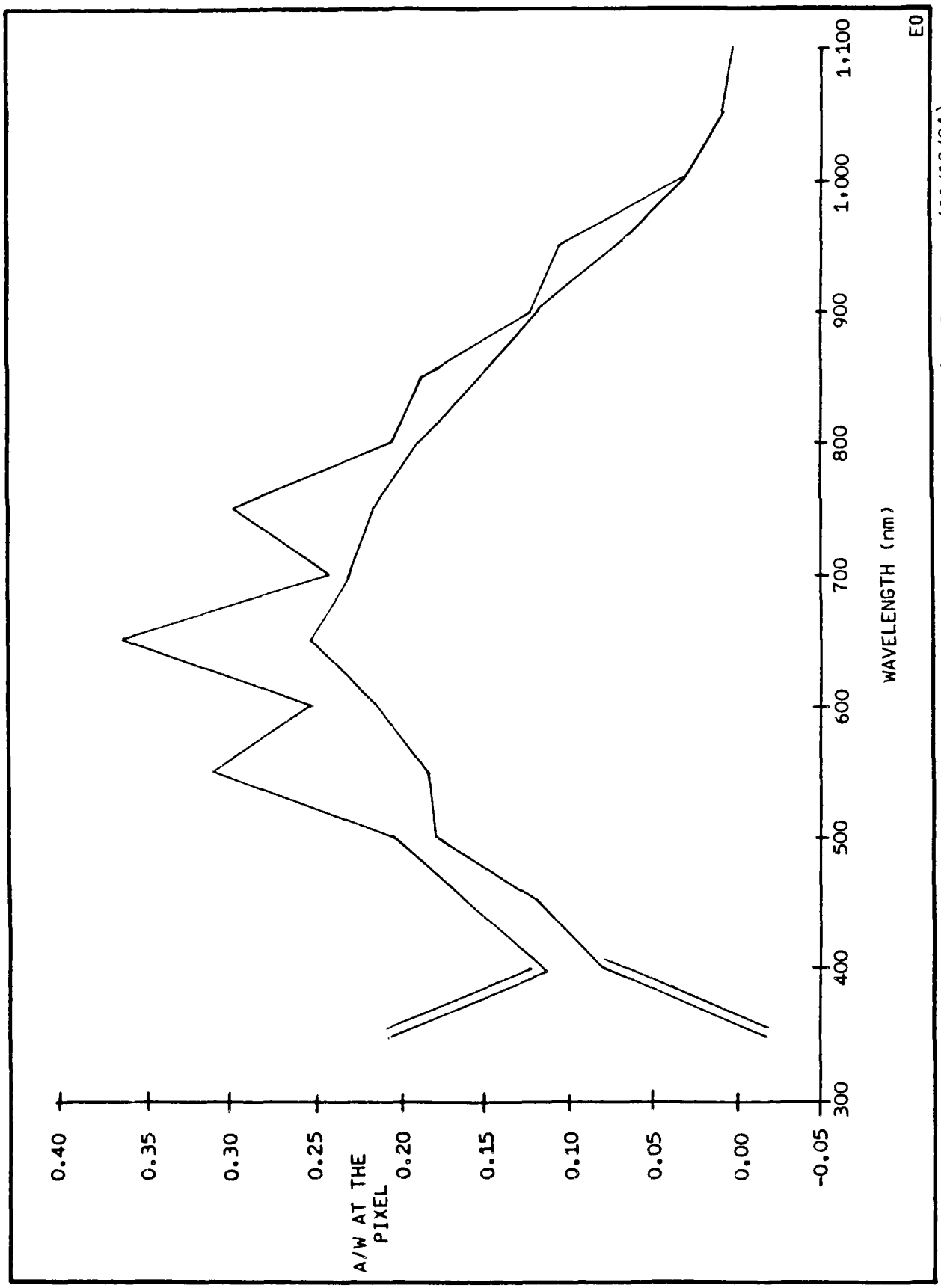

Figure 6-4 Spectral Response for STS-256 5-5-2, Pre- and Postradiation Response (11/13/84)

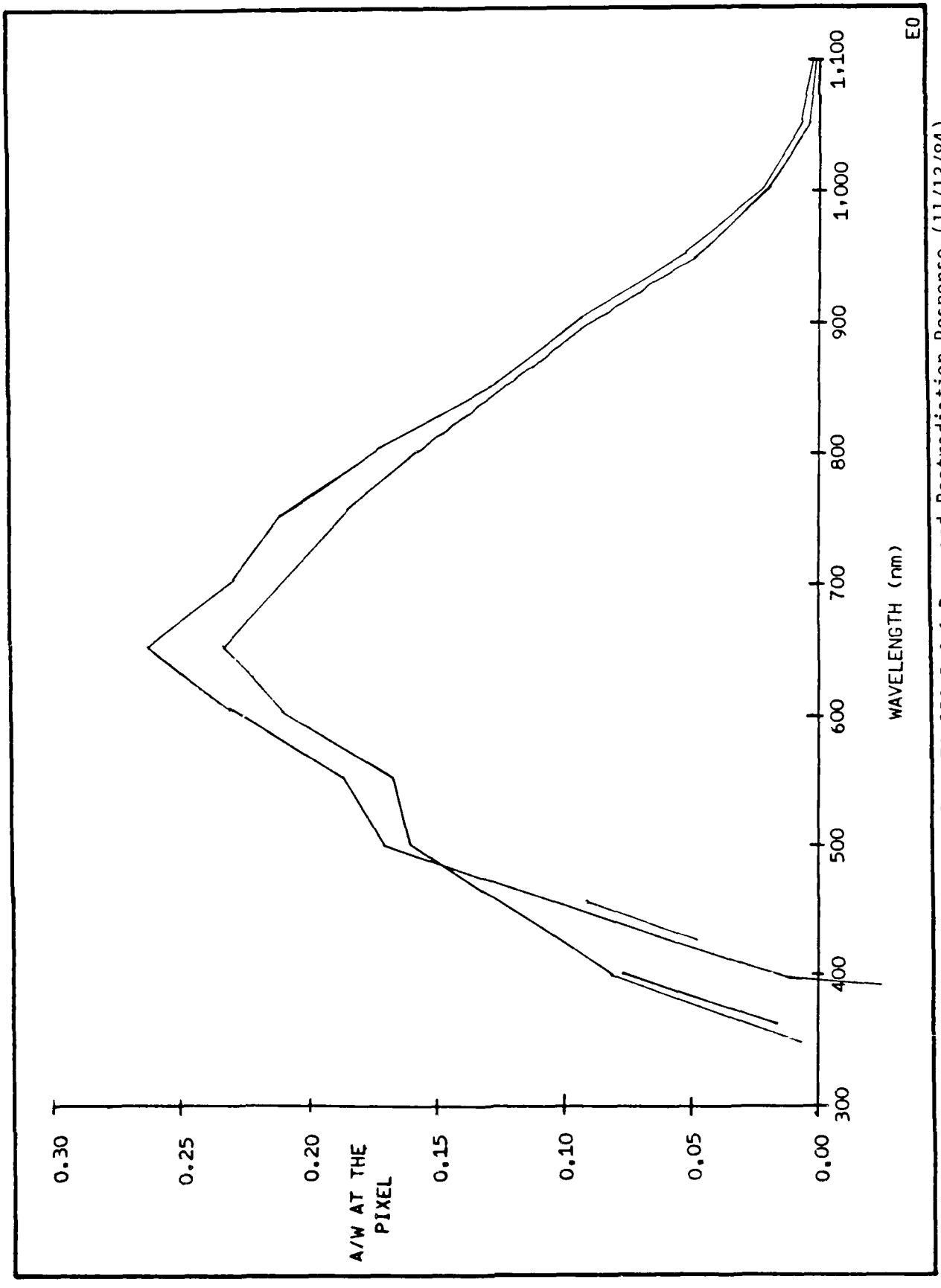

Figure 6-5 Spectral Response for STS-256 5-6-1, Pre- and Postradiation Response (11/13/84)

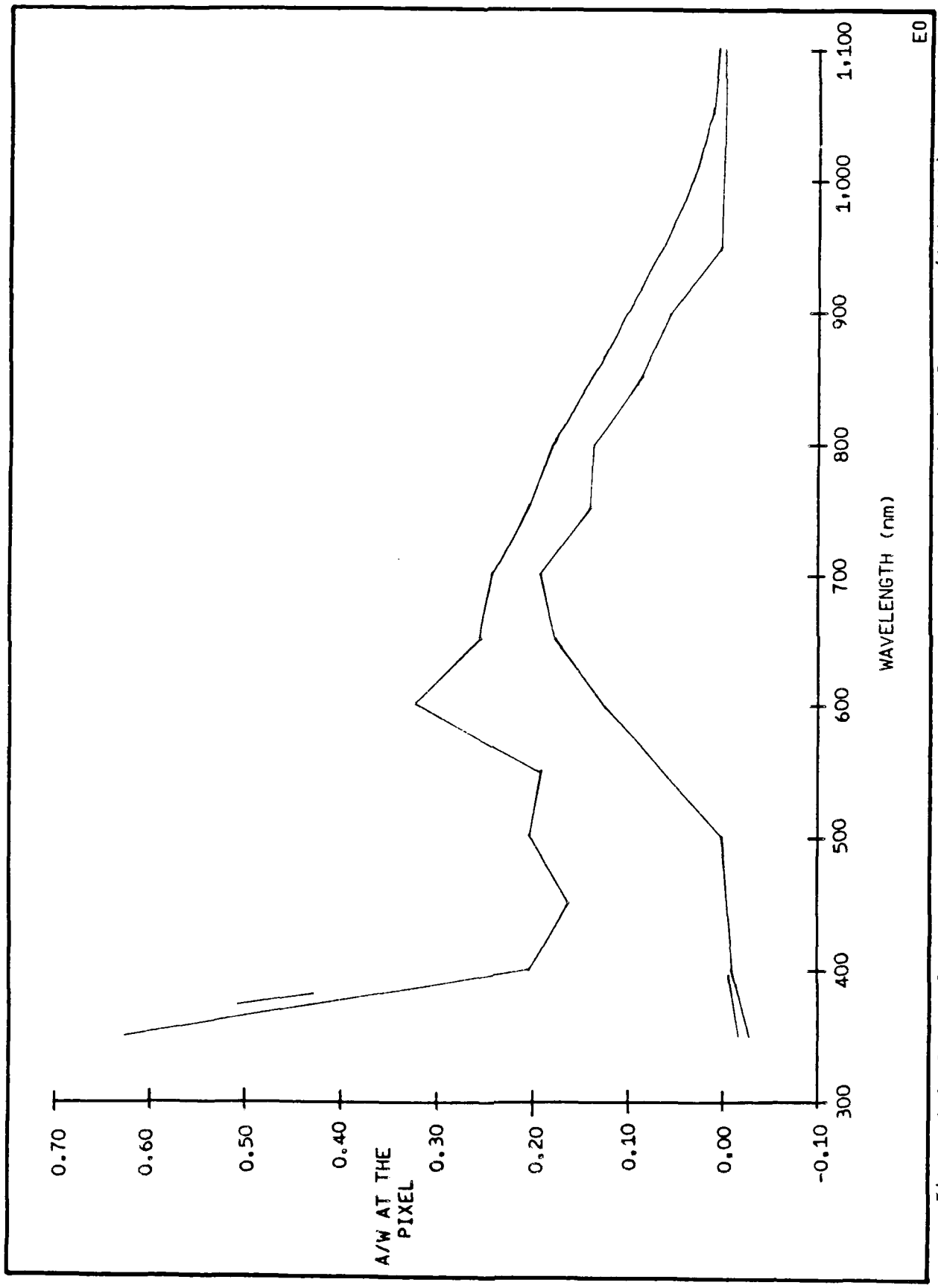

Figure 6-6 Spectral Response for STS-256 5-6-2, Pre- and Postradiation Response (11/13/84)

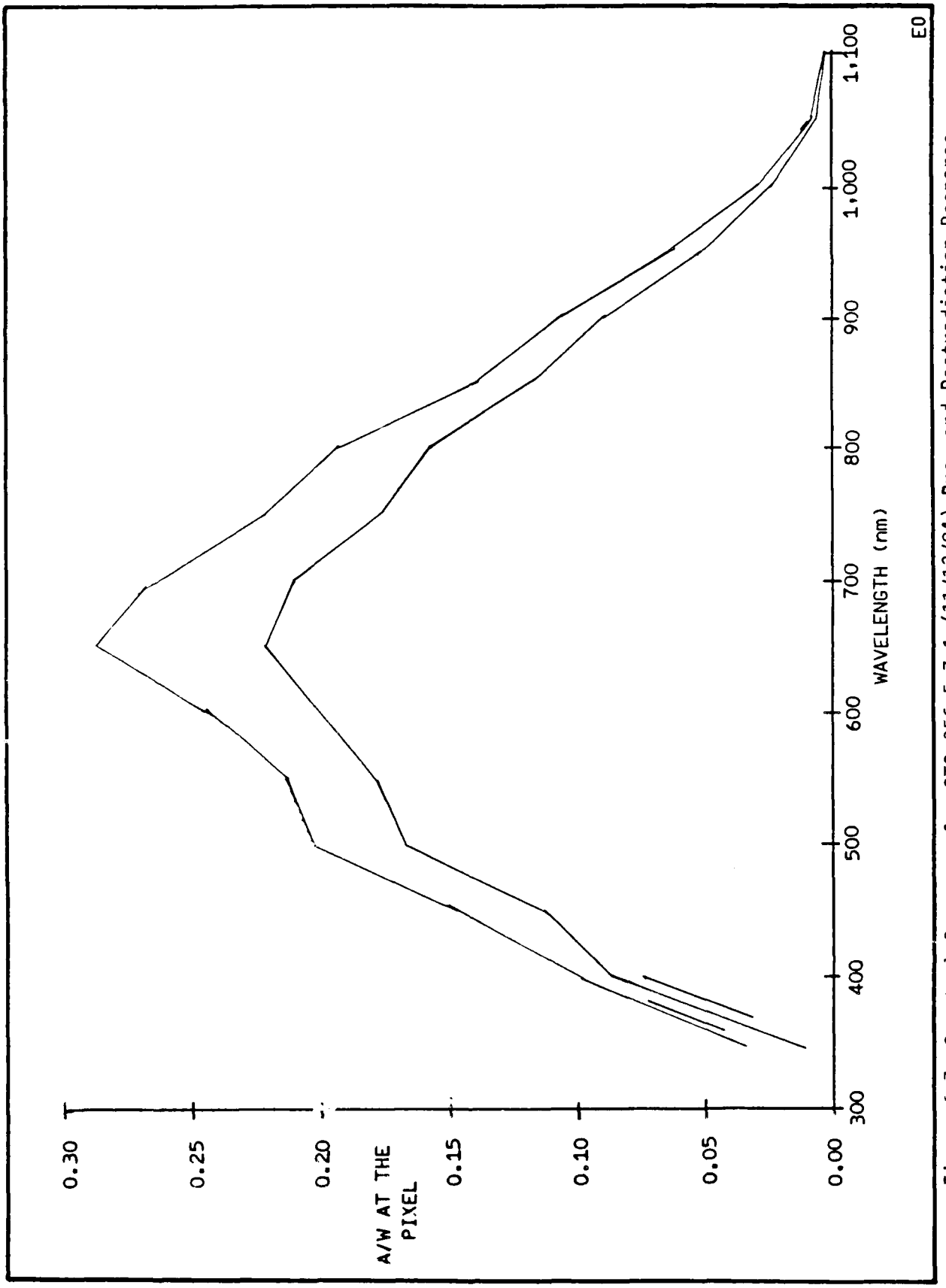

Figure 6-7 Spectral Response for STS 256 5-7-1 (11/13/84) Pre- and Postradiation Response

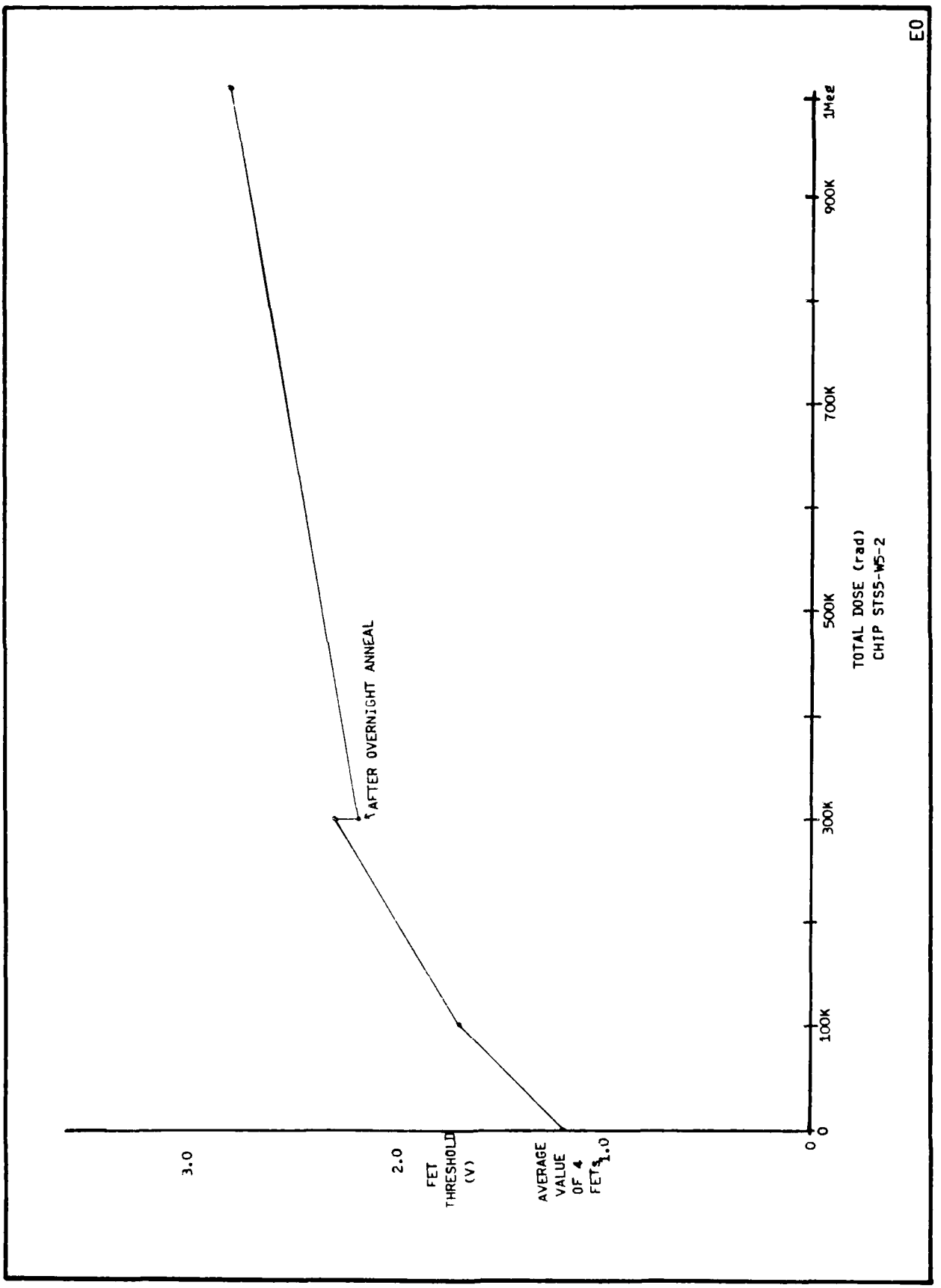

Figure 6-8 FET Threshold vs. Total Dose (5-5-2)

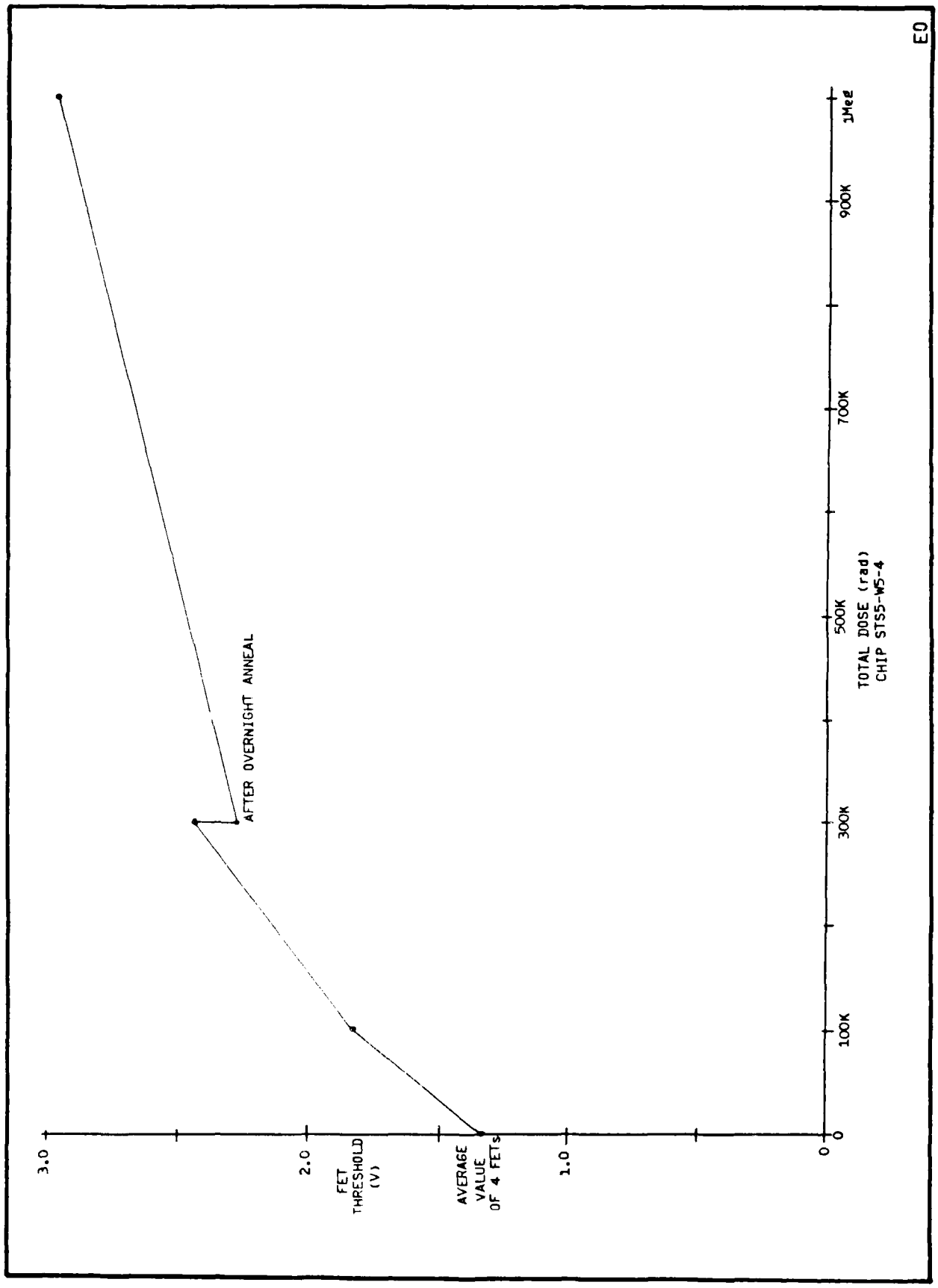

Figure 6-9 FET Threshold vs. Total Dose (5-5-4)

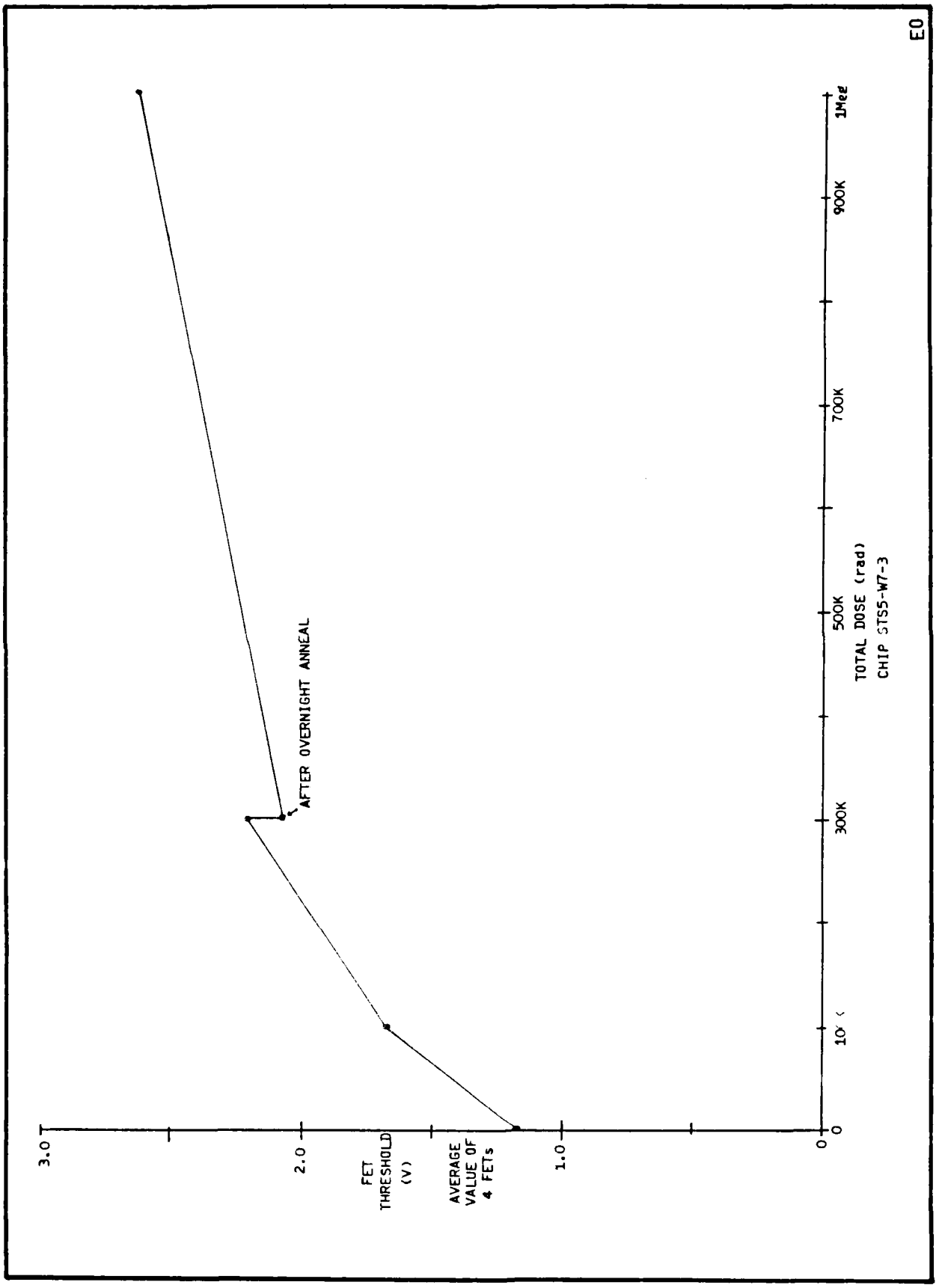

Figure 6-10 FET Threshold vs. Total Dose (5-7-3)

Section 7
BREADBOARD TRACKER RADIATION TESTS

Section 7
BREADBOARD TRACKER RADIATION TESTS

Radiation tests were performed at NRL using cobalt 60 for low-rate transient tests and electrons for high-rate and total dose tests. In general, all tests were conducted in a manner consistent with the operation of the cobalt source machine and the LINAC machine.

7.1 COBALT 60 TESTING

For dose rates from 0.5 rad/min to 20 rad/min, the star tracker was set up so that its side faced the cobalt source output. The star simulator and star source were used to track stationary targets using the simple tracking program. For the 36-rad/min dose rate, the star simulator and star source were removed and the star tracker lens was placed up against the cobalt source output. The read 4 pixel program was implemented for this dose rate.

Table 7-1 summarizes the results obtained from the cobalt 60 testing. Although at the 36-rad/min dose rate there was some change in star magnitude, this testing showed no loss of star tracking.

Table 7-1
COBALT 60 RADIATION TESTING

DOSE RATE	TIME	TOTAL DOSE	PARTS EXPOSED	COMMENTS
0.5 RAD/min	5 min	2.5 RAD	Detector	No observable change
5.4 RAD/min	6.75 min	36.4 RAD	Detector	No observable change
5.4 RAD/min	4 min	21.6 RAD	Detector	No observable change
5.4 RAD/min	3 min	16.2 RAD	Detector/ Electronics	No observable change
20 RAD/min	6 min	120 RAD	Detector/ Electronics	No observable change
*36 RAD/min	4 x 1 min	144 RAD	Detector	Some change in star magnitude. No observable effect on system.

*Performed after LINAC total dose testing to approximately 100 krad.

7.2 DOSE RATE TESTING

NRL's LINAC machine was used for all high-rate testing. Scatter plates were placed at the waveguide output to diverge the beam. TLDs were placed on the star tracker to measure dose levels.

Initially, the star tracker was irradiated from the side. This seemed to produce a fairly even coverage of radiation throughout the star tracker up to a dose rate of 1.2×10^9 rad/sec. At this point, the uniformity of radiation coverage dropped significantly, which prompted the star tracker to be irradiated at the back (power supply end).

The electronics were exposed to dose rates up to 1.2×10^9 rad/sec, and the detector with rates up to 1.4×10^{11} rad/sec. In order for the detector to be exposed to higher dose rates, the electronics were shielded with approximately 1 inch of lead.

Table 7-2 shows the results of the dose rate testing. At the 10^6 rad/sec dose rate and single-pulse application, there was no observable change in star tracker performance. When 10- and 100-pulse bursts were applied, false acquisitions with no track during the search mode occurred. This seemed to be more of a timing problem during the read cycle than a problem with integrating pulses. At the 10^8 dose rate, a loss of track (upset) and interruption of performance occurred. The program was reset to the beginning and continued a partition search until a target was acquired. The total recovery time was approximately 1 second. Latch-up occurred at 10^9 rad/sec with single-pulse and 10-pulse burst applications.

With only the detector exposed, upset/recoveries occurred at 10^9 rad/sec. At 10^{10} rad/sec and 10^{11} rad/sec, there was no observable change in performance.

The total dose accumulated by the detector and the electronics after the completion of dose rate testing was 51.3501 krad and 4.7172 krad, respectively.

Table 7-2

DOSE RATE TESTING
40 MeV electrons; 0.8-1A, 50-nsec pulses

RUN	DOSE RATE (rad/sec)	TOTAL DOSE (rad)	SETS/ PULSE BURST	PARTS EXPOSED	COMMENTS
1	2×10^6	0.4	4/1s	Detector	No performance change.
2	3.5×10^6	2.0	11/1s	Detector/ Electronics	No performance change.
3	3.5×10^6	352	20/100s	Detector/ Electronics	False acquisition. No track during search mode; no change during track mode.
4	2.5×10^6	277	20/100s 20/10s	Detector	No change during track; false acquisition, no track during search.
5	1.8×10^7	458	20/1s 1/500s	Detector	Star magnitude increased. No performance change.
6	2.1×10^7	277	10/1s 5/10s 2/100s	Electronics	Star magnitude changes. No performance change.
7	1.4×10^8 at center; 5.6×10^7 at edge	1,500	5/1s 10/10s 2/100s	Electronics	Power supply current increased. Star magnitude changed. Upset/Reset ~1 sec.
8	7.5×10^7	411	10/1s 10/10s	Detector	Star magnitude change. No performance change.
9	1.2×10^9	450	15/1s	Electronics	Upset/Reset ~1 sec.
10	1.2×10^9	1,000 for detector; 2,000 for electronics	22/1s 3/10s	Detector/ Electronics	Power supply current increased. Upset/Reset ~1 sec; Latch-up.
11	1.2×10^9	1,853	10/1s 2/10s	Detector	Magnitude changed. Upset/Recovered
12	4×10^{10}	40,000	10/1s 1/10s	Detector	Magnitude increased. No performance change.
13	1.4×10^{11}	6,800	1/1s	Detector	Magnitude decreased; No performance change.

7.3 TOTAL DOSE TESTING

All total dose testing was performed using NRL's LINAC machine with scatter plates placed at the waveguide output to diverge the beam. TLDs were placed throughout the star tracker to measure dose levels.

For test runs 1 through 10, the star tracker was pointed with its back (power supply end) toward the waveguide output. The simple tracking program was implemented along with the star simulator and star source. As shown in Table 7-3, the total dose for the electronics was applied in 10-krad increments, and 1.675-krad increments for the detector. During these first ten runs, only one latch-up occurred. However, after cycling the power, the star tracker was functional again. Functional testing consisted of performing an acquisition search around the entire CID array.

For test run 11, the star simulator, star source, and lens were removed. Another latch-up occurred at this point, but power was cycled and the testing resumed.

The star tracker was set up with the detector pointing toward the LINAC waveguide output for test runs 12 and 13. Only upsets/resets occurred with recovery times of approximately 1 second.

For the remaining test runs, the star tracker was placed so that its side was irradiated. Total dose was accumulated until latch-up with no recovery occurred. The total dose for the detector and electronics at this point was 192.3941 krad and 216.4072 krad, respectively.

After a crude parts check, it was discovered that the level shifter D139 ICs were not functioning correctly. These parts were replaced and testing resumed. Again, total dose was accumulated until failure occurred. After preliminary examination of the electronic parts, the D139 ICs seemed to be the cause of the second failure. However, further investigation is required to examine the degradation of other parts.

Table 7-3

TOTAL DOSE TESTING
40 MeV electrons; 2 mA, 1.5-μsec pulses

RUN	TOTAL DOSE DETECTOR (krad)	TOTAL DOSE ELECTRONICS (krad)	COMMENTS
1	53.0251	14.7172	Upset/Reset ~1 sec; functional
2	54.7001	24.7172	Upset/Reset ~1 sec; functional
3	56.3751	34.7172	Upset/Reset ~1 sec; functional
4	58.0501	44.7172	Upset/Reset ~1 sec; functional
5	59.7251	54.7172	Upset/Reset ~1 sec; functional
6	61.4001	64.7172	Upset/Reset ~1 sec; functional
7	63.0751	74.7172	Latch-up; cycled power; functional
8	64.7501	84.7172	Upset/Reset ~1 sec; functional
9	66.4251	94.7172	Upset/Reset ~1 sec; functional
10	68.1001	104.7172	Upset/Reset ~1 sec; functional
*	68.2441	--	Cobalt testing on detector, add 144 rad
11	68.8641	108.3172	Latch-up; cycled power; functional
12	78.0841	109.8172	Upset/Reset ~1 sec
13	87.3041	111.3172	Upset/Reset ~1 sec
14	90.6941	114.7072	Upset/Reset ~1 sec
15	141.5441	165.5572	Upset/Reset ~1 sec
16	192.3941	216.4072	Latch-up; upset with continuous search, no recovery.
*	--	--	Replaced level shifter D139 ICs
17	243.2441	267.2572	Upset/Reset ~1 sec; 50.85 krad on D139s
18	294.0941	318.1072	Upset/Reset ~1 sec; 101.70 krad on D139s
19	344.9441	368.9572	Latch-up; no recovery; 152.55 krad on D139s

Appendix A
CONTROL, INTERFACE, AND OPERATING PROCEDURES

Appendix A
CONTROL, INTERFACE, AND OPERATING PROCEDURES

TABLE OF CONTENTS

Appendix A
CONTROL, INTERFACE, AND OPERATING PROCEDURES

A.1 TEST COMPUTER

The test computer, shown in Figure A-1, is a Hewlett Packard Series 200 Model 16 (HP 9816). It is based on the Motorola MC68000 16-bit microprocessor with a 32-bit architecture. This computer operates as a stand-alone unit or as an instrument controller. Included with the HP 9816 are a 9-in. CRT, a detachable keyboard, memory from 128 to 768 kbytes, an HP-IB interface, and an RS-232-C interface. The external peripherals include an HP 9121D dual 3-1/2-in. flexible disk drive and an HP 2673A thermal printer.

The 3-1/2-in. single-sided disk drive has a storage capacity of 270 kbytes, which is the same capacity as that of the 5-1/4-in. double-sided drive. The 3-1/2-in. drive storage capacity is due to its increased track density, which is 135 tracks per inch, compared with 48 tracks per inch for the 5-1/4-in. drive.

The 3-1/2-in. flexible disks are protected in three ways:

1. The media are completely enclosed in shirt-pocket-sized, hard plastic envelopes;

2. An auto-shutter feature of the drive prevents contamination from getting inside;

3. A monitor indicates when a piece of media needs to be replaced.

Features of the HP 2673A thermal printer are:

- 120 cps bidirectional printing;
- 9 x 15 dot matrix character cell;
- HP-IB, RS-232-C, HP or Centronics Parallel, Factory Data Link, HP-IL interfaces;

AD-A162 777 RADIATION-HARD BREADBOARD STAR TRACKER(U) BALL AEROSPACE SYSTEMS DIV BOULDER CO M W HUBBARD ET AL. SEP 85 BASD/F85-03 N00014-82-C-2488 2/2

UNCLASSIFIED F/G 17/3 NL

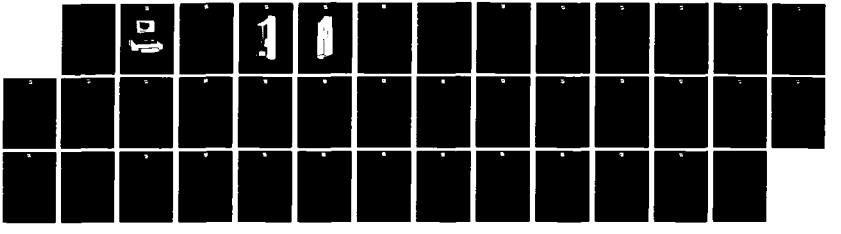

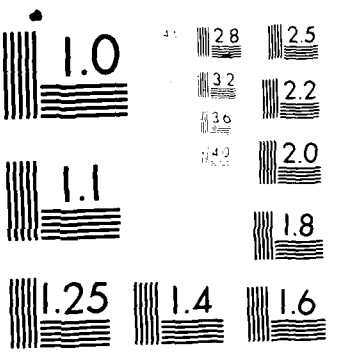

EO

Figure A-1 Test Computer

- Fanfold or roll paper;
- Full 128 USASCII, Roman Extension, and line drawing character sets;
- Capability to generate copies of text pages, program output, or test results;
- 90-dots-per-inch raster graphics capability;
- Autocentering, windowing, and framing;
- Offsets, expanded characters 5 cpi, and high-density printing; and
- JASCII, HPL, Katakana, and nine ISO languages.

Print features and formatting are selected by the control panel and are stored in the printer's nonvolatile memory. Once the features have been selected, they appear automatically when the printer is turned on. Features can be turned on or off by escape sequence commands from the host without altering the setting in the memory.

A.2 INTERFACE BOX

The interface box, shown in Figures A-2 and A-3, allows the star tracker to communicate with the HP 9816 computer. Specifically, the interface box:

- Receives data from the star tracker and transfers data to the HP 9816, and
- Sends commands from the HP 9816 to the star tracker.

Two Motorola MC68705U3 microprocessors that perform data and command tasks are incorporated into the design of the interface box.

Signals that come from the star tracker into the interface box include data, clock, flag, and command acknowledge. Signals that are sent to the star tracker through the interface box include data, clock, and flag.

Figure A-4 is a block diagram of the interface box, and Figure A-5 is the schematic diagram. Attachment I-1 lists the program, written in BASIC, that controls star tracker operation. A flowchart of the program is included in Attachment I-2. The interface box is discussed further in this Appendix, subsections A.2.1 and A.2.2.

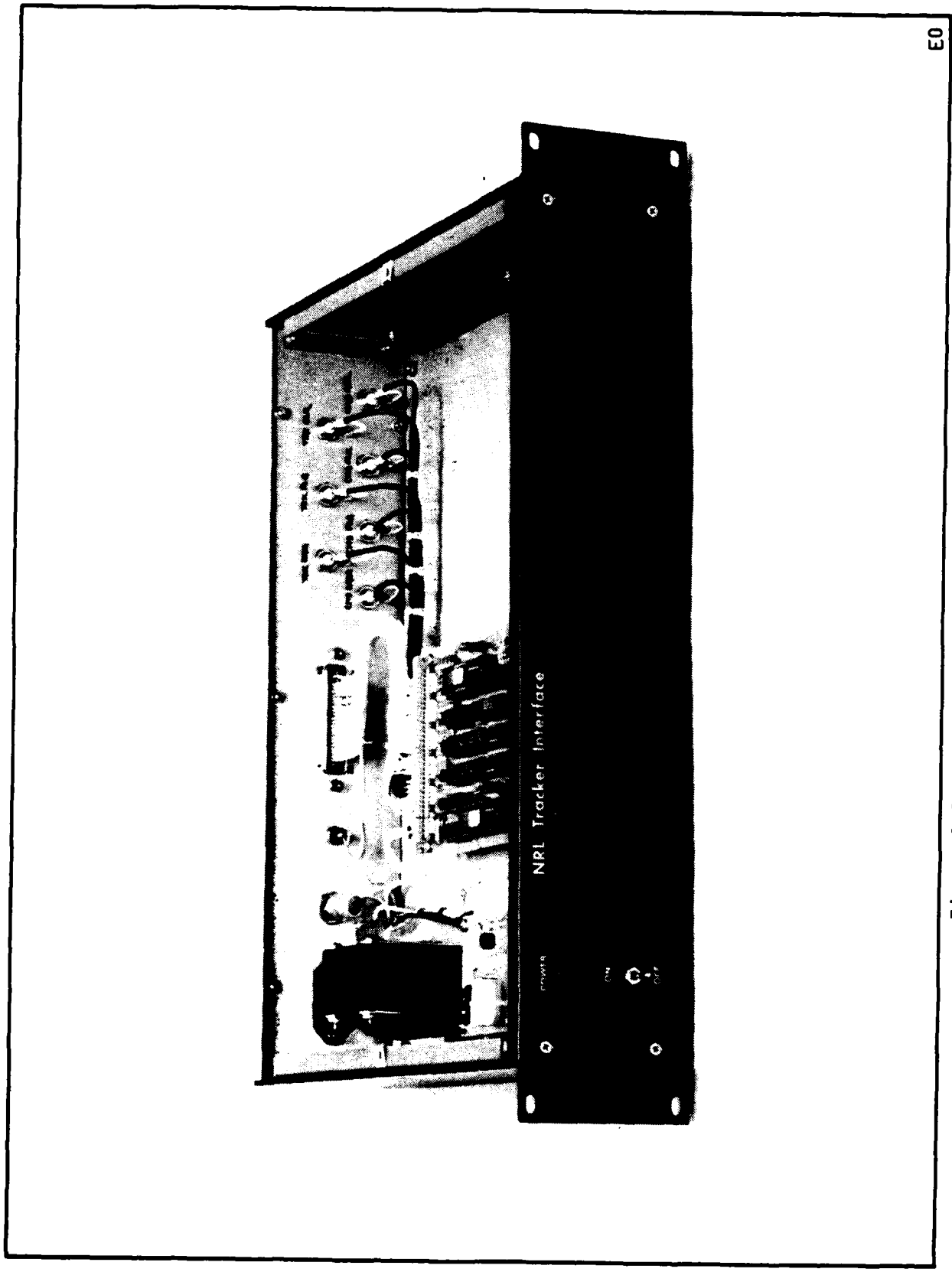

Figure A-2 Star Tracker Interface Box (Front)

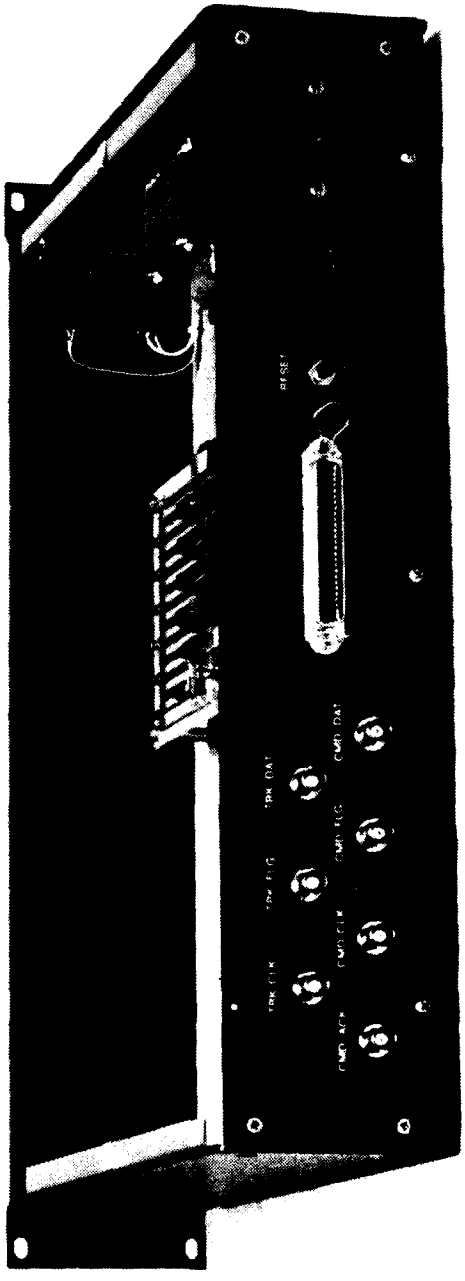

Figure A-3 Star Tracker Interface Box (Back)

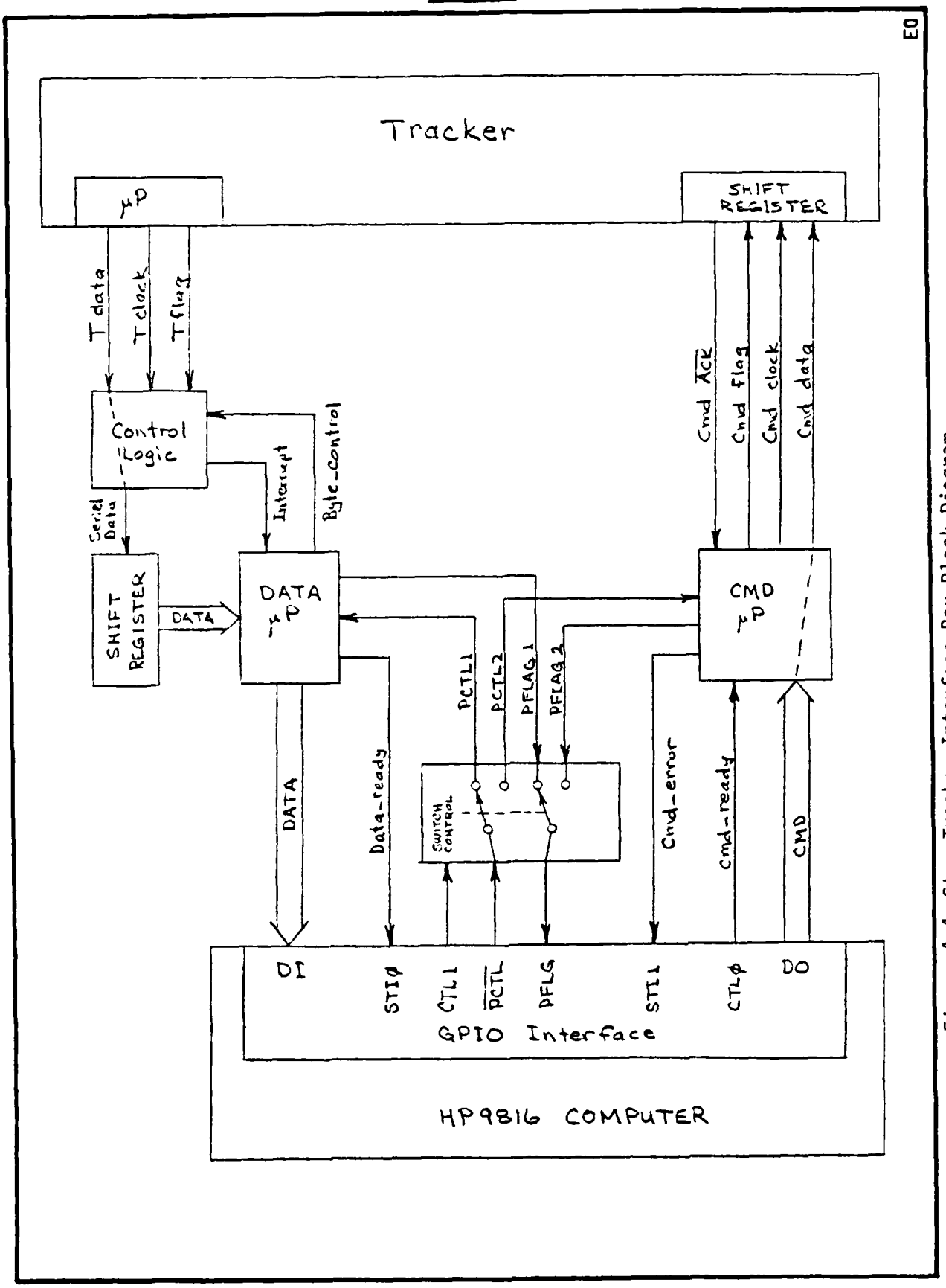

Figure A-4 Star Tracker Interface Box Block Diagram

A.2.1 Receive Data and Transfer

One of the two microprocessors in the interface box is used strictly for data tasks. It receives data from the star tracker and transfers it to the HP 9816 computer. Figure A-6 is a flowchart of the program used to handle data from the star tracker.

Figure A-7 is a timing diagram of key signals involved in transferring nine words of star tracker data to the HP 9816. Figure A-8 illustrates what happens when a 16-bit word is sent by the star tracker and received by the interface electronics. The end of word read cycle is shown in Figure A-9. Attachment I-3 contains the program used by the data microprocessor.

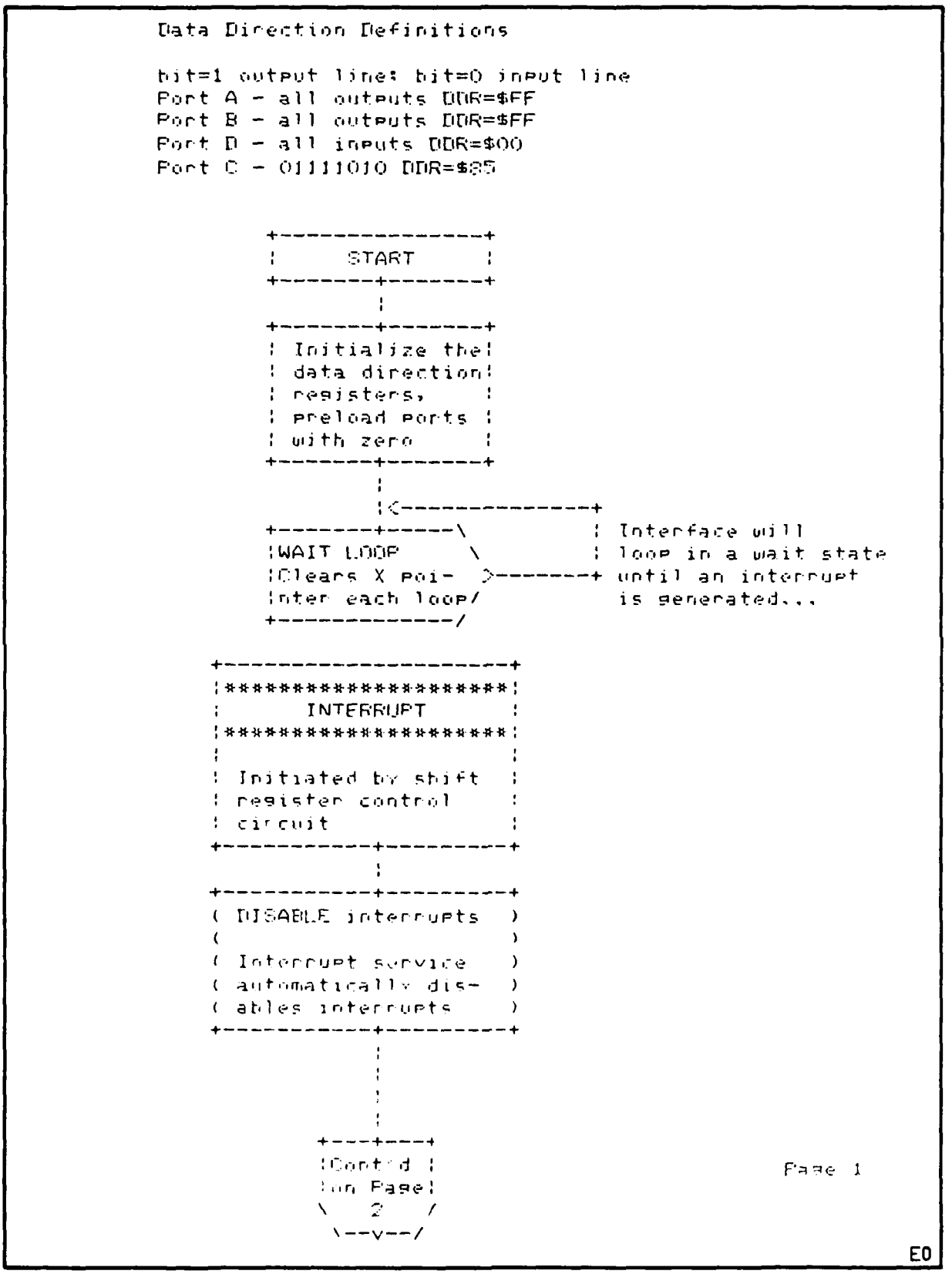

Figure A-6 Flowchart of Data Receiving and Transfer between Interface and HP 9816

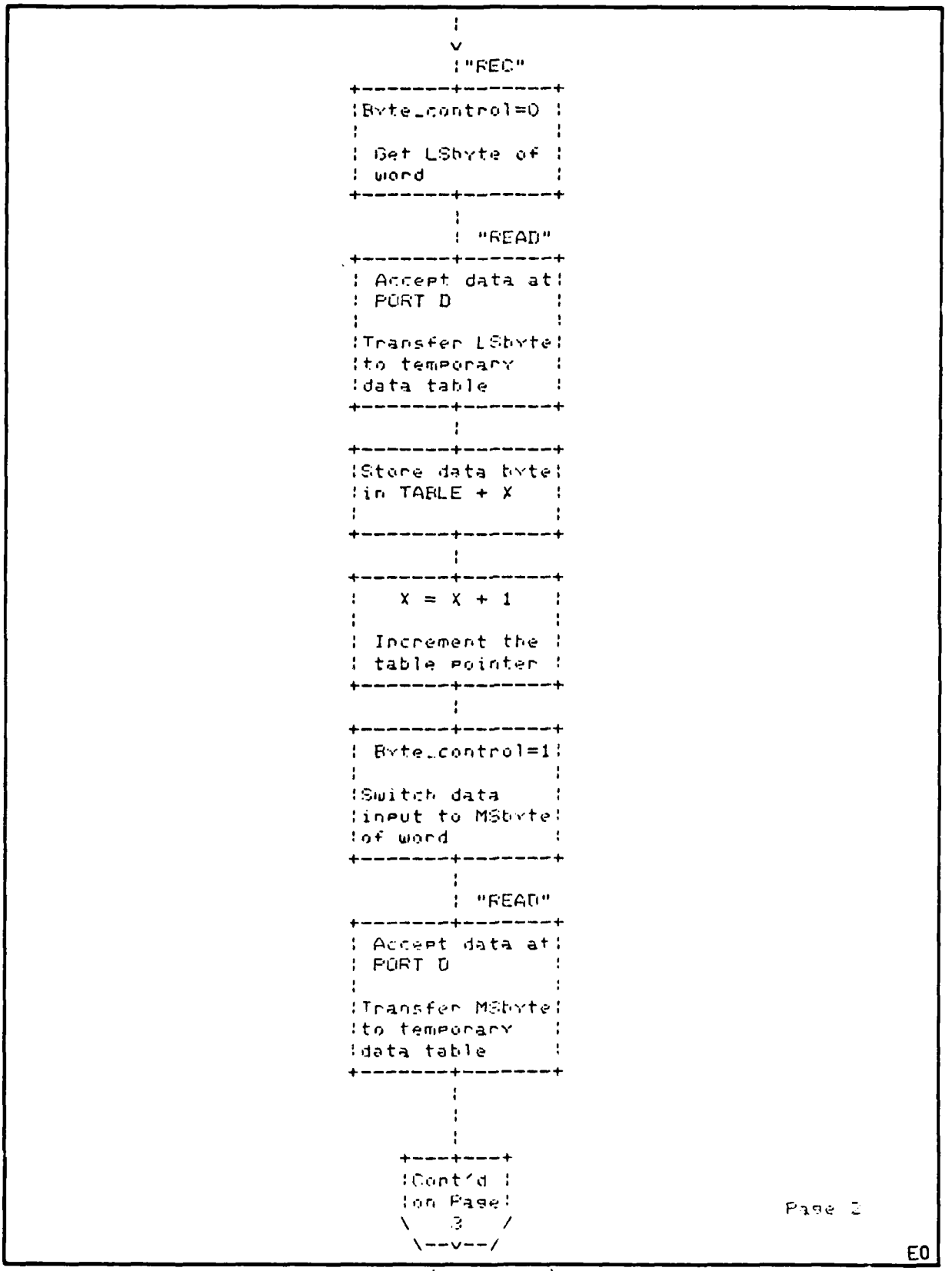

Figure A-6 (Continued)

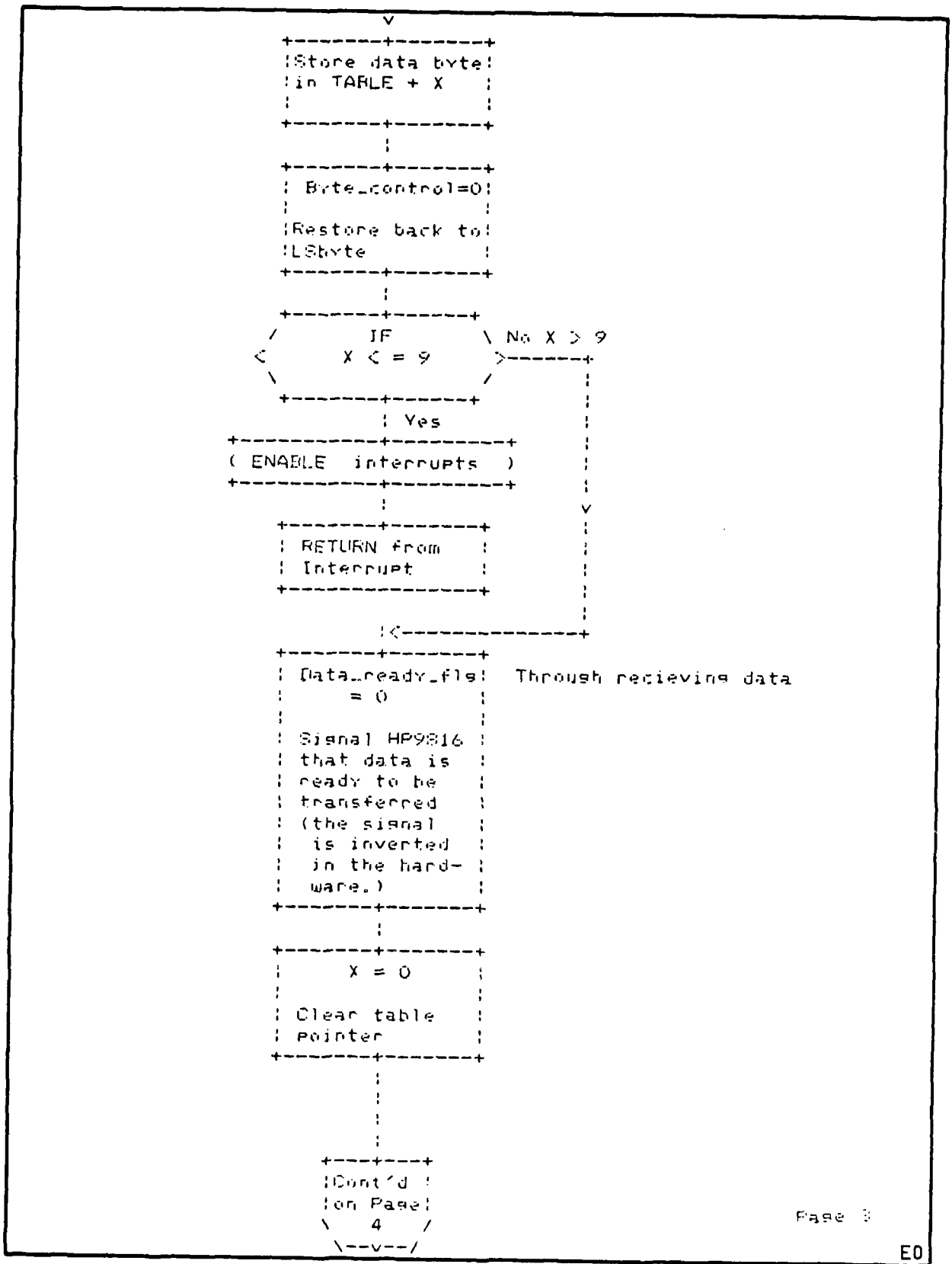

Figure A-6 (Continued)

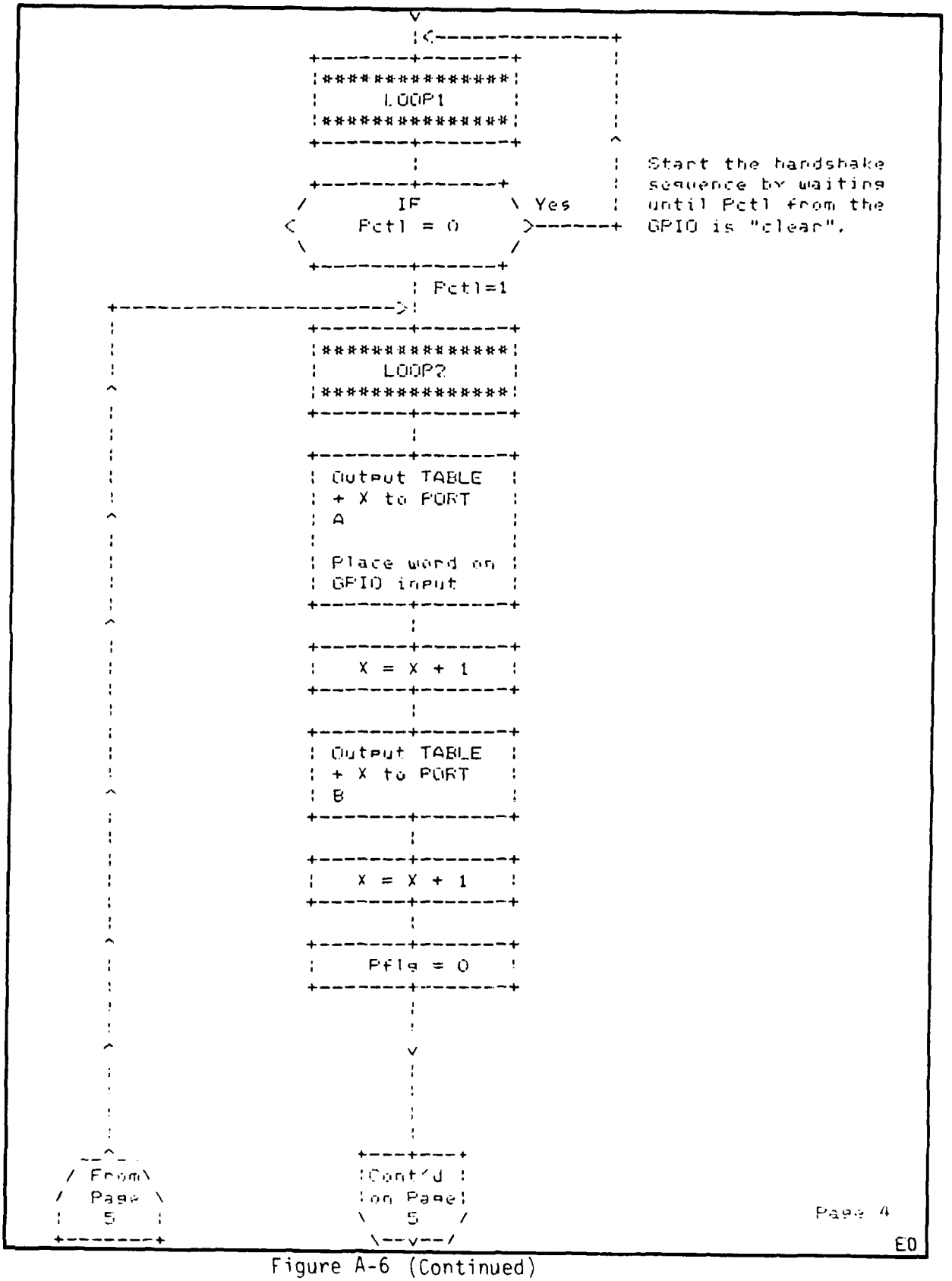

Figure A-6 (Continued)

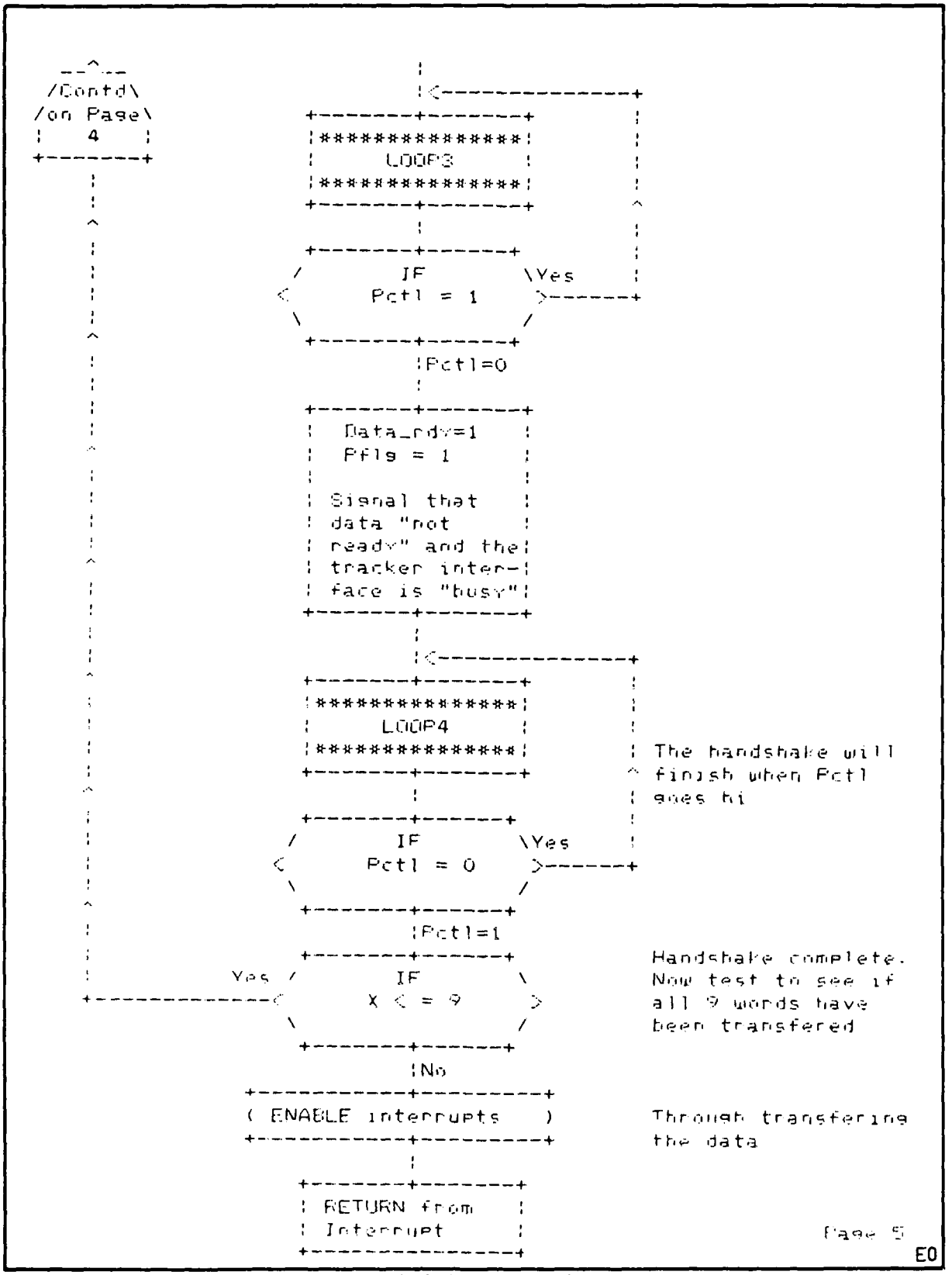

Figure A-6 (Concluded)

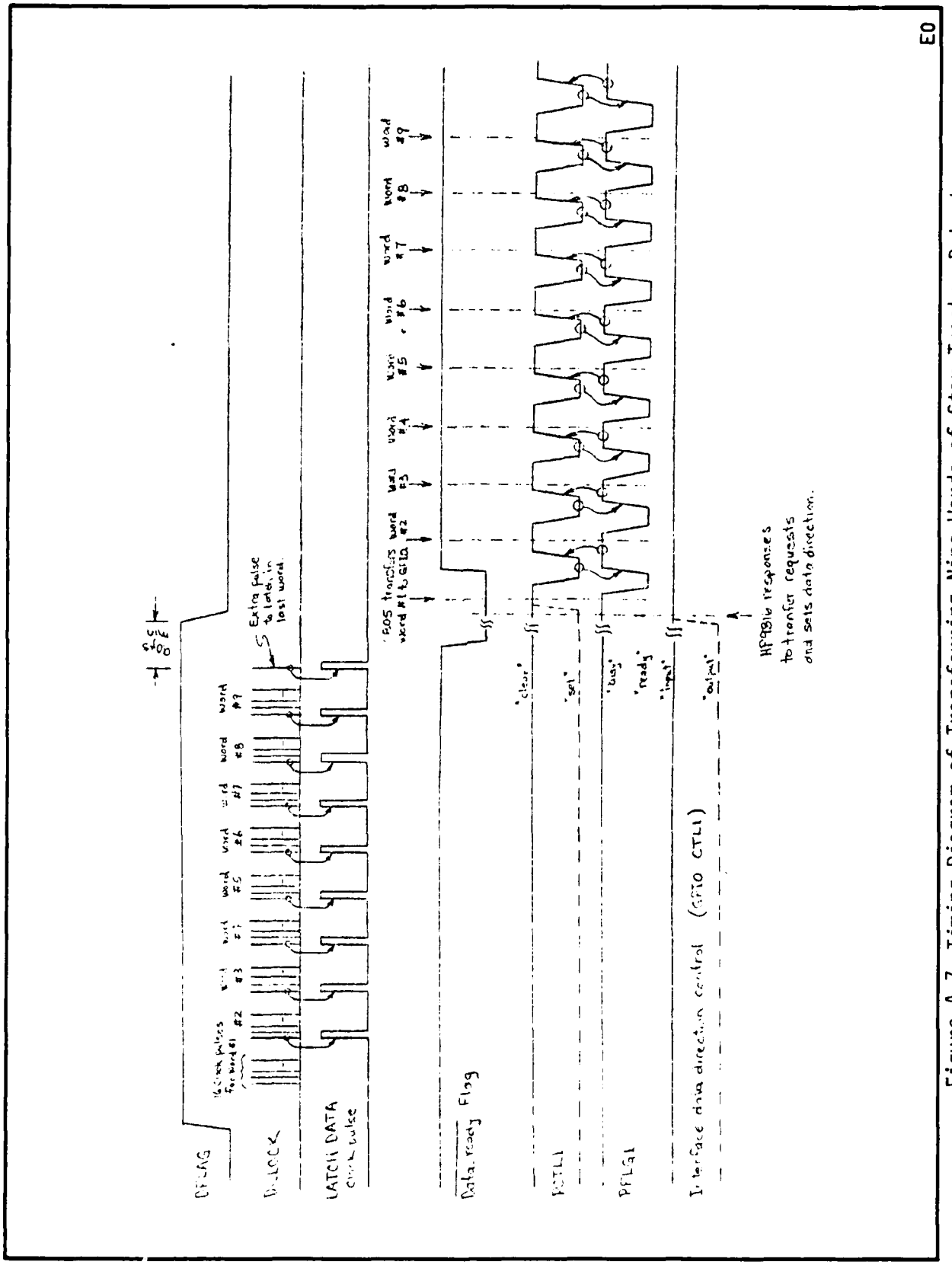

Figure A-7 Timing Diagram of Transferring Nine Words of Star Tracker Data to HP 9816

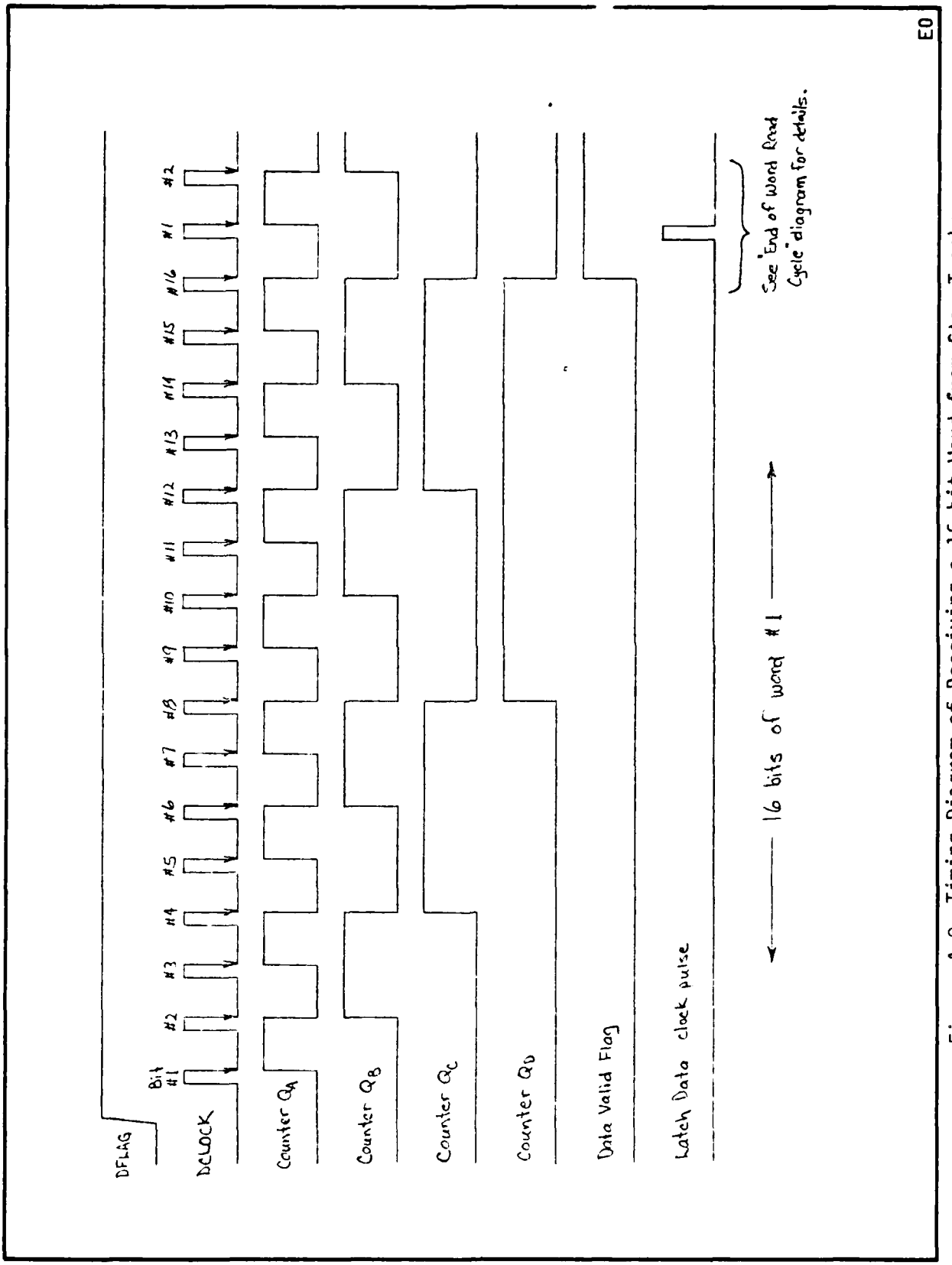

Figure A-8 Timing Diagram of Receiving a 16-bit Word from Star Tracker

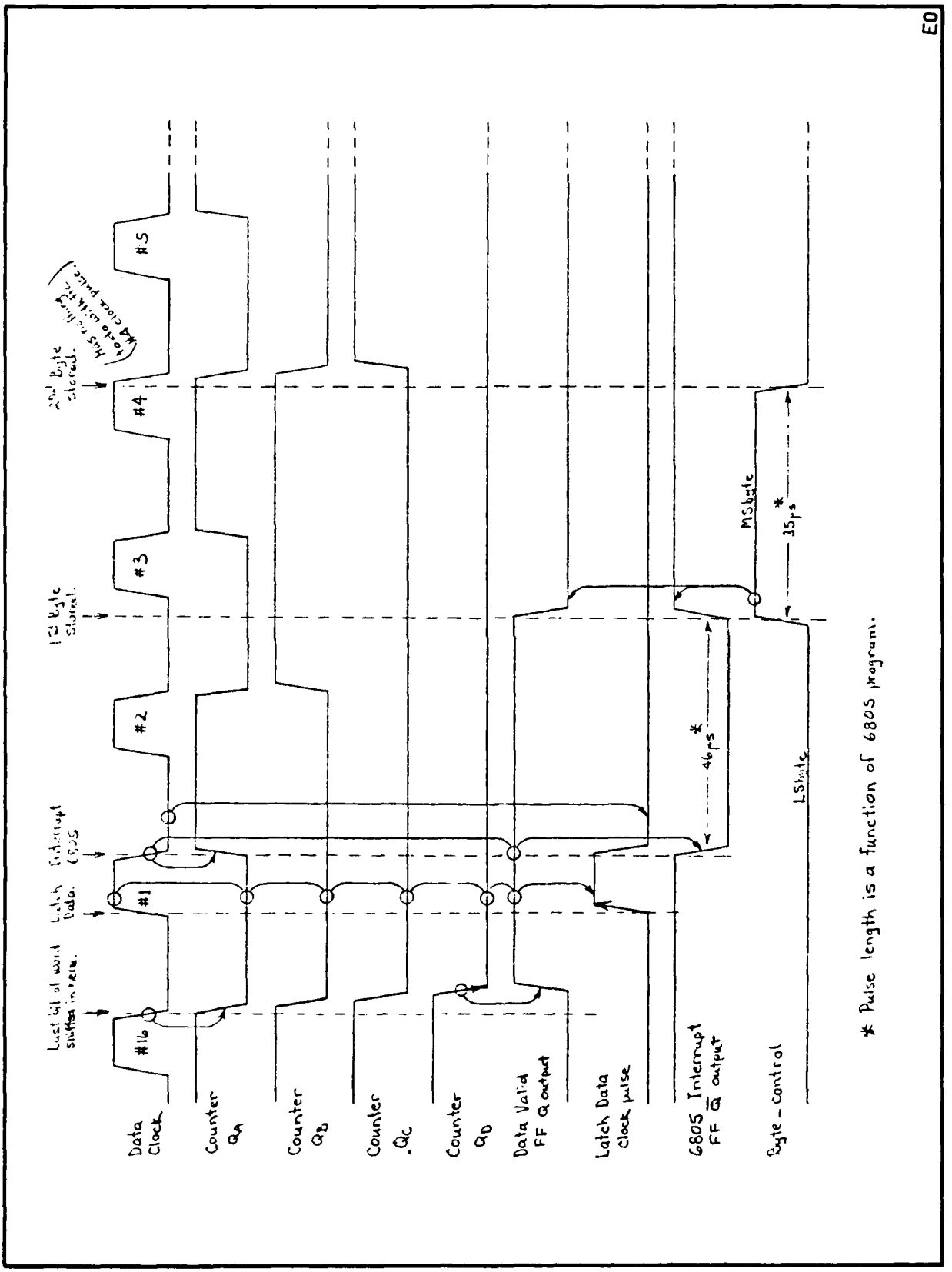

Figure A-9 End-of-Word Read Cycle

A.2.2 Send Command

The second microprocessor in the interface box is used to send commands from the HP 9816 to the star tracker. Figure A-10 is a flowchart of the microprocessor program used to send commands, and Attachment I-4 is a listing of the program.

When a command is sent from the HP 9816 to the star tracker, one of three things can occur:

- Both commands are received by the star tracker and they match,
- One command is sent to the star tracker and there is no acknowledge, or
- Both commands are sent to the star tracker but there is a mismatch.

The command sequence is as follows:

1. A command is sent to the star tracker.
2. A command acknowledge is sent from the star tracker.
3. A command mismatch is sent to the star tracker because only one command is sent.
4. The second command is sent.
5. A second acknowledge is sent from the star tracker.
6. A command mismatch may or may not occur. If the commands match, the star tracker will proceed to execute the command.

All commands that are received are acknowledged, and if the star tracker is not in the proper mode, the command will be ignored. Figure A-11 illustrates what happens when a command is sent.

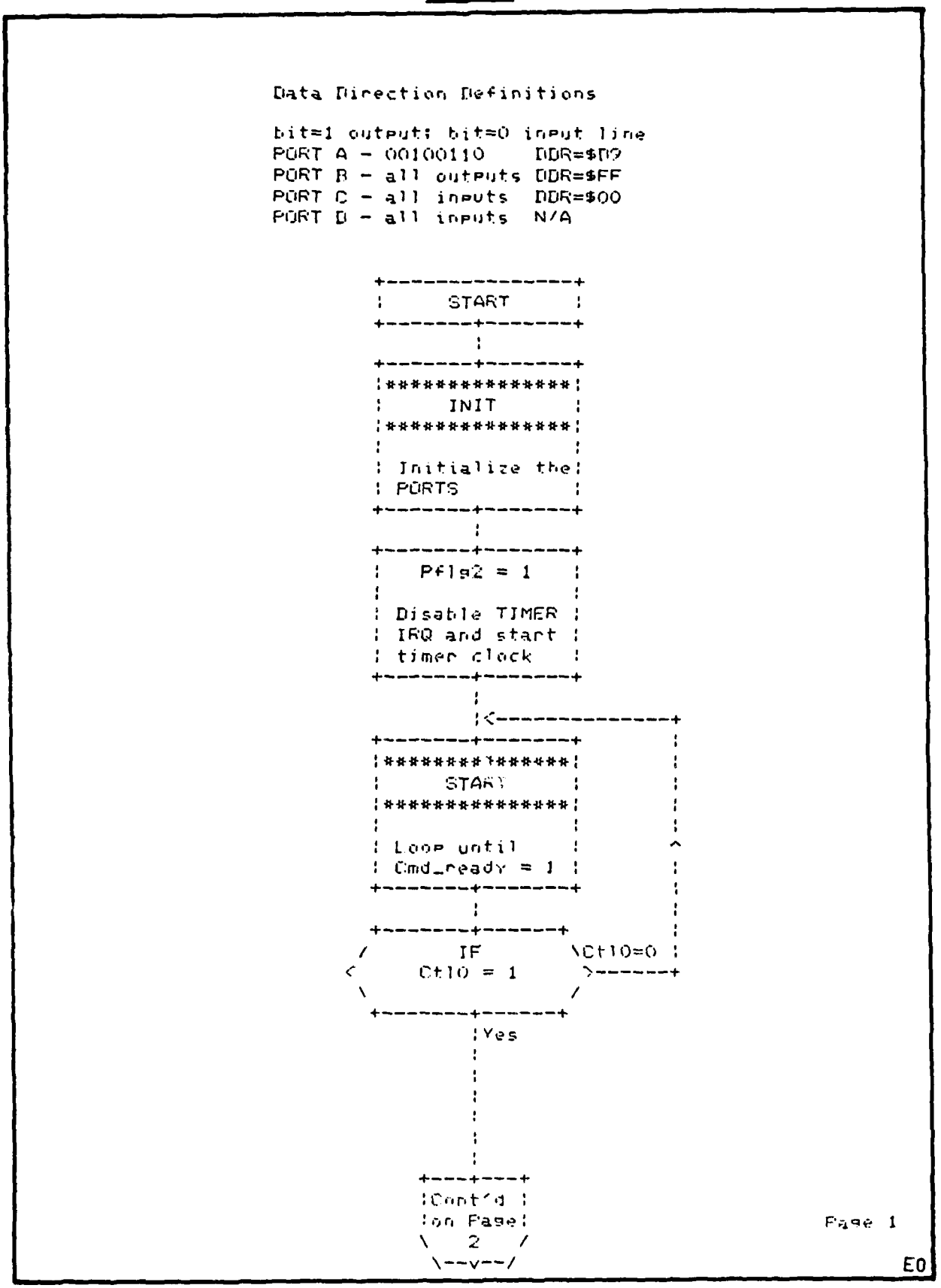

Figure A-10 Sending Commands Flowchart

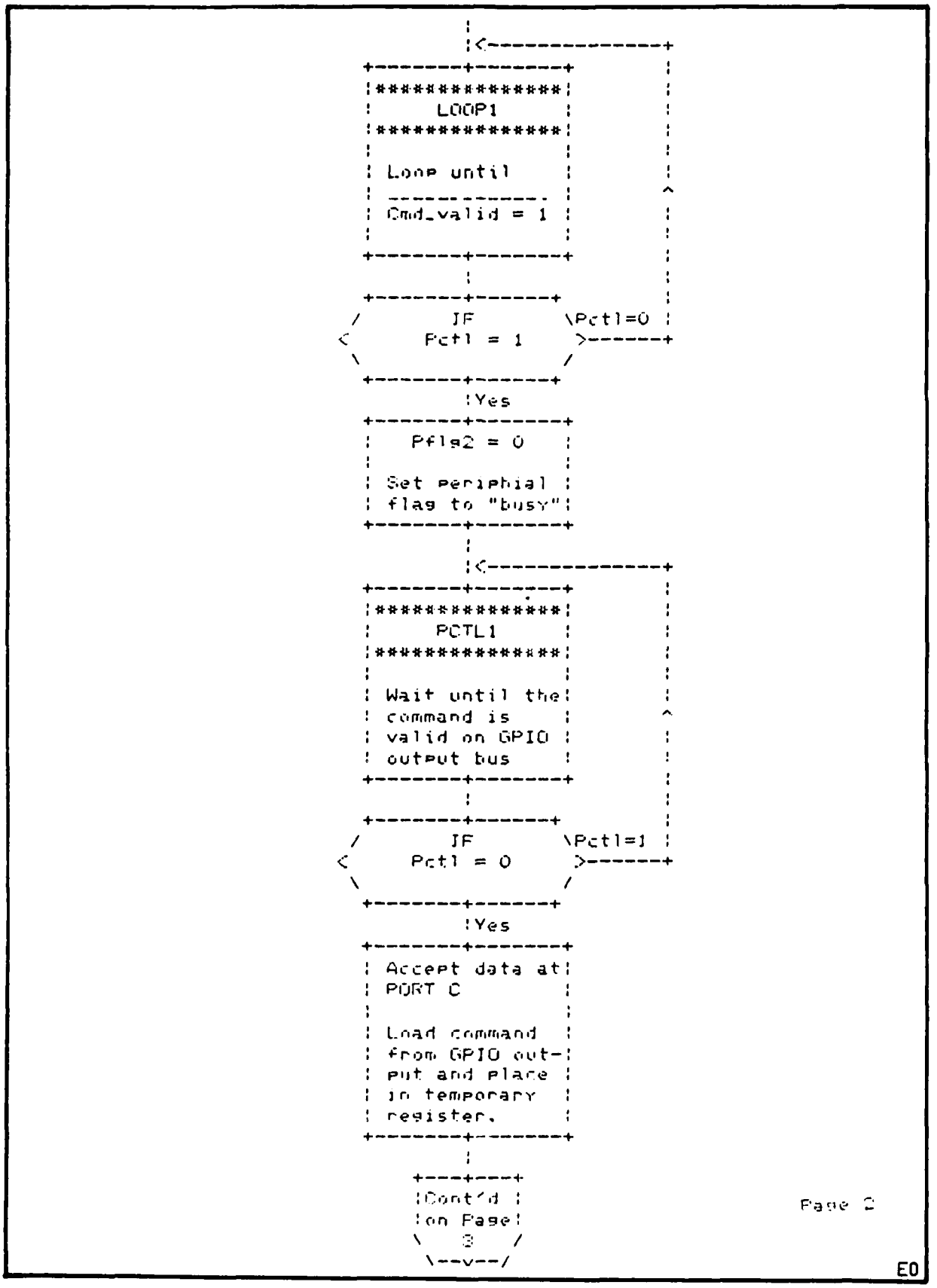

Figure A-10 (Continued)

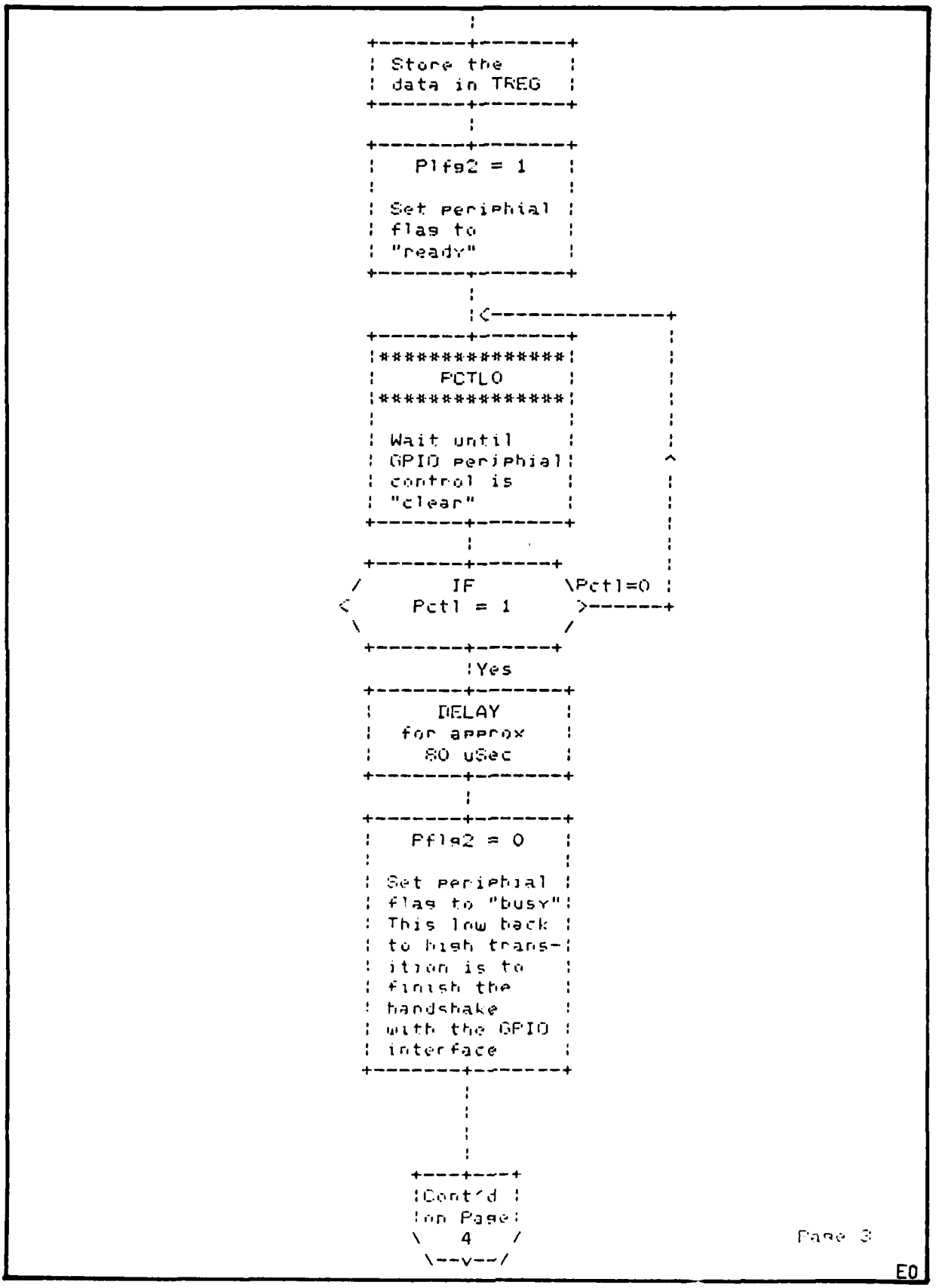

Figure A-10 (Continued)

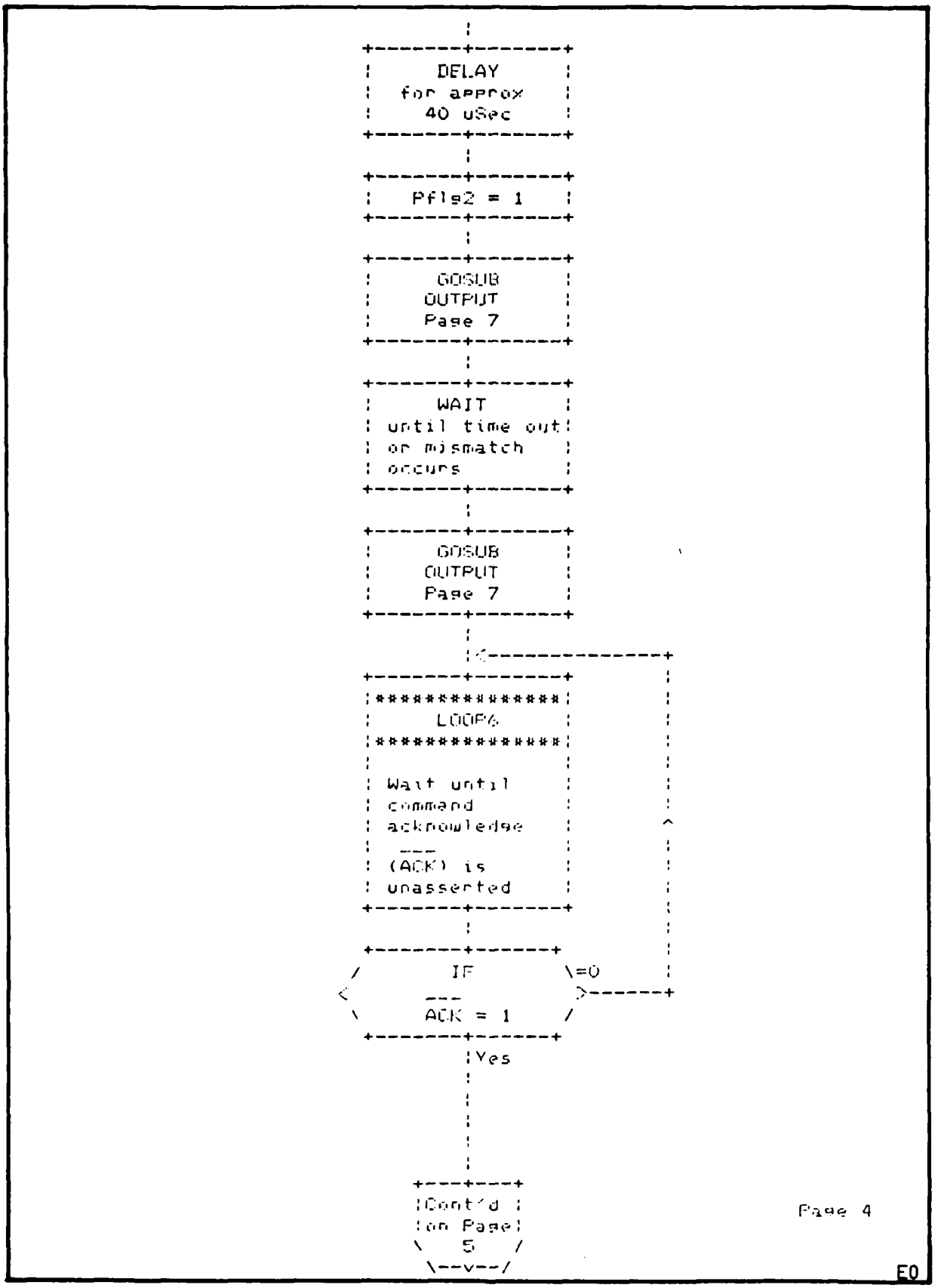

Figure A-10 (Continued)

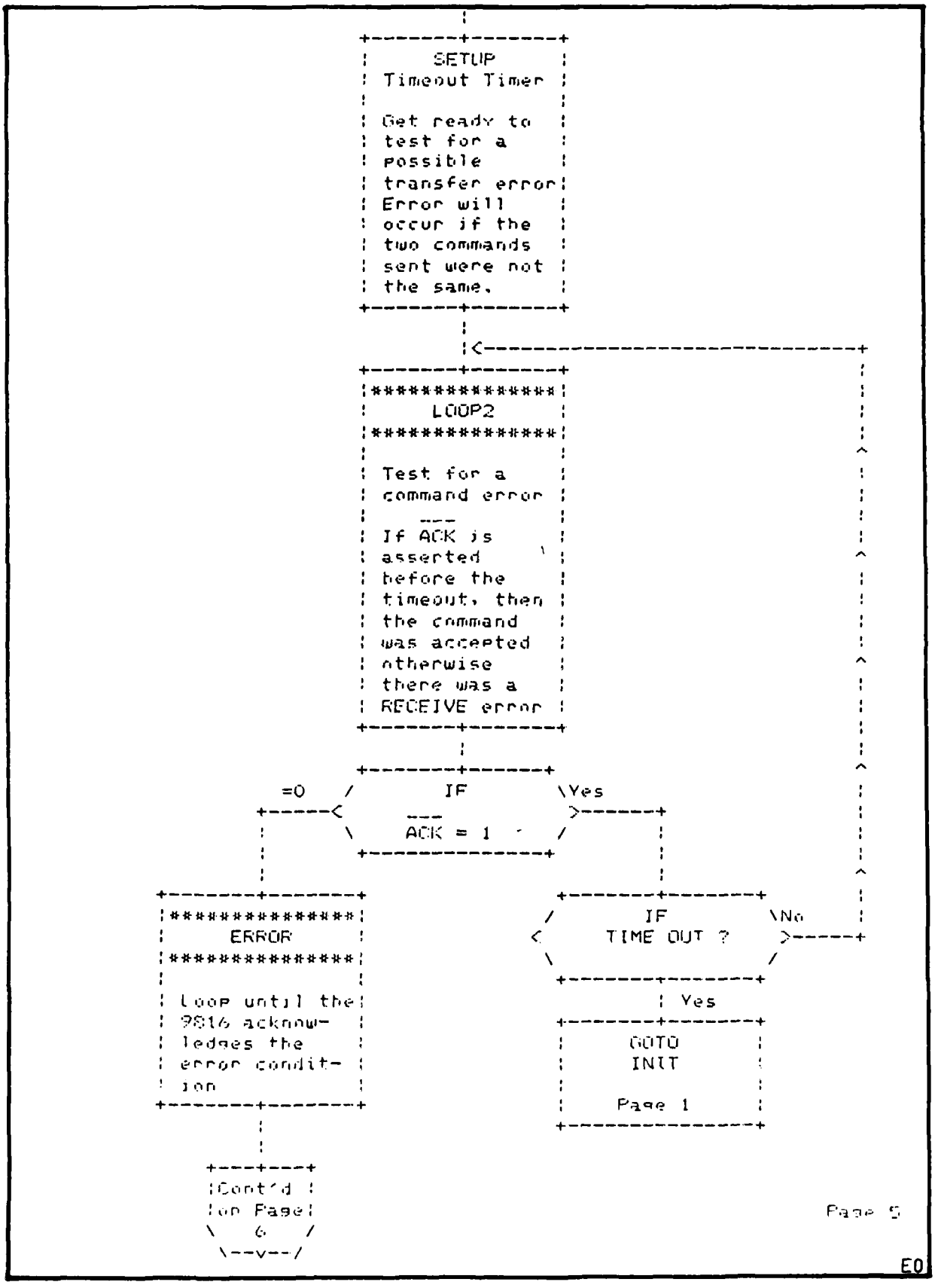

Figure A-10 (Continued)

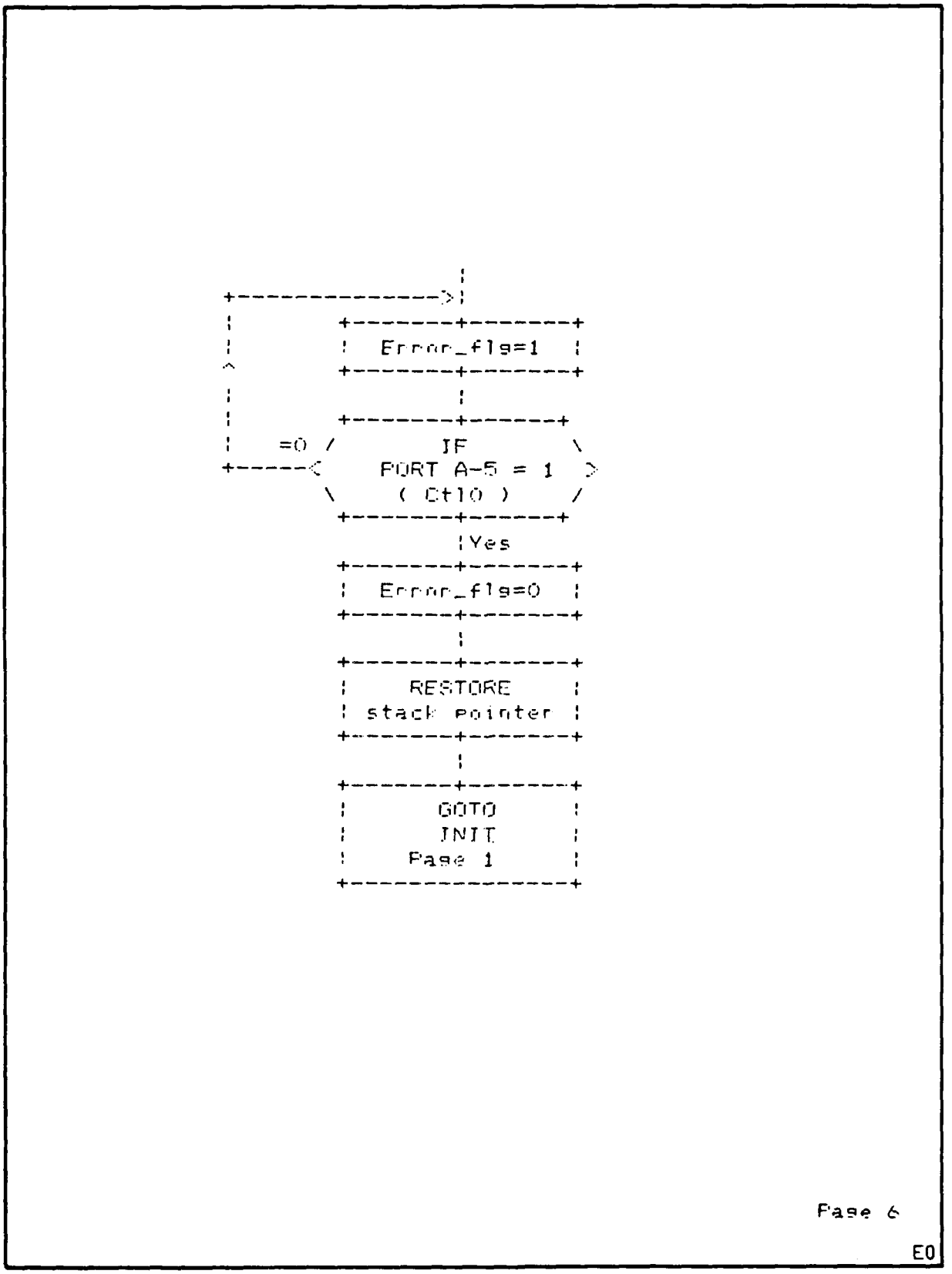

Figure A-10 (Continued)

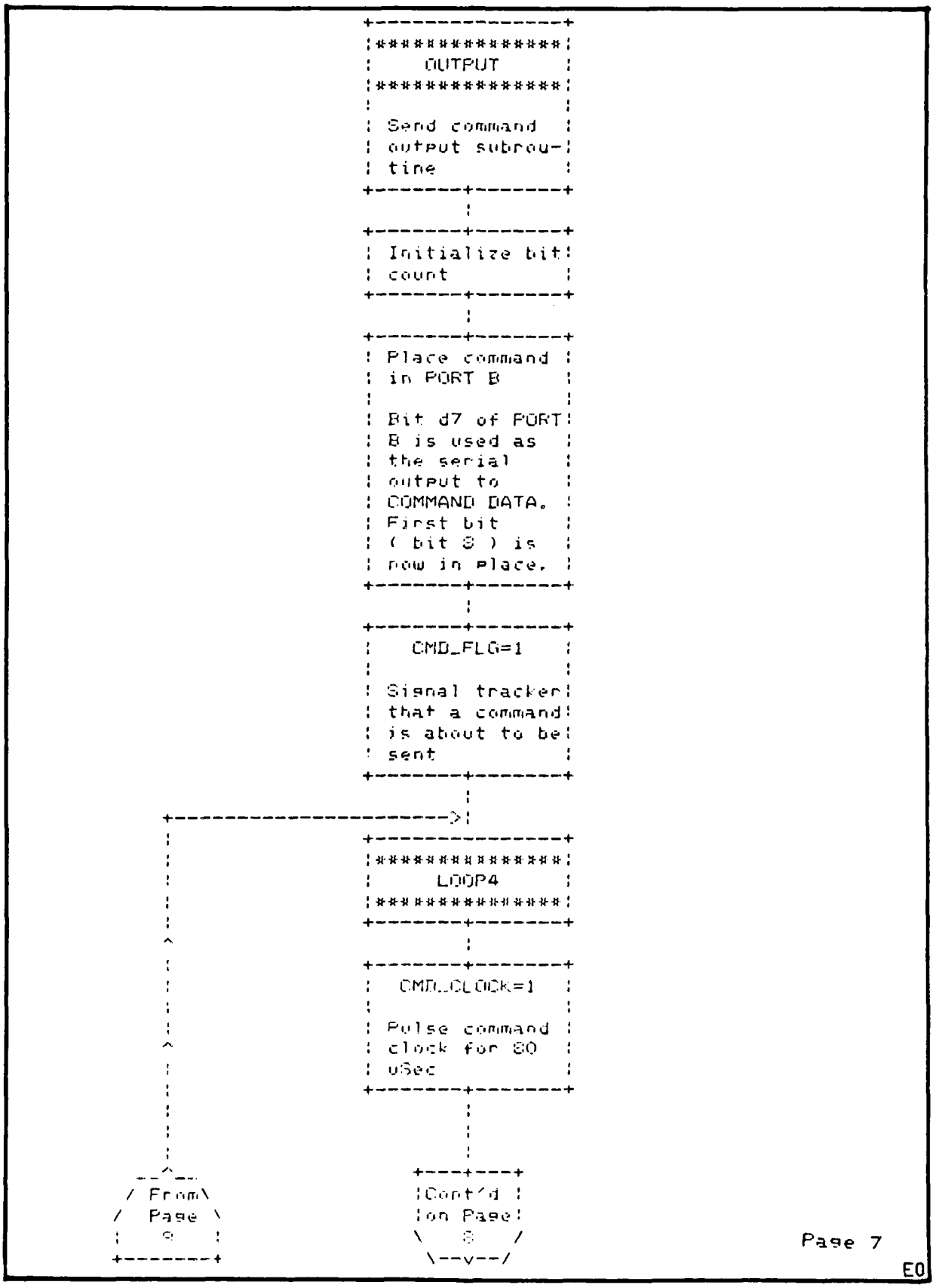

Figure A-10 (Continued)

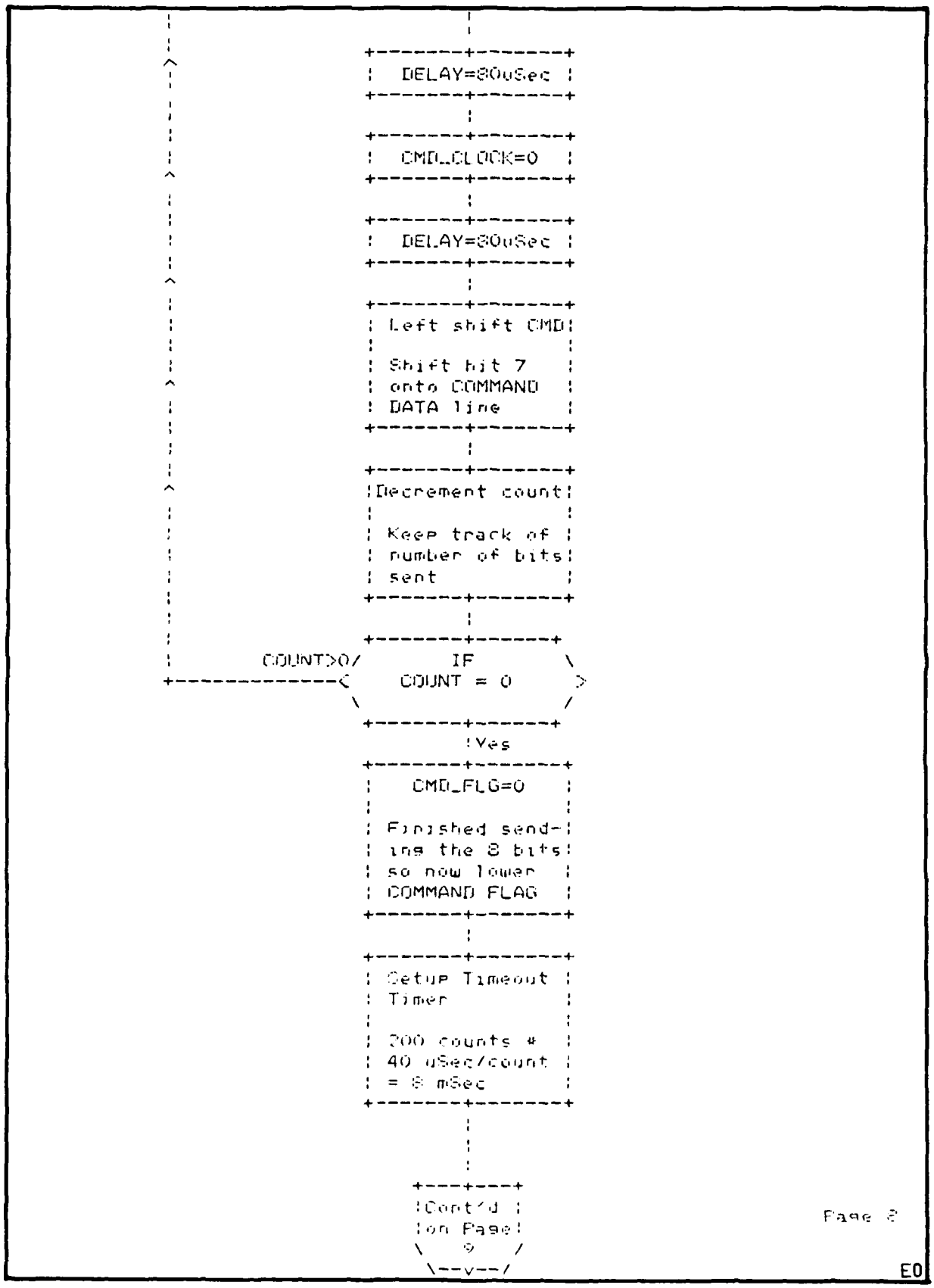

Figure A-10 (Continued)

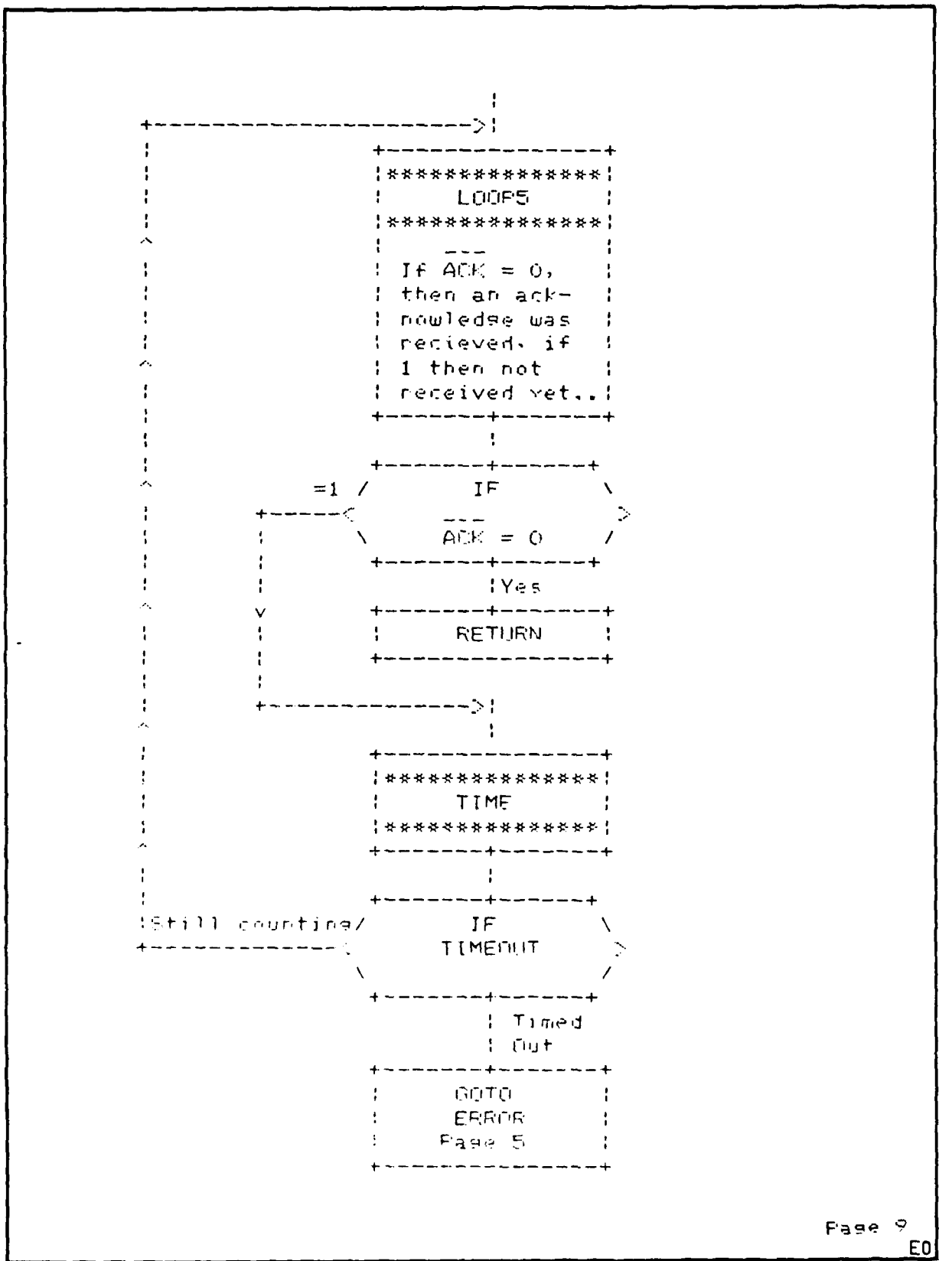

Figure A-10 (Concluded)

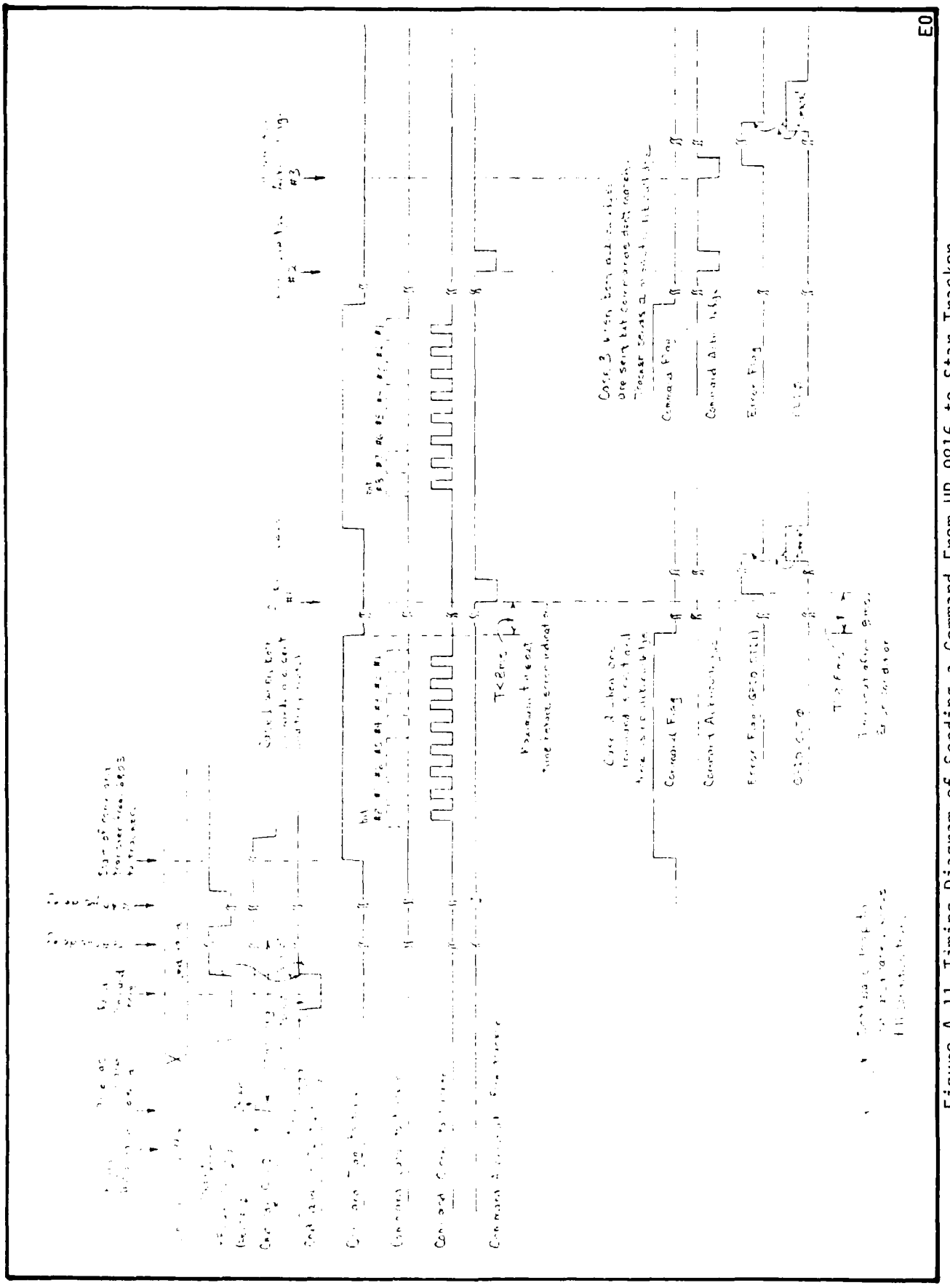

Figure A-11 Timing Diagram of Sending a Command From HP 9816 to Star Tracker

A.3 XY DISPLAY AND INTERFACE BOX

An XY display and its interface box are included in the system configuration for test purposes. The XY display is an HP Model 1300A and is used to visually monitor star tracker operation.

The star tracker operations that can be identified by observing the display are:

- Star tracker sequence,
- Star position within ±2 pixels,
- Tracking of stars,
- Star acquisition and deacquisition,
- Star enable and disable,
- Number of stars being tracked,
- Partition read,
- Partition location,
- Partition size,
- Local injection,
- Automatic gain control (AGC) operation, and
- Self-test.

The XY display interface box generates the signals needed to operate the XY display. These signals first enter the interface box as digital signals from the microprocessor. The digital signals are converted to analog signals, which is the form required by the display. Figure A-12 is a schematic diagram for the interface box and Figure A-13 is its timing diagram.

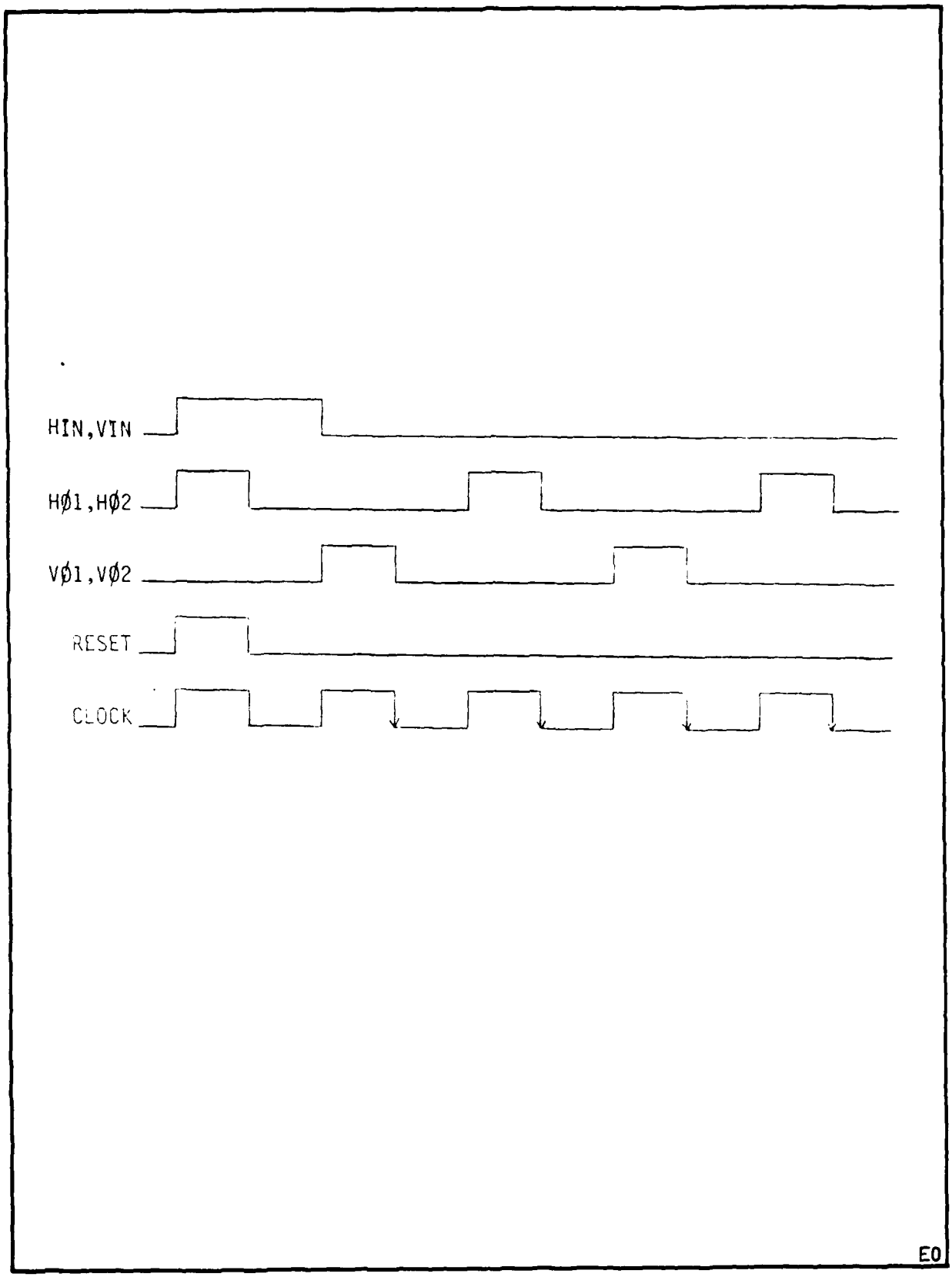

Figure A-13 XY Display Generator Timing Diagram

A.4 OPERATING INSTRUCTIONS FOR THE HP 9816

A.4.1 Booting Up the System

Place the boot disk in the left-hand drive. (Do NOT push it in all the way yet.) Next, turn on the following equipment: interface box, printer, terminal, and disk drive units. Push in the boot disk and the system will automatically boot up. A program called "AUTOST" will then instruct you to replace the boot disk with the disk containing the programs. Place a data disk in the right-hand drive. The program "SET_TIME" will then automatically be loaded and run. After setting the system clock, the program "AUTOST" will then display a menu of the available programs. Choose your option, and the program will be loaded and start to run.

A.4.2 Running the Program "NRL"

The menu-driven program "NRL" will be used to interface operator inputs with the tracker setup. This program has many options that the operator can choose by using the programmable function keys to initiate certain commands. These commands will be explained in detail in the following pages. If the user would like to observe only the data coming out of the tracker, no operator inputs are required, and the program will act only as a monitor.

Menu 1 Options

Redisplay the current screen:

REDISPLAY SCREEN (Option <SHIFT> k0)

Toggle the self-test status flag between ON and OFF and then send the command to the tracker:

SELF TEST (Option <SHIFT> k1)

Send the star disable command to the tracker (the star disabled is the one that is displayed as the current star):

STAR DISABLE (Option <SHIFT> k2)

Send the star enable command to the tracker (the star enabled is the one that is displayed as the current star):

STAR ENABLE (Option <SHIFT> k3)

Toggle the condition of the adaptive rate flag between ON and OFF and then send the command to the tracker:

ADAPTIVE RATE (Option <SHIFT> k4)

Toggle the condition of the acquisition flag between MANUAL and AUTO and then send the command to the tracker. If the mode is MANUAL, the operator has the four choices of the acquisition mode: 0-OFF, 1-FULL FIELD OF VIEW, 2-FULL EDGE, 3-VECTORED EDGE.

ACQUISITION (Option k5)

Toggle the condition of the taking data flag between ON and OFF. If data are being taken for the first time, the program queries the user for a data file number into which data will be stored. An initialized disk must be in the right disk drive. If a large amount of data will be taken, the NRL program should be loaded into memory, and the program disk should be removed from the right disk drive and replaced with an initialized **blank** disk. When the disk is full, the program will ask the user to replace it with another disk to continue taking data.

TAKE DATA (Option k6)

NOTE: For data processing purposes, the internal clock should be set to the correct date and time before taking any data. The SET_TIME program was created to simplify this process. First, load the SET_TIME program into memory (from the program disk) and then execute it.

Access the options listed in the second menu:

MENU 2 OPTIONS (Option k7)

Check the status of the tracker, and set and display the program flags to reflect the actual running conditions of the tracker:

GET TRACKER STATUS (Option k8)

Stop the program execution:

EXIT PROGRAM (Option k9)

Menu 2 Options

Redisplay the current screen:

REDISPLAY SCREEN (Option <SHIFT> k0)

Use the current star number, X position, and Y position as the data sent to the tracker for the commanded-to-track option:

TRACK STAR AT X,Y (Option <SHIFT> k1)

Query the user for the new drop criteria, which has a valid range of 1 to 15, and send the drop criteria command to the tracker, which sets up the number of times a possible star is to be tracked before dropping it:

DROP CRITERIA (Option <SHIFT> k2)

Query the user for a new X position, which has a valid range of 0 to 256:

X POSITION (Option <SHIFT> k3)

Query the user for a new Y position, which has a valid range of 0 to 256:

Y POSITION (Option <SHIFT> k4)

Query the user for a new star number, which has a valid range of 1 to 3:

STAR NUMBER (Option k5)

Toggle the condition of the taking data flag between ON and OFF. If taking data for the first time, the program queries the user for a data file number into which to start storing data. An initialized disk must be in the right disk drive. If a large amount of data is being taken, load the NRL program into memory, remove the program disk from the right disk drive, and replace it with an initialized **blank** disk. The program will indicate when the disk is full, and it will ask the user to replace it with another disk to continue taking data.

TAKE DATA (Option k6)

Access the options listed in the first menu:

MENU 1 OPTIONS (Option k7)

Check the status of the tracker, and set and display the program flags to reflect the actual running conditions of the tracker:

GET TRACKER STATUS (Option k8)

Stop the program execution:

EXIT PROGRAM (Option k9)

Possible Error Conditions

An error checking code has been included in the areas of user inputs, transmit errors between the interface box and tracker, and writing data to a file on a disc.

Transmit errors occur when the redundancy check fails while sending a command to the tracker, or receiving data from the tracker. When the transmit error occurs while sending a command, the user can try to send it again.

Input errors occur when an invalid input is received, such as a number outside the prescribed range. These errors will be trapped by the program, which then allows the user to correct the problem immediately. Consult Menu 1 Options and Menu 2 Options for details for each command, and the valid range of inputs will be listed there.

Data file errors occur when data are being taken to be stored on a disk. The program traps three specific errors and advises the user what to do next. These errors are:

1. **Duplicate file name.** The file name already exists. To correct the error, input a different data file number. If unsure what number to use, exit from the program and type:

   CAT <EXEC>

   to display a list of the files on the disk. (FILE_0 through FILE_999 are valid names for the data files.) To delete a file, e.g., file number 0, type:

   PURGE "FILE_0" <EXEC>

2. **Mass storage overflow.** The data disk is full, replace it with a new one.

3. **Media not present in the right disk drive.** A disk must be in the right disk drive to record data.

4. All other errors encountered in this section of the program are trapped, and are listed in Attachment I-6.

A.4.3 Running the Program without the Interface Box

When running the program without the interface box, the user must change one line in the program source code. Exit from the NRL program and type EDIT. Then change the line that contains the following code:

```
Test_flag=0     ! For use w/ the interface box
```

To reach the end of this line of code, move the cursor by using the arrow keys or the rotating knob. Change the flag equal to 1 by typing over the 0. To register the change, hit the <ENTER> key. To exit the edit session, simply press the shift key concurrently with the <PSE/RSET> soft key. Press the <RUN> soft key to run the program.

A.4.4 Running the Data Processing Program PLOTXY

PLOTXY is a menu-driven program that will be used to process data received from the tracker. The programmable function keys can be used to initiate many different commands. The program listing for PLOTXY is provided in Attachment I-5.

To load the program PLOTXY into memory, type:

LOAD "PLOTXY" <EXEC>

(the symbol <EXEC> signifies pressing the soft key labeled EXEC)

To begin execution, press the soft key labeled RUN:

<RUN>

Menu Options

Clear the graphics from the screen and redisplay the option menu:

REDISPLAY SCREEN (Option <SHIFT> k0)

Toggle the flag for star 1 to indicate whether that star will be plotted on the next graph:

STAR #1 (Option <SHIFT> k1)

Toggle the flag from star 2 to indicate whether that star will be plotted on the next graph:

STAR #2 (Option <SHIFT> k2)

Toggle the flag from star 3 to indicate whether that star will be plotted on the next graph:

STAR #3 (Option <SHIFT> k3)

Choose the data file to be used for the plots:

DATA FILE # (Option <SHIFT> k4)

NOTE: The program will not allow the user to plot any graphs until a data file has been read.

Plot the graph (X position versus Y position) of the stars that are currently turned ON (via options k1, k2, and k3) for the last data file read:

X VS Y (Option k5)

Plot the graphs (X and Y positions versus time) of the stars that are currently turned ON (via options k1, k2, and k3) for the last data file read:

POSITION VS TIME (Option k6)

Dump the graphics currently on the terminal screen to the thermal printer (after printing the graph, the screen is then cleared):

DUMP SCREEN GRAPHICS (Option k7)

Stop the program execution:

EXIT PROGRAM (Option k8)

Possible Error Conditions

An error checking code has been included in the areas of user inputs and writing data to a file on a disk.

Input errors occur when an invalid input is received from the user, such as a number that may have been outside the prescribed range. These errors should be trapped by the program, which allows the user to correct the problem immediately.

Data file errors occur when reading data from a disk. The program will trap three specific errors and advise the user what to do next. These errors are:

1. **File name is undefined.** The specified file name does not exist in the directory. Check the contents of the directory by typing:

   CAT <EXEC>

   to display a list of the files on the disk. (FILE_0 through FILE_999 are valid names for the data files.) To delete a file, e.g., file number 0, type:

   PURGE "FILE_0" <EXEC>

2. **Media not present in the right disk drive.** To read data, a disk must be in the right disk drive.

3. All other errors encountered in this section of the program are trapped, and are listed in Attachment I-6.

END

FILMED

DTIC